

THE ROLE OF INHIBITION IN THE DEVELOPMENT OF PATTERN VISION IN
HUMAN INFANTS

by

LETICIA A. GARCIA-QUISPE

A dissertation submitted to the Graduate Faculty in Biology in partial fulfillment of the requirements for the degree of Doctor of Philosophy, The City University of New York

2008

UMI Number: 3296945

Copyright 2008 by
Garcia-Quispe, Leticia A.

All rights reserved.

UMI[®]

UMI Microform 3296945

Copyright 2008 by ProQuest Information and Learning Company.
All rights reserved. This microform edition is protected against
unauthorized copying under Title 17, United States Code.

ProQuest Information and Learning Company
300 North Zeeb Road
P.O. Box 1346
Ann Arbor, MI 48106-1346

© 2008

LETICIA A. GARCIA-QUISPE

All Rights Reserved

This manuscript has been read and accepted for the
Graduate Faculty in Biology in satisfaction of the
dissertation requirement for the degree of Doctor of Philosophy.

Date

Chair of Examining Committee
Dr. James Gordon, Hunter College

Date

Executive Officer
Dr. Richard L. Chappell

Dr. Richard L. Chappell, Hunter College

Dr. Joshua Wallman, City College

Dr. E. Eugenie Hartmann, The University of Alabama

Dr. Vance Zemon
Ferkau Graduate School of Psychology, Yeshiva University

Supervisory Committee

THE CITY UNIVERSITY OF NEW YORK

ABSTRACT
THE ROLE OF INHIBITION IN THE DEVELOPMENT OF PATTERN VISION IN
HUMAN INFANTS

by

Leticia A. García-Quispe

Adviser: Professor James Gordon

There are major developmental changes in the visual system early in infancy which continue throughout childhood and possibly even later. The purpose of this study is to describe the development of cortical responses to gratings of different contrasts and spatial frequencies in order to characterize the neural mechanisms that contribute to these responses. In spatial tuning functions from infants we examined the changes in the low spatial frequency limb of the function, the peak of the amplitude and the acuity limit, as well as differences between the eyes. In the contrast response functions, we obtained representative data from infants in order to quantify amplitude and phase functions using a nonlinear model based on shunting inhibition. The model generates estimates of shunting inhibition and integrative time constants in the visual system.

The stimuli were horizontal square-wave gratings contrast-reversed at 7.5 Hz. For spatial tuning functions, spatial frequency was swept in six octave steps from 0.8 c/deg to 24 c/deg in infants (1.6 c/deg to 48 c/deg in adults). Five or ten runs were obtained from each participant (6.4 s each). For the contrast response functions, gratings of 0.75 c/deg or 1.5 c/deg were used, and contrast was swept in eight octave steps from 0 to 64%. Ten runs were obtained (8.5 s each). Infants from 10 through 31 weeks of age were tested. Some children and adults were tested for comparison. The amplitude and phase of the second harmonic were computed and plotted versus spatial frequency or contrast.

The results indicate that in general, infants' spatial functions have a less pronounced low-spatial frequency fall-off, their amplitudes tend to be larger, the peak of their functions is at lower spatial frequencies, and they have lower acuities than adults. Infants show slight but adults show steep phase lags with increasing spatial frequency. Most infants had well-matched right versus left eye responses (a significant difference at one spatial frequency or none). In general, contrast response functions in infants are more linear with increases in contrast, and they do not show amplitude saturation. Infant phases are relatively flat whereas adult phases advance with increases in contrast. Adults show high contrast gain control (amplitude compression and phase advance) but it is lacking or weakly present in most infants. In general, infants have longer time constants than adults, and time constants decrease with increasing contrast. These results are consistent with greater inhibitory cortical activity (lateral inhibition and shunting inhibition) in adults than in infants.

ACKNOWLEDGEMENTS

I thank all the members of my Committee for their constructive comments and their important role in reviewing and in the development of this manuscript. Special thanks go to my mentor and Chair of the Examining Committee, Dr. James Gordon, for his advice and his constant guidance and words of encouragement during my years as a Graduate student. I offer my appreciation to Dr. Vance Zemon for his invaluable discussions during the course of this study and the Dissertation writing period. I express my gratitude to Dr. Mirjana Nesin for her key role in the recruitment of infants, and Dr. Genie Hartmann for her thorough proofreading of this manuscript. I also thank all the students who helped with data collection. I am especially grateful to my husband, Jose Luis, for his support and belief in me during my graduate school journey.

TABLE OF CONTENTS

Abstract	iv
Acknowledgements	vi
List of Tables and List of Figures	ix
Introduction	1
Development of the Human Visual System	8
Anatomical Studies	8
Behavioral Studies	11
Visual Acuity	11
Spatial Contrast Sensitivity	15
Temporal Contrast Sensitivity	17
Summary	19
Electrophysiological Studies: The Visual Evoked Potential as a Tool to Study Functional Subsystems in Infants	20
Transient versus Steady State VEPs	21
Visual Acuity: VEP Estimates	23
Contrast Sensitivity: VEP Estimates	25
Amblyopia	28
Inhibition in the Visual System	30
Goals of the Study	38
Research Design and Methods	39

Instrumentation	39
Data Recording Techniques	39
Data Collection Procedure	40
Analysis of the VEP	40
Specific Experiments	41
Spatial Frequency Sweep	42
Contrast Sweep (15 Cycles per Screen)	43
Contrast Sweep (30 Cycles per Screen)	44
Participants	45
Spatial Frequency Sweep Participants	46
Contrast Sweep (15 Cycles per Screen) Participants	47
Contrast Sweep (30 Cycles per Screen) Participants	47
Results	48
Spatial Frequency Sweep	48
Monocular Differences	79
Contrast Sweep (15 Cycles per Screen)	86
Contrast Sweep (30 Cycles per Screen)	93
Discussion	99
Spatial Tuning Functions	99
Contrast Response Functions	108
References	113

LIST OF TABLES

Table 1	Summary of parameters for the stimuli used in this study	45
Table 2	Number of participants recruited per stimulus condition and distance used	47
Table 3	Pearson correlations between phase and age for the right (OD) and left (OS) eyes by each spatial frequency tested at 114 cm	52
Table 4	Binocular and monocular mean acuities in infants and adults for the 5-runs and 10-runs analyses only for participants in which binocular data was obtained	69
Table 5	Monocular mean acuities in all infants and adults for the 5-runs and 10-runs analyses	69
Table 6	Number of participants (n), t values (t), and probabilities (p) for monocular and binocular comparisons (one tail) in infants and adults. (OD: right eye, OS: left eye, OU: both eyes)	70

LIST OF FIGURES

Figure 1	Comparison of binocular (top panel) and monocular (bottom panel) acuity estimates as a function of age from the behavioral studies reviewed in the text	14
Figure 2	Comparison of binocular (top panel) and monocular (bottom panel) acuity estimates as a function of age from VEP studies reviewed in the text	26
Figure 3	Example of a spatial frequency sweep used as stimulus	43
Figure 4	Example of a contrast sweep pattern used as stimuli	45
Figure 5	Monocular amplitude and phase of the second harmonic response versus spatial frequency for a 16-week old tested at a viewing distance of 114 cm	49

Figure 6	Monocular amplitude and phase of the second harmonic response versus spatial frequency for a 23-week old tested at a viewing distance of 114 cm	50
Figure 7	Monocular amplitude and phase of the second harmonic response from a 4-year old tested at a viewing distance of 114 cm	53
Figure 8	Amplitude and phase of the second harmonic response from a 30-year old adult tested at a viewing distance of 228 cm.	54
Figure 9	Monocular amplitude and phase of the second harmonic response from a (a) 24-week old tested at a viewing distance of 114 cm, a (b) 2-year old tested at 114 cm, and a (c) 23-year old adult tested at 228 cm	55
Figure 10	Scatter plots of phase (in degrees) versus age (in weeks) for the right eye (OD) by each of the spatial frequencies tested at 114 cm (ten-runs analysis)	58
Figure 11	Scatter plots of phase (in degrees) versus age (in weeks) for the left eye (OS) by each of the spatial frequencies tested at 114 cm (ten-runs analysis)	59
Figure 12	Scatter plots of phase (in degrees) versus age (in weeks) for the right eye by each of the spatial frequencies tested at 114 cm (five-runs analysis)	60
Figure 13	Scatter plots of phase (in degrees) versus age (in weeks) for the left eye by each of the spatial frequencies tested at 114 cm (five-runs analysis)	61
Figure 14	Scatter plots of phase (in degrees) versus age (in years) for the right (column a) and left eye (column b) by each of the spatial frequencies tested at 228 cm	64
Figure 15	Mean phase versus spatial frequency bar graphs	65
Figure 16	Scatter plots of acuity versus age (ten runs)	66
Figure 17	Scatter plots of acuity versus age (five runs)	67
Figure 18	Scatter plots of acuity versus age for the right eye (top), left eye (middle) and both eyes (bottom) in children and adults tested at 228cm	68

Figure 19	Bar graphs of mean monocular and binocular acuity in infants	71
Figure 20	Bar graphs of mean monocular and binocular acuity in adults	72
Figure 21	Scatter plots of the LOG value of the ratio of the signal to noise value at 0.8 c/deg and the signal to noise value at the peak spatial frequency as a function of age	73
Figure 22	Scatter plots of the LOG value of the ratio of the signal to noise value at 1.5 c/deg (1.6 c/deg) and the signal to noise value at the peak spatial frequency as a function of age	74
Figure 23	Bar graph of mean log value of the ratio of the S/N value at 0.8 c/deg and S/N value at the peak of the response in infants and adults	75
Figure 24	Bar graph of log value of the ratio of the S/N value at 1.5 c/deg and S/N value at the peak of the response	76
Figure 25	Frequency distribution plots of location of peak of response based on amplitude values and signal to noise ratios	77
Figure 26	Bar graphs of mean acuity in infants by gender	78
Figure 27	Monocular responses from two 21-week olds (a and b) and a 24-week old (c) showing significant differences between the eyes	82
Figure 28	Monocular responses from a 9-year old (a), an 11-year old (b) and a 14-year old (c) showing significant differences between the eyes	83
Figure 29	Monocular responses from a 21-year old (a), a 23-year old (b) and a 36-year old (c) showing significant differences between the eyes	84
Figure 30	Spatial tuning functions for a 46-year old diagnosed amblyope	85
Figure 31	Monocular amplitude and phase of the second harmonic response to the 0.75 c/deg contrast grating sweep from a 19-week old, a 23-week old, a 28-week old, a 10-year old and a 26-year old	87

Figure 32	Monocular amplitude and phase of the second harmonic response to the 0.75 c/deg contrast grating sweep from a 22-week old, a 24-week old and a 20-year old showing negative shunting coefficients	89
Figure 33	Scatter plots of each of the model's parameters versus age for the 0.75 c/deg contrast sweep responses	90
Figure 34	Scatter plots of each of the model's parameters versus age showing only the infants from Figure 33 (0.75 c/deg contrast sweep responses)	91
Figure 35	Bar graphs of each of the parameters mean values for adults and infants corresponding to the data shown in Figure 33	93
Figure 36	Monocular amplitude and phase of the second harmonic response to the 1.5 c/deg contrast grating sweep from a 16-week old, a 21-week old, a 3-year old, a 14-year old and a 26-year old	95
Figure 37	Scatter plots of each of the model's parameters versus age for the 1.5 c/deg contrast sweep responses	97
Figure 38	Bar graphs of each of the parameters mean values for adults and infants corresponding to the data shown in Figure 37	98
Figure 39	Amplitude and phase of the second harmonic response as a function of spatial frequency from the 16 week-old from Figure 5 (right eye) and the 23 year-old from Figure 9 (left eye) superimposed to emphasize the adult and infant differences	102
Figure 40	Comparison of mean acuity results from the present study and VEP acuity from previous studies	103

INTRODUCTION

Invasive studies on diverse species of animals have demonstrated that various components of the nervous system form distinct and parallel subsystems, which govern different functional aspects of visual information processing. It has become clear that an important functional dichotomy exists within the primate visual system for processing brightness (positive-contrast) and darkness (negative-contrast) information. It has long been recognized that white and black (brightness and darkness) are distinct sensations (Hering, 1964).

Hartline (1938) studied the responses of optic nerve fibers in the frog's eye. He defined the "receptive field" of an optic nerve fiber as "the region of the retina which must be illuminated in order to obtain a response." He also indicated that individual ganglion cells fall under one of three distinct types: 1) Fibers that respond throughout the duration of the light stimulus, 2) Fibers that respond only at the onset and cessation of illumination, and 3) Fibers with activity confined only when a light stimulus is withdrawn. Subsequently, Kuffler (1953) studied the responses of cat retinal ganglion cells to small spots of light. He described the general organization of a receptive field as a concentric area with a center and an antagonistic surround. The center and the surround had opposite discharge patterns. Kuffler classified receptive fields into "on" center and "off" center fields. When he placed a small spot of light in the center of an ON center retinal ganglion cell, the cell's firing rate increased; when the spot was placed on the surround, the firing rate decreased. The OFF center cell's firing rate increased and decreased when the spot of light was placed in the surround and in the center of its receptive field respectively.

It appears that the ON/OFF dichotomy is established at the level of bipolar cells (reviewed in Tessier-Lavigne, 2000). These subsystems are distinct both morphologically (Famiglietti & Kolb, 1976; Dacey, 1993) and pharmacologically (Slaughter & Miller, 1981).

By mid 1970's, there was evidence that flat cone bipolar cells hyperpolarized to photic stimulation whereas invaginating cone bipolar cells depolarized under the same conditions of illumination. It was also known that synaptic terminals of flat cone bipolar cells ended high in the inner plexiform layer (IPL), and invaginating cone bipolar cells ended low, toward the ganglion cell layer (reviewed in Famiglietti and Kolb, 1976). Famiglietti and Kolb (1976) provided anatomical evidence for the presence of distinct pathways which they proposed were the structural basis for the ON- and OFF-center responses in mammalian retinas. Two morphological types of ganglion cells in the cat retina were observed. One type of ganglion cells branched exclusively in the region of flat cone bipolar cells, and the other type branched only among the terminals of invaginating cone bipolar cells. They interpreted these findings as indicating that flat cone bipolars were OFF-center cells whereas invaginating cone bipolar cells were ON-center cells.

Dacey (1993) distinguished two midget ganglion cell types in the human retina on the basis of their dendritic stratification in either the inner or outer portion of the inner plexiform layer (IPL), which presumably correspond to ON- and OFF-center cells respectively. Midget and parasol ganglion cells in the inner portion of IPL (presumed ON-center) were consistently larger in diameter than their counterparts in the outer IPL

(presumed OFF-center). Moreover, the smaller diameter outer cells formed a higher density mosaic than the larger-diameter inner cells.

ON and OFF cells form independent pathways up to the level of the primary visual cortex where significant interactions occur. Schiller (1982) recorded cell responses from the LGN and striate cortex of the rhesus monkey before and after infusion of APB (DL-2-amino-4-phosphonobutyric acid) into the eye. APB had been previously shown to block ON responses in retinal bipolar, amacrine and ganglion cells of the mudpuppy and the rabbit (Slaughter and Miller, 1981). Retinal APB infusion was found to block the responses of the LGN ON-center cells while the OFF-center cells were unaffected. Some responses were affected at the level of the cortex (e.g. light edge responses) while others showed no discernible effect (e.g. orientation and direction specificity). These results indicated that ON and OFF systems interact significantly at the level of the striate cortex, but not at the level of the LGN. Schiller, Sandel and Maunsell (1986) found that detection of light increment but not of light decrement was severely impaired in rhesus monkeys (trained to make saccades to targets which were either lighter or darker than the background) after injection of APB into the vitreous.

Zemon, Gordon and Welch (1986, 1988) designed separate positive- and negative-contrast bright- and dark- isolated-check stimuli over a static background to emphasize respectively contributions from the ON and OFF pathways to the visual evoked potential (VEP). The luminance of the checks was modulated sinusoidally either above or below the static background. Temporal frequency, check size and contrast level were varied parametrically. [Temporal frequency refers to how fast a pattern changes as a function of time (Wurtz & Kandel, 2000)]. Amplitudes and phases of the fundamental

component were compared across check size, temporal frequency and contrast. The negative-contrast stimuli elicited larger responses than the positive-contrast stimuli at most check sizes, over a wide temporal range and at each level of contrast used. The response to stimulation of the OFF cells showed finer spatial tuning than the ON pathway response. The authors indicated that OFF cells appear to have smaller diameter center mechanisms than ON cells, and that the OFF pathway has a greater contrast gain than the ON pathway (Zemon et al., 1988). These results are consistent with the anatomical differences reported by Dacey (1993) between the ON- and OFF-cells, namely the smaller diameter and higher density of the OFF-center cells compared to the ON-center counterparts.

It has also been found that negative contrasts prevail over bright contrasts in natural scenes which coincides with the asymmetry between the ON and OFF ganglion cell mosaics (Ratliff, Sterling & Balasubramanian, 2005).

Further study results have demonstrated a lack of maturity in the ON and OFF pathways well into childhood. Zemon et al. (1995) used appearing-disappearing bright or dark isolated checks over a static background to examine contrast-dependent responses in humans from 4 to 42 years of age. They found that fundamental responses to the dark-check condition were greater in magnitude than those of the bright-check condition. Children's responses were larger than those of adults, and the phase lag appeared to increase with increasing age under each condition. In addition, they used a conventional contrast-reversing checkerboard to record transient VEPs. Their transient VEP waveforms showed a small initial positive deflection (P_{60}) and a later prominent positive deflection (P_{100}) that peaked at about 60 and 100 milliseconds respectively. They found

that the latency of P₁₀₀ decreased whereas the latency of P₆₀ increased with increasing age. The authors indicate that P₆₀ latency reflects delay due to precortical processing and conduction time. Myelination of the visual pathways which increases conduction velocity in nerve fibers has been cited as an explanation for decreases in response latency. Zemon et al. (1995) emphasize that myelination would predict a decrease in latency of both P₆₀ and P₁₀₀ with age. If myelination is not the main contributor to these latency changes, they suggest it is possible P₆₀ latency is shorter in infants and children due to shorter optic nerve fibers (precortical input reaches the cortex faster in infants and children than adults). On the other hand, faster intracortical processing in adults than in children could account for the observed decreased P₁₀₀ latency with age.

Sokol and Moskowitz (1990) found that as early as 2 months of age, infants showed greater responses to negative contrast stimuli compared to positive contrast stimuli. Peak amplitudes occurred between 20 and 40 min of arc, and the phase differences between the ON and OFF responses were larger than in adults. Hartmann Hitchcox and Zemon (1992a, 1992b) also observed larger amplitudes to the contrast-decrement stimuli compared to amplitudes to the contrast-increment condition in 6- and 12-week olds. In infants less than 6 weeks of age, the difference of the response phases for the bright and dark conditions fall mainly between 90° and 180°; however, in infants older than 6 weeks, the phase differences are less than 90°, indicating that the responses in younger infants are mediated primarily by local luminance rather than pattern signals (Hartmann et al., 1992a).

Another major dichotomy in the visual system is the processing of contrast information: 1) The Magnocellular (M) pathway which originates in the retina and

projects to the two ventral layers of the dorsal lateral geniculate nucleus (LGN), exhibits high contrast sensitivity; 2) The Parvocellular (P) pathway which also originates in the retina but projects to the four dorsal layers of the LGN, exhibits low contrast sensitivity (Kaplan & Shapley, 1986). “Contrast sensitivity is the inverse of the lowest stimulus contrast that can be detected” (Wurtz & Kandel, 2000). The M and P streams, each of which is subdivided into ON and OFF subsystems, remain segregated at the initial cortical level, where they project to different strata of layer IVc in V1 (Hubel & Wiesel, 1972; Hendrickson, Wilson & Ogren, 1978). Relatively little knowledge of these pathways, however, exists for humans of any age. Recent electrophysiological studies using the visual evoked potential (VEP) as a noninvasive measure indicate that these pathways can be probed selectively in humans (Zemon et al., 1988; Zemon, Siegfried & Gordon, 1991; Zemon et al., 1995).

Neurons in M layers of the primate LGN are known to have contrast sensitivities about ten times greater than those in P layers (Kaplan & Shapley, 1986). Derrington and Lennie (1984) studied spatial tuning between neurons in the M and P layers of the LGN and found a higher spatial frequency roll-off in P cells than in M cells. There are also differences in spatial tuning of VEP responses to high- and low-contrast stimuli (Zemon & Gordon, 1988), consistent with the differences in spatial tuning found between cells in the M and P pathways (Derrington & Lennie, 1984). Responses elicited by high-contrast stimuli peak at finer checks than do the responses elicited by low-contrast stimuli.

M and P streams also differ with regard to their temporal phase characteristics: M-cells exhibit a relative phase advance with increasing contrast, whereas P-cells do not (Derrington & Lennie, 1984). This difference suggests that greater contrast gain control

is exerted on the M pathway than on the P pathway. The concept of contrast gain control (amplitude compression and phase advance in contrast functions) was introduced by Shapley and Victor (1978, 1981) in their studies of cat retinal ganglion cells.

Postnatal development of neurons in M and P layers of the human LGN has also been studied (Hickey, 1977). Different time courses for cellular growth were discovered for these two populations. P cells had a rapid growth phase ending at about six months and a more gradual growth phase during the subsequent six months. In contrast, M cells increased rapidly in size for one full year and then continued to increase gradually for another year.

Another important distinction between M and P streams is their sensitivity to wavelength (Shapley, 1982): M cells are broadband in their spectral sensitivity, whereas P cells exhibit color-opponency. There have been attempts to separate contributions from M and P pathways to the VEP using luminance-contrast and isoluminant chromatic-contrast stimuli, respectively (Murray, Parry, Carden & Kulikowski, 1987). Dramatic differences in transient VEPs elicited by these two types of stimuli have been found. More recent efforts using isoluminant chromatic stimuli to emphasize contributions from the P pathway to the VEP indicate that the properties of this system have been successfully isolated and examined (Zemon, Gordon, Greenstein, Holopigian & Seiple, 1990; Zemon, et. al. 1991). In the luminance case, amplitudes saturate at about 16% contrast, whereas in the chromatic case, amplitudes increase with contrast in an approximately linear fashion. Again, these results are consistent with the hypothesis that VEPs to low contrast luminance and isoluminant chromatic stimuli reflect activity from M and P pathways, respectively.

DEVELOPMENT OF THE HUMAN VISUAL SYSTEM

Development of the neural pathways involved in processing visual information has been investigated using a variety of anatomical, biochemical, physiological, and behavioral techniques.

ANATOMICAL STUDIES

Anatomical evidence indicates that significant maturational processes take place during the first few years of life in human infants (Abramov, Gordon, Hendrickson, Dobson & LaBossiere, 1982; Hendrickson & Yuodelis, 1984; Yuodelis & Hendrickson, 1986; Hickey, 1977; Garey & de Courteen, 1983). The different time courses of development for different structures in the visual system are likely to be the underlying mechanisms for the different physiological and behavioral responses observed in infants. Abramov et al. (1982) provided anatomical evidence that the peripheral retina of the human infant is well developed eight days after birth, but the macular area is not. Some notable features of the immaturity of the macular area were: (1) the poorly formed foveal depression due to incomplete migration of ganglion cell and inner nuclear layers, (2) the presence of a split in the inner nuclear layer near the fovea (“transient layer of Chievitz”), (3) the paucity of cones in the foveal region and (4) the short and stumpy appearance of the foveal cones rather than the slim, elongated shape seen in cones from adults. Other researchers (Hendrickson & Yuodelis, 1984; Yuodelis & Hendrickson, 1986) have also reported that the foveal area is immature at birth. Yuodelis and Hendrickson (1986) reported that foveal development in humans may not be complete until after 4 years of

age. Foveola width and cone diameter decreased to reach adult values (650-700 μm and 2 μm respectively) at 45 months of age. However, outer segment length and cone packing density were only half the adult values at this age. Foveolar cone density increased from 18 cones/100 μm at 1 week after birth to 42 cones/100 μm in the adult. Yuodelis and Hendrickson (1986) propose that the large foveolar cones of the newborn and their low density impose a severe limitation on visual acuity levels.

Differential maturation has also been observed at the level of the lateral geniculate nucleus (LGN). As previously mentioned, Hickey (1977) studied the cells in the LGN of human brains. He noted that cells in the parvocellular layers increased in size rapidly during the first six months after birth, but continued to grow until they reached their adult sizes near the end of the first year. However, the time course of development for cells in the magnocellular layers was different. Magnocellular layer cells grew rapidly until one year after birth and reached their adult sizes at the end of the second year. In monkeys (reviewed in Boothe, Dobson & Teller, 1985), the parvocellular layers showed no significant growth after eight days, but there was significant growth in the magnocellular layers between eight days and adulthood. The importance of studying visual development in monkey infants resides in the possible use of the monkey as a model for normal and abnormal visual development in humans (reviewed in Boothe et al., 1985).

In the early 80's, Garey and de Courteen (1983) found that the LGN doubles its size between birth and six months of age, and that the presence of a large number of spines on dendrites and soma is the most striking difference between immature and adult LGN neurons. The number of spines reaches a peak around birth and then decreases so

that LGN neurons have an adult appearance by about 3 months in monkeys. In humans, the number of spines peaks at 4 months postnatally and reaches adult values by 9 months.

The human visual cortex has also been shown to undergo extensive postnatal development. The primary visual cortex increases 4-fold in volume between birth and 4 months, reaching its adult size at this age according to some studies (Huttenlocher, de Courten, Garey & Van der Loos, 1982; Garey & de Courten, 1983). Some researchers have found that the volume of cortical area 17 reaches maturity around 8 months (Leuba & Kraftsik, 1994). Other macroscopic features of area 17 which have been studied and found to reach maturity at different ages include the caudorostral length (6 months), the cortical thickness (7 months) and cortical surface (10 months) (Leuba & Kraftsik, 1994). Synaptogenesis in the cerebral cortex begins early in fetal life. It has been reported that vertical (intracolumnar) connections between layers of striate cortex develop at the beginning of the third trimester of gestation, whereas long horizontal (intercolumnar) connections within layers do not appear until shortly before birth and continue to develop throughout the first year of age and possibly even later (Burkhalter, Bernardo & Charles, 1993). The number of synapses in area 17 peaks at about 8 months postnatally and then decreases to reach an adult value by about 11 years of age (Huttenlocher et al., 1982; Garey & de Courten, 1983). In monkeys (for review see Boothe et al., 1985), the number of spines in cortical cells increases until eight weeks after birth and then decreases to adult values. The cortical cells in layers that receive input mainly from parvocellular layers reach their adult levels of spine frequency faster than cells in layers receiving primarily magnocellular input. Studies of cerebral glucose utilization with Positron Emission Tomography (PET) have found there is an increase in glucose metabolism in

primary visual cortex around 2 to 3 months of age (Chugani, 1998). There is also a dramatic increase in the absolute rates of cerebral-cortex-glucose utilization between birth and four years of age when rates are about twice as those of adults. These rates are maintained between four and ten years of age, and then there is a gradual decrease toward adult levels by 16 to 18 years of age.

BEHAVIORAL STUDIES

Visual Acuity

Some behavioral studies of visual acuity have used the Forced-choice Preferential Looking Procedure (FPL) (for reviews see Dobson, 1993, 1994; Hartmann, 1995, 1996). In the FPL technique, each infant is shown a set of black and white gratings (that vary in spatial frequency from trial to trial) paired with a gray stimulus of equal space-average luminance. An adult, masked to the location of the grating, observes the infant's looking behavior through a central peephole situated between the grating and the gray stimuli. The observer makes a decision regarding the position of the grating (right versus left) based on the infant's looking behavior. The observer's responses are objectively scored as correct or incorrect. A plot of observer's percent correct versus stripe width is constructed. Acuity is estimated as the spatial frequency that yields a specific level of accuracy, usually set to a correct criterion of 75%. ["Spatial frequency refers to the number of repetitions of a pattern over a given distance", usually given in cycles/degree (Wurtz & Kandel, 2000)].

The acuity card procedure, a modification of the FPL procedure, was developed to shorten the length of time necessary to obtain an acuity estimate in an infant. The most important difference between the acuity card and the FPL procedure is not the configuration of the stimuli, but the incorporation of subjective judgments on the part of the tester (reviewed in Dobson, 1993, 1994; Hartmann, 1995, 1996). There is; however, reliable accordance between mean acuities for FPL and acuity card estimates (Dobson, 1993).

Despite variations in the FPL procedure and stimulus configuration used, there is good agreement among studies in the development of acuity during infancy. In general, acuity improves rapidly during the first postnatal months, with little measurable improvement between 6 and 12 months (Dobson, 1994).

Birch (1985) obtained monocular acuities from 106 normal infants and binocular acuities from 40 infants aged 0-11 months with a preferential-looking technique. She found that monocular acuity improved rapidly from 2 c/deg at 0-2 months to 9.6 c/deg at 9-11 months. Binocular acuity had a similar course of development as monocular acuity before 6 months of age, but it became superior from 6 to 11 months of age. No adult comparison data were presented in this study.

McDonald, Sebris, Mohn, Teller and Dobson (1986) obtained monocular and binocular acuity estimates from 36 normal infants aged 4, 8 and 16 weeks and 6, 9 and 12 months. They used the acuity card procedure and cards with gratings that varied in spatial frequency from 0.2 to 24 c/deg in about 1-octave steps when viewed at 33 cm. Reported mean monocular and binocular acuities were as follows respectively: 0.6 and 0.8 c/deg at 4 weeks, 1.4 and 2.0 c/deg at 8 weeks, 2.3 and 4.5 c/deg at 16 weeks, 3.7 and 5.3 c/deg at

6 months, 4.1 and 5.0 c/deg at 9 months, and 3.3 and 6.3 c/deg at 12 months of age.

Acuity estimates shift to higher spatial frequencies in infants from 4 weeks to 6 months of age, but there is only minimal or no increase from 6 to 12 months.

Courage and Adams (1990) assessed binocular visual acuity from birth to three years of age using the acuity card procedure and the Teller Acuity Cards. The spatial frequencies of the gratings ranged in half-octave steps from 0.3 to 38 c/deg when viewed at 55 cm. They tested 140 infants and children, and reported mean acuities in cycles per degree for newborns (0.9 c/deg), 1-month (1.1 c/deg), 3-month (2.6 c/deg), 6-month (5.9 c/deg), 12-months (9.6 c/deg), 24-month (13.2 c/deg) and 36-month-olds (18.6 c/deg).

Mayer, Beiser, Warner, Pratt, Raye and Lang (1995) measured monocular acuities in 460 children between 1 month and 4 years of age in order to derive grating acuity norms using the acuity card procedure and the Teller Acuity Cards. The gratings ranged from 0.32 to 26 c/cm in approximately half-octave steps. The authors found that mean monocular acuity was 0.94 c/deg at 1 month, 2.16 c/deg at 2.5 months, 2.68 c/deg at 4 months, 5.65 c/deg at 6 months, 6.79 c/deg at 9 months, 6.42 c/deg at 12 months, 8.59 c/deg at 18 months, 9.57 c/deg at 24 months, 11.52 c/deg at 30 months, 21.81 c/deg at 36 months, and 24.81 c/deg at 48 months of age. Mean acuity showed a 2.6 octave increase between 1 and 6 months, and a 2.1 octave increase between 6 and 48 months. Mean acuity improved rapidly in the first 6 months and more gradually thereafter.

Salomao and Ventura (1995) obtained binocular (N=646) and monocular (N=624) acuity norms from infants and children aged 0 to 36 months of age using the Teller Acuity Cards and a modified staircase procedure. The spatial frequency of the gratings

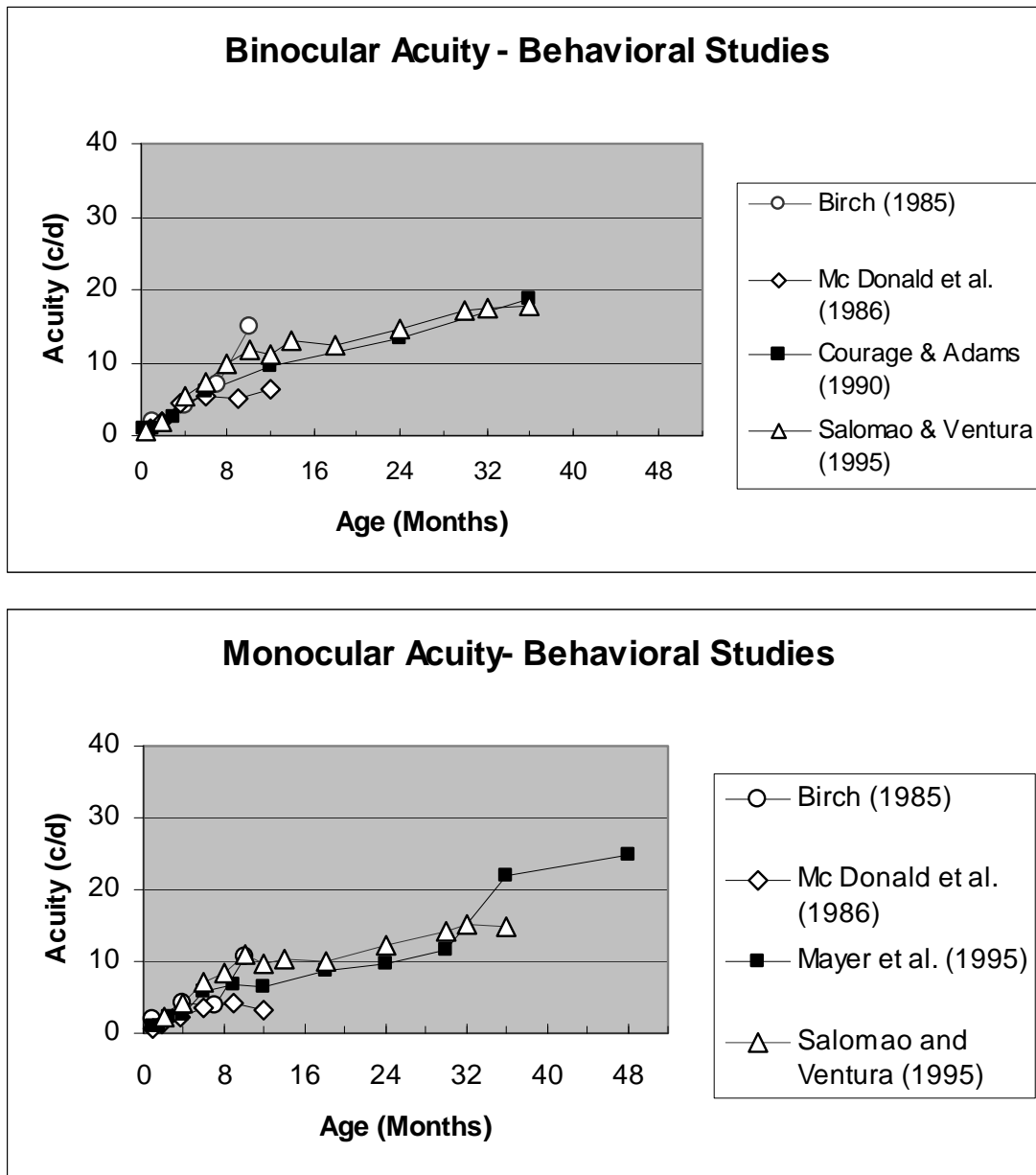


Figure 1. Comparison of binocular (top panel) and monocular (bottom panel) acuity estimates as a function of age from the behavioral studies reviewed in the text. Techniques used are indicated: Birch (1985)- preferential looking technique; McDonald et al. (1986)-acuity card procedure (ACP); Courage & Adams (1990)- ACP and Teller Acuity Cards (TAC); Mayer et al. (1995)- ACP and TAC; Salomao & Ventura (1995)- TAC and modified staircase procedure.

ranged from 0.23 to 38 c/cm in half-octave steps. Some of their reported binocular and monocular mean acuities are respectively: 2.02 c/deg and 2.31 c/deg at 2 months, 5.48 c/deg and 4.15 c/deg at 4 months, 7.44 c/deg and 7.18 c/deg at 6 months, 9.81 c/deg and 8.31 c/deg at 8 months, 12.39 c/deg and 9.95 c/deg at 18 months, 11.08 c/deg and 9.82 c/deg at 12 months, 14.64 c/deg and 12.31 c/deg at 24 months and 17.82 c/deg and 14.98 c/deg at 36 months of age.

Figure 1 summarizes the estimated monocular as well as binocular acuities as a function of age from the behavioral studies reviewed above. Despite some variations in the procedures used to obtain acuity estimates, the results of these studies agree well and are consistent with continued development of the visual system beyond the first year of life.

Spatial Contrast Sensitivity

Banks and Salapatek (1978) measured contrast sensitivity functions in 1-month-olds ($n=6$), 2-month-olds ($n=10$), and 3-month-olds ($n=8$) using a behavioral paradigm. The stimulus consisted of two adjacent half fields: one contained stationary vertical sinewave gratings and the other an unpatterned stimulus. The first eye movement (to the right or to the left) made by the infant was recorded. Thresholds were determined using a staircase procedure. They found that contrast sensitivity increased during the first three months of life, but it was still well below adult contrast sensitivity. The authors noted that the presence of a low-frequency fall-off at 2 and 3 months but not generally at 1 month of age is related to an increase in the strength of lateral inhibitory processes (implying

center-surround antagonism in retinal ganglion and lateral geniculate cells) during the first months of life.

Gwiazda, Bauer, Thorn and Held (1997) tested 83 infants (aged 0 to 8 months of age) with preferential looking and 84 children (aged 3 to 8.6 years) and 15 adults (aged 18 to 30 years) with operant techniques in order to examine the development of spatial contrast sensitivity. The stimuli were vertical sine wave gratings (contrast reversed at 0.5 Hz), paired with a gray field. They found that the shape of the contrast sensitivity function changes between 2 and 4 months of age: the peak shifts from 0.38 c/deg to about 1 c/deg, and the sensitivity decreases by about 1 octave at 0.38c/deg. The authors also attribute this low spatial frequency reduction in sensitivity to an increase in lateral inhibition in the visual system during early infancy. From 4 months to 4 years of age, the peak of the function shifts from about 1 c/deg to approximately 3.0 c/deg. Sensitivity at the peak increases by about two log units from infancy through adulthood.

Movshon and Kiorpes (1988) reanalyzed published data by Boothe, Kiorpes, Williams and Teller (1988) on spatial contrast sensitivity development obtained from macaque monkeys with operant techniques and by Banks and Salapatek (1978, 1981) obtained from human infants tested with a preferential looking paradigm. The authors point out that the shape of the contrast sensitivity function does not change significantly during development; there is only a shift in the horizontal and vertical scales. They mention that there is no reason to believe “that low-level processes such as lateral inhibition are of late onset.” They also analyzed sweep visual evoked potential data from human infants published by Norcia, Tyler and Hamer (1987). They note that there is no indication that the shape of the contrast sensitivity function from infants 12 weeks of age

or less differs from the function from infants 13 weeks of age or more. However, they indicate that the contrast sensitivity functions are more low-pass than bandpass possibly because the gratings were contrast modulated at relatively high temporal frequencies.

Eye movements have also been used to assess the development of contrast sensitivity. Hainline and Abramov (1997) observed directionally appropriate eye movements in infants 12 days through 146 days (5 months) of age in response to vertical sine wave gratings drifting either to the right or to the left at a velocity of 7 deg/s. The gratings varied in spatial frequency between 0.07 c/deg and 2.4 c/deg (up to 4.7 c/deg in adults) in octave steps. Contrast of these gratings ranged from 0.70 to 89% in 1-, 2- and 3-month olds and from 0.17 to 22% in 3-, 4-, 5- month olds and adults. The authors note that there is a marked increase in contrast sensitivity at the peak of the contrast sensitivity function, as well as a shift in the peak and the acuity limits to higher spatial frequencies with age. These results agree well with the literature. The authors also indicate that the general shape of the contrast sensitivity function does not change considerably between 1 month of age and adulthood.

Temporal Contrast Sensitivity

Temporal contrast sensitivity functions (CSFs) represent the sensitivity of an observer to a stimulus flickering sinusoidally as a function of temporal frequency. Hartmann and Banks (1992) studied CSFs in infants 1.5 and 3 months of age (with the FPL procedure). The stimuli were 0.1 c/deg sinewave gratings (0.5 c/deg in adults) contrast reversed at 1, 2, 5, 10 and 20 Hz. Average adult temporal CSF was found to be bandpass with peak sensitivity at 10 Hz. Average infant temporal CSF was low pass at

1.5 months, but it was bandpass by 3 months of age. The authors indicate that temporal contrast sensitivity in infants is most adult-like at high temporal frequencies, but spatial contrast sensitivity is most adult-like at low spatial frequencies.

Swanson and Birch (1990) also studied temporal contrast sensitivity functions with forced-choice preferential looking (FPL) in infants of 4, 6 and 8 months of age. The stimuli were 1.0 and 0.35 c/deg grating patches temporally modulated in contrast at 2, 4, 8 and 17 Hz. There was a considerable increase in sensitivity between 4 and 8 months of age for 1 c/deg patches modulated at temporal frequencies of 8 and 17 Hz; however, overall sensitivity was lower than in adults. The temporal contrast sensitivity function was low-pass for 1 c/deg at 4 months, and it was band-pass at 6 months. Temporal tuning curves were bandpass at 0.35 c/deg in 4-month old infants. Adult temporal tuning functions changed from bandpass to lowpass as spatial frequency increased from 0.35 c/deg to 4.6 c/deg. Swanson and Birch (1990) suggest that increased inhibition, either cortical or retinal in origin, could be responsible for the narrowing of temporal tuning of spatiotemporal mechanisms. It is important to note that temporal tuning functions in adults are bandpass at low spatial frequencies and lowpass at high spatial frequencies (Robson, 1966; Swanson & Birch, 1990). Bandpass temporal functions are observed at progressively higher spatial frequencies with increasing age (Hartmann & Banks, 1992).

Kiorpes and Stavros (2007) studied the development of temporal contrast sensitivity in 11 monkeys 5 weeks to 4 years of age. The stimulus was an unpatterned field of light modulated sinusoidally at different temporal frequencies (1 to 40 Hz). Sensitivity to high temporal frequencies appeared to develop earlier than sensitivity to low temporal frequencies. The authors indicate there is a change in the shape of the

temporal contrast sensitivity function during development. Moreover, peak temporal contrast sensitivity matured earlier than peak spatial contrast sensitivity.

Summary

In adults, temporal CSFs are band pass at low spatial frequencies, but low pass at high spatial frequencies, and spatial CSFs are bandpass at low temporal frequencies but low pass at high temporal frequencies (Robson, 1966). The infant literature usually deals with spatial and temporal contrast sensitivity functions separately at a specific temporal or spatial frequency respectively. However, the shape of the CSF changes depending on the spatial and temporal characteristics of a stimulus. The development of spatiotemporal interactions in infants needs to be studied further.

Although there are contradicting reports concerning the development of the shape of the contrast sensitivity function (namely, change from low pass to bandpass versus no major change), there is in general, agreement that the peak shifts to a higher spatial frequency, and there is an increase in peak sensitivity with age. The low-spatial frequency fall-off is thought to be associated with lateral inhibition in the visual system, “the result of an antagonism between signals from the center and surround regions of receptive fields” (Robson, 1966). In summary, behavioral testing of visual functions in infants indicates that the human visual system is immature at birth, develops very rapidly during the first year of life, but continues to develop throughout childhood.

ELECTROPHYSIOLOGICAL STUDIES: THE VISUAL EVOKED POTENTIAL AS A TOOL TO STUDY FUNCTIONAL SUBSYSTEMS IN INFANTS

The visual evoked potential is a gross electrical signal which is generated by the occipital region of the cortex in response to visual stimulation (Sokol, 1976). The VEP, recorded from the surface of the head, is the sum of a large number of excitatory and inhibitory postsynaptic potentials occurring on apical dendrites of pyramidal cells in superficial layers of cortex (for a review see Zemon, Kaplan & Ratliff, 1986). It reflects the complex sum of responses of a very large number of visual neurons. It is considered to be a measure of the visual pathway from the optic nerve to the visual cortex (reviewed in Hartmann, 1995).

The VEP has been used for decades to study visual development. VEP stimuli can either be unpatterned (flash) or patterned (e.g. gratings, checkerboards). Flash VEPs are used to assess the gross responsivity of the visual system (reviewed in Hartmann, 1995). A pattern stimulus is particularly useful in the study of the human visual system because it generates electrical signals that reflect, in part, the activity of mechanisms that underlie the processing of pattern information from photoreceptors to visual cortex (Sokol, 1982).

Dustman and Beck (1966) studied 215 normal participants 1-month through 81 years of age. They reported changes with age in amplitudes of waves in the first 250 ms of the response in flash VEPs. Amplitude increased rapidly, reaching a maximum at 5-6 years of age. The increase was followed by a rapid decline in amplitude until the ages 13 to 14 when another sudden increase occurred. The amplitudes stabilized at approximately age 16.

Transient versus Steady State VEPs

Depending on the rate of stimulation, VEPs can be classified into either transient or steady-state. Waveforms that result from low stimulation rates are called transient VEPs. In the transient condition, the relevant brain mechanisms for the response are in their resting states before each successive stimulus. As displayed by a conventional averager, a transient VEP is a graph of voltage versus time. An averaged transient VEP consists of one or more positive and negative deflections (e.g. P₆₀, P₁₀₀). Analysis of such VEPs are aimed at decomposing the waveform into elementary components that presumably originate in different parts of the brain or different neural organizations (Regan, 1982).

Steady-state VEPs are elicited by temporal modulation of sufficiently high frequency to result in overlap of the individual responses (Regan, 1982, 1989). The ideal steady-state VEP is a response whose constituent harmonic frequency components remain constant in amplitude and phase over an infinitely long time period (Regan, 1989). A stimulation frequency somewhere between 3 and 5 Hz marks the shift between transient and steady-state responses such that a stimulus varying at a frequency of 2 Hz would be considered transient while a varying frequency of 6 Hz (or greater) would be considered steady-state (reviewed in Hartmann, 1995).

Visual development has been explored using steady-state VEPs (Harris, Atkinson & Braddick, 1976; Sokol, 1978; Atkinson, Braddick, & French, 1979; Moskowitz & Sokol, 1980; Norcia, Tyler & Hamer, 1988, 1990; Peterzell & Kelly, 1997). Both acuity (Sokol, 1978; Atkinson et al., 1979; Norcia et al., 1988, 1990) and contrast sensitivity functions (CSFs) have been measured (Harris et al., 1976; Atkinson et al., 1979; Norcia

et al., 1988, 1990). VEP resolution acuity is defined as the largest stimulus to which a zero amplitude response can be obtained; however, direct measurement of this parameter is not possible (Hartmann, 1995). The contrast sensitivity (the reciprocal of contrast at threshold) function plots the contrast required to just detect a sinusoidal grating as a function of spatial frequency (in cycles per degree) (Banks, 1985).

Transient VEPs, like steady-state VEPs, reflect a dramatic maturational process that occurs during approximately the first half year of life. Crognale, Kelly, Chang, Weiss and Teller (1997) explored the differentiation of VEP components during the course of development in infants using two paradigms: large checkerboard pattern reversal (at 1.4 Hz) and low frequency pattern onset. They showed systematic developmental sequences for responses recorded within individuals. Adult responses were much smaller than the infant responses. The latency of the positive wave decreased rapidly from more than 240 ms at 2 weeks to reach adult values of about 100 ms at 3 months of age for the pattern reversal response. Latencies decreased from about 200 ms at 1 to 2 weeks to about 100 ms at 3 months of age for the pattern-onset response. Fiorentini and Trimarchi (1992) found that the peak latency of the infant VEP in response to a vertical sinusoidal grating (spatial frequency 0.5 c/deg) square-wave reversed at 1 Hz also decreased with age in a group of 14 infants 3 to 22 weeks of age.

Several studies have collected VEPs elicited by a stimulus display that has one of its parameters swept rapidly in time (e.g. Seiple, Kupersmith, Nelson & Carr, 1984; Norcia & Tyler, 1985; Norcia, Tyler, Hamer & Wesemann, 1989; Zemon, Hartmann, Gordon & Prünke-Glowazki, 1997). This efficient form of VEP recording permits the measurement of a variety of visual functions in a short period of time, making it a

potentially valuable tool for probing visual processing in subjects of limited attention span, such as infants. Thus far, applications of the sweep VEP technique have demonstrated its usefulness for monitoring the development of visual acuity (Norcia & Tyler, 1985; Zemon et al., 1997) and of contrast sensitivity (Norcia et al., 1988, 1989).

Visual Acuity: VEP Estimates

Atkinson et al. (1979) estimated acuity in 97 human neonates by using vertical sinusoidal contrast-reversing (10 Hz) grating stimuli. The spatial frequency at which 50% of the infants gave a significant VEP was used to obtain a neonatal group acuity of 0.85 c/deg. Norcia and Tyler (1985) measured visual acuities of 197 infants from 1 week to 53 weeks of age using the sweep VEP in response to contrast reversing gratings (6 Hz). VEP acuity was defined as the pattern element size at which a VEP could no longer be elicited from visual cortex, and it was estimated by linear extrapolation to zero microvolts of the highest spatial frequency peak in the amplitude versus spatial frequency function. Grating acuity increased gradually from a mean of 4.5 c/deg at 2.5 weeks (at 65.5 cm from display) to 22.0 c/deg at 50.5 weeks (at 262 cm). Adult VEP acuity averaged 24.3 c/deg (at 262 cm). The authors required that the phases of the VEP responses had to be constant over a considerable period or gradually lagging the stimulus as spatial frequency increased in order to consider the record for visual acuity estimation. However, the authors did not present any phase data as a function of age.

In a subsequent study, Norcia et al. (1988) estimated grating acuities of 7.4 ± 1.7 c/deg and 33.9 ± 1.0 c/deg for 10-week-olds (ten infants) and adults respectively. Similar results were obtained in a later study with 37 infants from 4 weeks to 31 weeks of age

(Norcia et al., 1990). A gradual increase in grating acuity from 5 c/deg during the first month to 16.3 c/deg at 8 months postnatal age was reported.

Hamer, Norcia, Tyler and Hsu-Winges (1989) measured monocular and binocular grating acuities in 87 infants between 2 and 52 weeks of age using the sweep VEP. The authors found that binocular acuity was nearly identical to monocular acuity. There was a small binocular acuity superiority (0.17 octaves higher than monocular) only in the 11 to 20 week age group. Interocular acuity differences were small (averaging 0.22 octaves across all age groups). The authors concluded that these differences are primarily determined by the inherent variability of the VEP measure. Mean acuity increased from about 6 c/deg in the first month to around 14 c/deg by 8 months of age for both monocular and binocular viewing. No developmental phase data were presented.

Recently, Zemon et al. (1997) examined spatial processing in humans over a broad range of ages using a variant of the sweep VEP under monocular viewing conditions. The stimulus consisted of a brief sweep of horizontal square-wave grating patterns which were contrast reversed in a square-wave temporal modulation (7.94 Hz). Data collection was synchronized (time-locked) to the stimulus presentation; noise was estimated using the T_{circ}^2 statistic (Victor & Mast, 1991), and acuity estimates were obtained by linear interpolation of the signal-to-noise measure. They found that acuity estimates increased as a function of age (26-week-old at 114 cm: 9.41 c/deg; 33-week-old at 114 cm: 13.93 c/deg; 17-year-old at 228 cm: 22.76 c/deg; 33-year-old at 228 cm: 32 c/deg). Phase functions decreased consistently with spatial frequencies greater than 4 c/deg. Infants produced relatively flat phase functions at low spatial frequencies showing

a nearly 180° phase shift (at 2 c/deg) relative to the older observers. Moreover, response amplitudes for adults were much smaller than those for infants.

Figure 2 shows a summary graph of the developmental acuity results obtained with VEP testing. The top panel shows binocular mean acuity as a function of age. The bottom panel shows monocular acuity. The data points for the Zemon et al. (1997) study do not represent mean acuity values but their reported data for a single participant at each age. For the Hamer et al. (1989) study, their reported acuity at 8 months (e.g. 14 c/deg) was plotted, although from their figures, acuity at this age seems closer to 11 c/deg. VEP acuity estimates are in general higher than behavioral estimates. Infants at 8 months (for monocular data) or 13 months (for binocular data) of age have not yet reached adult acuity values (with the exception of the Norcia and Tyler (1985) study in which the authors reported that adult acuities were achieved by 8 months of age). As with the behavioral studies, there is also very good agreement between the VEP estimated acuities, despite differences in the methodology used to obtain them. Moreover, VEP binocular and monocular acuities are consistently higher than their respective behavioral acuities (see Figures 1 and 2).

Contrast Sensitivity: VEP Estimates

Atkinson et al. (1979) used vertical sinusoidal gratings contrast-reversed at 10 Hz to examine contrast sensitivity in 97 human infants 1 to 10 days old. Spatial frequencies of 0.15, 0.4, 0.75 and 1.2 c/deg were combined with 25%, 40%, 63% and 98% contrast levels. The contrast at which 50% of the infants gave a significant VEP was used as an estimate of threshold. They estimated an optimal group contrast threshold of 50%.

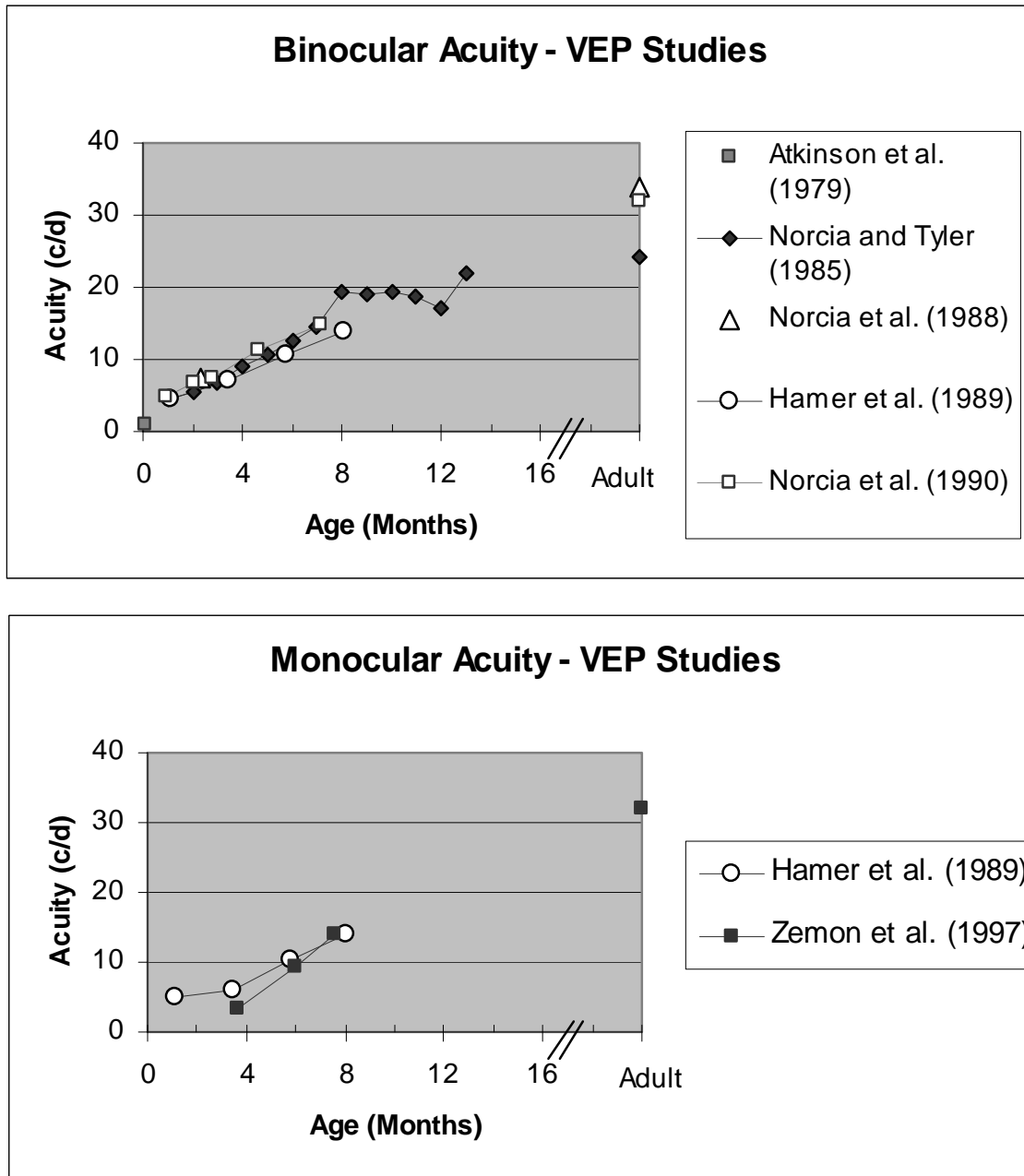


Figure 2. Comparison of binocular (top panel) and monocular (bottom panel) acuity estimates as a function of age from VEP studies reviewed in the text.

Norcia et al. (1988) compared adult and infant (10-week olds, n=10) contrast sensitivity for sinusoidal luminance gratings contrast-reversed at 6 Hz. They used a sweep VEP technique in which grating contrast increased in a series of 19 logarithmic steps that started well below threshold and ended above it. The VEP contrast sensitivity of 10-week-old infants (maximum average=200= 0.5% contrast) was close to that of the adults(maximum sensitivity=340) for spatial frequencies below about 1 c/deg. The infant contrast sensitivity function showed a 4.5 times faster fall off with increasing spatial frequency than the adult contrast sensitivity function. In a subsequent study, Norcia et al. (1990) assessed the development of contrast sensitivity in 48 infants between 2 and 40 weeks of age. They found that contrast sensitivity at low spatial frequencies developed rapidly during the first 10 weeks of age. Little development was evident after 10 weeks. Peak contrast sensitivity was about 200 compared to 450 for adults.

In summary, the anatomical, physiological as well as psychophysical studies reviewed indicate that there is extensive maturation of the visual system in human infants early in life, particularly during the first year of postnatal life. It is important to study the development of monocular as well as binocular visual functions (e.g. visual acuity, lateral interactions, contrast information processing). In some clinical conditions, such as in amblyopia, only one eye may be affected. Learning about the normal maturation of these visual functions in human infants could eventually lead to the development of useful diagnostic tools.

AMBLYOPIA

The term amblyopia is derived from the Greek word meaning dull or blunt vision (The American Heritage Dictionary of the English Language, 1971). Amblyopia is commonly referred to as “lazy eye”. It is the most common cause of visual loss in infants and young children, and it results when normal visual development is disturbed, leading to neural impairment (Levi, 2006). The incidence of amblyopia in the general population ranges from 2-4% (reviewed in Kiorpes & McKee, 1999 and Wu & Hunter, 2006), and it is probably higher in the medically underserved (Simons, 2005).

The first accurate clinical description of human amblyopia is attributed to Le Cat in 1713 (reviewed in Ciuffreda, Levi & Selenow, 1991). Almost 300 years later, we still have many gaps in our understanding of this condition and the mechanisms underlying it. Amblyopia is a complex condition with a wide array of deficits which may include: loss of Snellen, grating and vernier acuity, “loss of sensitivity to the contrast in a stimulus, distortions in the shape of a stimulus, some uncertainty about the position of a stimulus, motion deficits and an increase in the magnitude of the crowding effect or separation difficulty” (reviewed in Daw, 1998). The period during which any form of stimulus deprivation is effective in causing amblyopia ranges from a few months to seven or eight years of age (Daw, 1998; Harwerth, Smith III, Duncan, Crawford & von Noorden, 1986), and the conditions leading to functional amblyopia include strabismus, anisometropia, astigmatism, myopia, cataracts and other types of stimulus deprivation (Daw, 1998). In view of this information, the need to identify individuals at risk as early as possible so treatment can take place becomes apparent.

There are several forms of amblyopia, but they all have in common the symptoms of abnormal binocular vision, poor spatial vision (acuity and contrast sensitivity), or both. (Boothe et al., 1985). According to Wu and Hunter (2006), there are three main types of amblyopia classified on the basis of their cause: refractive amblyopia, strabismic amblyopia and deprivation amblyopia. Anisometropia (unequal refractive error in the two eyes) is a subclass under refractive amblyopia. Strabismus is the most common cause of amblyopia and involves a misalignment of the visual axes and cortical suppression of the deviating eye (Wu & Hunter, 2006).

Although amblyopia is usually classified into three main types (strabismic, anisometropic and deprivation amblyopia), the literature often describes more than three categories, and their boundaries are not clear cut; for example, “anisometropic amblyopia involves both deprivation and abnormal binocular interaction” (Simons, 2005). A great deal of the literature focuses on anisometropic and strabismic amblyopia or a combination of both.

McKee, Levi and Movshon (2003) classify amblyopes based on their pattern of visual function deficits rather than on the cause of the visual loss. They state that “strabismics” show modest losses in acuity combined with better-than-normal contrast sensitivity, “anisometropes” also have modest losses in acuity, but worse-than-normal contrast sensitivity, and “strabismic anisometropes” have very poor acuity and normal or subnormal sensitivity. The authors also indicate that strabismics have higher sensitivity, but lower acuity than anisometropes. According to Ciuffreda et al. (1991), the Snellen acuity of strabismic amblyopes may be more affected than their grating resolution.

Data from amblyopic monkeys suggest that no functional abnormalities exist earlier than the primary visual cortex, area V1 (Kiorpes & McKee, 1999; Kiorpes, 2006). There is evidence, however, that there are neural processing deficits further along the visual pathway in extrastriate visual areas (reviewed in Kiorpes, 2006; Levi, 2006).

The present study aims to contribute to the understanding of normal visual development with the expectation that this knowledge will help to clarify the mechanisms underlying amblyopia, and that in the future, the VEP could possibly be used as a screening or diagnostic tool for this disorder.

INHIBITION IN THE VISUAL SYSTEM

Inhibition is a very important phenomenon that is ubiquitous in the nervous system. Lateral inhibition was first reported by Ernst Mach in 1866 in his description of Mach bands, but it was mainly the work of Hartline in 1949 that introduced the idea of lateral inhibition in the visual system (reviewed in Von Békésy, 1967). Many cells in the brain are spontaneously active, and synaptic inhibition can determine their pattern of firing (“sculpturing role of inhibition”) (reviewed in Kandel & Siegelbaum, 2000). The development of cortical inhibition has been used to explain the transformation of low-pass into bandpass spatial frequency tuning (Wilson, 1988).

Gamma-aminobutyric acid (GABA) is a major inhibitory neurotransmitter in the brain (Kandel & Siegelbaum, 2000). Purpura, Girado and Grundfest (1957) demonstrated that GABA selectively blocks depolarizing, excitatory synapses when applied topically on the cerebral cortex of the cat. The surface-negative postsynaptic potential produced in the cortex by surface electric stimulation is reversed to a hyperpolarizing surface-positive

postsynaptic potential. Mitchell and Srinivasan (1969) provided some evidence that GABA is an important inhibitory transmitter in the cat visual cortex by showing that GABA is released during direct electrical stimulation of the lateral geniculate body and the cortex with stimuli which produced cortical inhibition. Moreover, Somogyi, Cowey, Halasz and Freund (1981) reported the presence of non-pyramidal (stellate cells) GABA-accumulating neurons in layers II and III of monkey visual cortex after injection of labeled GABA into layers V and VI.

Zemon, Kaplan and Ratliff (1980,1986) found that topical application of bicuculline (a GABA-A receptor blocker) over the cat visual cortex eliminates the P2 (P₁₀₀) positive wave, enhances the N1 (N₈₀) negative wave, while leaving the initial positive wave P1 (P₆₀) of VEPs nearly unaffected. In general, P₆₀ is associated with afferent activity from the LGN to the cortex and with early depolarization taking place deep in the cortex (most probably in layer IV), N₈₀ is linked to superficial depolarization and P₁₀₀ related to superficial hyperpolarization. The bicuculline-enhanced negative wave represents excitatory activity in the cortex, whereas the eliminated positive wave reflects an inhibitory process.

Increased cortical inhibition appears to be a major factor in triggering the onset of a critical period in primary visual cortex (Feldman, 2000). In a study (Fagiolini & Hensch, 2000) with mice lacking GAD65, a GABA-synthetic enzyme, it was found that these GAD65 knockout mice did not respond to brief monocular deprivation during the normal critical period. GAD65 knockouts retained ocular dominance plasticity into adulthood, but sensitivity to monocular deprivation could be induced by diazepam infusion, which enhances postsynaptic responses at inhibitory synapses. Murphy,

Beston, Boley and Jones (2005) studied the expression of glutamatergic receptors and GABA_A receptors in human primary visual cortex during the first five years of life. They suggest that the onset and closure of the critical period for visual plasticity is paced by mechanisms such as activation of N-methyl-D-aspartate (NMDA) receptors and GABA-mediated inhibition. The authors observed that during development of the human visual cortex, expression of GAD65 (found mainly in axon terminals) increased significantly by 1 to 3 years of age.

Primarily GABA_A and GABA_B receptors mediate synaptic inhibition in the central nervous system (Doiron, Longtin, Berman & Maler, 2000). In GABA_B receptor-mediated inhibition, activation of potassium channels results in large inhibitory postsynaptic potentials (IPSPs) and small changes in conductance. This type of inhibition, known as hyperpolarizing inhibition, is considered to be subtractive in nature because it diminishes the effect of the excitatory input linearly (Borg-Graham, Monier & Frégnac, 1998, Doiron et al., 2000). “In hyperpolarizing inhibition, negative and positive currents sum linearly to produce a net change in membrane potential” (Borg-Graham et al., 1998). In GABA_A receptor-mediated inhibition, opening of chloride channels causes an increase in membrane conductance while producing small shifts in membrane potential (chloride channels have a reversal potential close to the resting membrane potential). This type of inhibition (shunting inhibition or silent inhibition) has a nonlinear, divisive effect on the amplitude of the excitatory response (Borg-Graham et al., 1998; Doiron et al., 2000; Holt & Koch, 1997). If the membrane is in a depolarized state, opening of GABA_A-mediated chloride channels will cause re-polarization of the membrane.

Some research has also been devoted to the role of neural inhibition in the development of visual responses in infants. Sokol, Zemon and Moskowitz (1992) studied the development of lateral interactions in 84 human infants between 2 and 6 months of age using a windmill-dartboard stimulus. The stimulus consisted of a central disc surrounded by three concentric annuli, radially divided into light and dark segments. The segments of the central disc and second annulus were contrast-reversed sinusoidally at 4 Hz, while the contrast of the segments in the first and third annuli were held constant at either 0%, 30% or 100%. The contrast of the dynamic segments was set to either 30% or 100%. When static contrast was set to 0%, a partial windmill pattern resulted. When static and dynamic contrast was set to 30% or 100%, the windmill-dartboard pattern was created. Contrast-reversal of the partial-windmill pattern produced essentially identical waveforms for the two half-cycles of contrast reversal. The major component of the VEP was at twice the frequency of contrast reversal (the second harmonic component). Contrast reversal of the windmill-dartboard pattern produced an asymmetrical VEP waveform (Zemon and Ratliff, 1982). Based on previous study results in adults, the authors believe that a strong fundamental frequency response reflects short-range lateral inhibitory interactions, and attenuation of the second harmonic reflects long-range interactions. In their study, responses to the windmill-dartboard stimulus showed a dominant fundamental component in adults whereas an equal contribution from fundamental and second harmonic components was seen in 2-month old infants. There was a shift to a dominant first harmonic response by 6 months of age. Based on amplitude measures, they found that short-range interactions (the fundamental) were adult-like by 20 weeks of age, and long-range interactions (attenuation of second

harmonic) were adult-like by 8 weeks. However, phase data showed that both short- and long- range interactions are still immature at 20 weeks of age.

Grosec-Fifer, Zemon and Gordon (1994) expanded the work of Sokol et al. (1992) by studying the development of these lateral interactions over a range of temporal frequencies (1 Hz, 2 Hz, 4 Hz and 6 Hz) during the first six months of age. They found that the second harmonic attenuation was basically adult-like at all temporal frequencies for the majority of infants. However, the amplitude of the fundamental frequency component exhibited a low-pass temporal tuning function in infants that differed from the bandpass shape seen in adults.

Morrone and Burr (1986) studied cross-orientation inhibition in three infants over a period of 8 months. They obtained VEPs in response to sinusoidal gratings of variable contrast with no mask and with superimposed orthogonal or parallel high-contrast mask-gratings of different spatial frequencies. Stimulus and mask gratings were phase-reversed from 3 to 7 Hz. Contrast response functions at 3.5 months of age were virtually parallel for the no-mask, orthogonal-mask and parallel-mask conditions, with the latter two functions slightly shifted to the right. By 4 months, the orthogonal-mask function had shifted to the left coinciding with the no-mask curve. At 10 months of age, the curves had achieved a similar pattern as in the adults. The slope of the orthogonal-mask curve had changed, showing a greater amplitude reduction at higher than at lower contrasts. The authors indicated that this multiplicative (divisive) attenuation was not evident before 6 months of age.

Although there are different kinds of inhibition in the visual system (e.g. lateral inhibition, shunting inhibition, cross-orientation inhibition) which presumably are

GABA-mediated, in this study, the focus has been on lateral and shunting inhibition. The relationship between the different kinds of inhibition is still not clear.

Models of inhibition have been used to explain the responses of visual cells to contrast stimuli in monkeys as well as contrast response functions in humans. Carandini and Heeger (1994) proposed a model to characterize the responses of V1 simple cells in macaque monkey produced by sinusoidal gratings of different contrasts, orientations and spatiotemporal frequencies. Their model predicted that increasing stimulus contrast would result in an increase in membrane conductance which would also reduce the gain (amplitude saturation) and the time constant (phase advance) of the cell. Contrast gain control was first defined as amplitude compression and phase advance in cat retinal ganglion cells by Shapley and Victor (1978, 1981).

Zemon and Gordon (2006) used a biophysical model which incorporates a nonlinearity based on shunting inhibition to characterize the contrast gain control in contrast response functions obtained with the visual evoked potential in human adults. They used luminance-modulated bright or dark isolated checks to stimulate ON or OFF subsystems, and high or low contrast conditions to emphasize parvocellular or magnocellular pathway activity. Their proposed nonlinear model shows how the arrays of bright or dark isolated-checks might be processed independently by cortical neurons with low maintained discharge rates which receive input directly from ON or OFF cells, respectively, through the process of rectification. It has been shown that visual input signals increase the conductance of cortical neurons by increasing GABA_A-mediated shunting inhibition (Borg-Graham et al., 1998), which produces a decrease in cellular

temporal integration. Increases in stimulus contrast produce decreases in the time constant of the recipient cell.

Zemon and Gordon (2006) proposed that parallel ON and OFF streams enter V1 and remain segregated at their initial cortical projection sites: the spiny stellate neurons (simple cells) in layer IVc. The ON and OFF pathways also project to inhibitory interneurons (presumably GABAergic ones) in the cortex. These inhibitory interneurons average the signals from the ON and OFF fibers and hyperpolarize the spiny stellate simple cells lowering their maintained discharge rates to nearly zero spikes/second. Some of these GABAergic interneurons form synapses on distal locations on dendrites, and they probably mediate the subtractive (hyperpolarizing) inhibition that lowers the spontaneous discharge rate. Shunting inhibition may be mediated by other GABAergic interneurons which form synapses proximally near the cell body. According to the authors, the geometry of excitatory and inhibitory synapses acting on a neuron plays a key role on shunting inhibition. Activation of a nearby inhibitory synapse while an excitatory current is entering a cell, will cause part of this current to be shunted out of the cell before it can reach the axon hillock, the trigger zone for generation of action potentials. This effect is divisive in nature (Zemon & Gordon, 2006).

Borg-Graham et al. (1998) presented evidence that neurons in cat primary visual cortex show strong, transient shunting inhibition that increases the cell membrane conductance in response to visual stimuli. The timing of this change in conductance and its reversal potential point to the key connection to γ -aminobutyric acid (GABA_A) receptor-mediated synapses. Other membrane channels (associated with excitatory,

inhibitory, and leakage currents) are not thought to play a significant role in the stimulus-driven change in membrane conductance (Carandini and Heeger, 1994).

Zemon and Gordon (2006) assume that a “change in specific shunting conductance (g_s) of a neuron associated with stimulus modulation contributes to the VEP, and that this change is proportional to the sum of these stimulus-driven inhibitory signals (V_j) impinging on it”:

$$(g_s = \sum_{j=1}^n m_j V_j)$$

This shunting conductance is linearly related to contrast, or depth of modulation (D):

$$g_s = m(D - d_0)$$

“In these mathematical expressions, m is a coefficient of proportionality used as a parametric measure of the strength of this stimulus-driven shunting inhibition, and d_0 is threshold depth of modulation” (Zemon & Gordon, 2006). In their model, the time constant of the system (τ) is equal to:

$$\tau = \frac{C}{g_0 + g_s} = \frac{C}{g_0 + m(D - d_0)}$$

where C is the membrane capacitance, g_0 is the initial system conductance (without shunting inhibition) and g_s is the shunting conductance.

Increasing the shunting conductance, shortens the time constant of the system which results in contrast gain control.

GOALS OF THE STUDY

The specific goals of this project were:

- 1) To study the development of monocular acuity and contrast response functions in infants.
- 2) To determine if there are significant interocular differences during the development of monocular pathways.
- 3) To study phenomena in the visual evoked potential associated with neural inhibition: gain control in contrast response functions and low frequency fall-off in spatial tuning functions.

RESEARCH DESIGN AND METHODS

INSTRUMENTATION

The heart of the instrumentation is the ENFANT system (Neuroscientific Corp.). This is a complete system for stimulating the visual system, recording electrophysiological responses, and analyzing the data. The ENFANT system includes optically-isolated differential amplifiers, an analog-to-digital (A-D) converter, PC/AT compatible computer, one keypad interface for on-line control of the stimuli and data collection, the visual stimulator hardware, a Nokia monitor (Multigraph 447X) to be used as a stimulus display, and all the necessary software. Signals are amplified 10,000 times and filtered with a low- and a high-frequency cut-off of 0.5 Hz and 100 Hz respectively. The display has a mean luminance of 78 cd/m², and subtends visual angles of 20, 10 and 5 degrees at viewing distances of 57, 114 and 228 cm respectively.

DATA RECORDING TECHNIQUES

For all VEP recording sessions, the same three electroencephalogram (EEG) electrode placements were used. These placements are based on the International 10-20 System (Jasper, 1958), and standard gold-cup electrodes are attached to these midline sites. One electrode at Oz (positive lead; located at 10% of the distance from theinion to the nasion) is referenced to another one at Cz (negative lead; at 50% of the distance from theinion to the nasion) with a floating ground electrode placed at Pz (at 30% of distance from theinion to the nasion).

DATA COLLECTION PROCEDURE

Visual stimuli were presented on a TV-like monitor in a dark room. Infants sat on their parent's laps to view the stimuli. The electrical activity of the brain was recorded using electrodes attached to the scalp with water-soluble paste. Spatial frequency or contrast sweeps were performed during a single one hour session (which included time for breaks). Infants viewed the stimuli first monocularly, and if time permitted infants viewed the stimuli binocularly. During monocular testing, one eye was patched with a soft non-transparent eye patch, like the ones routinely used by ophthalmologists during the treatment of amblyopia. The order of eye tested was varied. In approximately half of the infants, the right eye was tested first; in the other half the left eye was tested first.

One person attracted the infant to focus on the stimuli with the aid of a small toy dangling on the center of the stimulus screen. Another person ran the stimuli and recorded the data files in a computer and a datasheet. Stimuli lasted a few seconds. The Infant System was used to record Visual Evoked Responses stimulating each eye separately or both eyes at the same time.

ANALYSIS OF THE VEP

The VEP is the constituent of the EEG that is synchronized to the temporal modulation of the visual stimulus. Conventional *steady-state* VEPs elicited by sinusoidal modulation signals are analyzed by a discrete Fourier transform, performed on a microcomputer, to extract the amplitudes and phases of frequency components that occur at multiples of the stimulus frequencies. These are the only driven components in the VEP response to such an input signal. The first harmonic component, or fundamental, is

at the stimulus frequency. The second harmonic component is at twice this frequency, and so on. In the analysis, response phase is defined relative to a cosine reference signal.

The T^2_{circ} statistic (Victor & Mast, 1991) which is specifically designed for the analysis of variability of Fourier components was used to estimate 95% confidence limits. Fourier components may be considered as vectors in the (x,y)-plane (x and y represent the cosine and sine components of the response). Individual estimates of the Fourier component form a cluster in the complex plane. The center of the cluster is a pooled estimate of the response, and the scatter of the cluster describes the reliability of that estimate. The T^2_{circ} statistic is applied to determine whether an observed set of Fourier components is consistent with random fluctuations alone, or whether the set of observations implies that a signal is present within a 95% confidence level.

SPECIFIC EXPERIMENTS

Steady-state VEPs, were recorded and analyzed in this study. The sweep VEP technique was used. Sweep VEPs have been used previously to assess the maturation of spatial mechanisms in infants (Norcia & Tyler, 1985; Zemon et al., 1997). Application of sweep VEPs makes data collection more efficient. Use of this technique allows the investigator to test infants in a single session with a battery of stimuli. Three different stimulus conditions were used: Spatial Frequency Sweep, Contrast Sweep-15 cycles per screen, and Contrast Sweep-30 cycles per screen. The stimulus parameters are summarized below (Table 1).

SPATIAL FREQUENCY SWEEP. This stimulus consisted of horizontal square-wave gratings contrast-reversed with a 7.5 Hz square-wave modulation (See Table 1 and Fig. 3). The duration of a single run was 6.4 seconds. The spatial frequency of the reversing grating decreased in six octave steps (0.8, 1.5, 3.0, 6.0, 12, 24 c/d at 114 cm and 1.6, 3.0, 6.0, 12, 24, 48 c/d at 228 cm). Infants viewed these gratings monocularly and binocularly at 114 cm from the stimulus monitor. Children viewed them at 114 cm and/or 228 cm. Most adults viewed them at 228 cm, although some viewed them at 114 cm. For some infants ten runs were collected, and for some only five runs. The amplitude (in μV) and phase (in degrees) of the second and fourth harmonic were computed and plotted versus spatial frequency (in c/deg). The T^2_{circ} statistic developed by Victor and Mast (1991) was used to obtain a measure of noise. The T^2_{circ} statistic defines a circular confidence limit around the tip of the mean response amplitude vector. The signal-to-noise ratio (S/N) is determined from the ratio of the response amplitude to the radius of the confidence circle. If the confidence region encompasses the origin, the S/N is less than one, and the response is not considered to be significantly different from noise. A two-sample T^2_{circ} statistic was also used to test for significant differences between corresponding monocular responses at each spatial frequency (see Zemon et al., 1997). Grating acuity was estimated from linear interpolation (see figure 5, right eye panel) between two successive points (lower confidence limits) on the amplitude versus spatial frequency plots, and it corresponds to the spatial frequency at which the signal-to-noise measure is equal to 1 (where the interpolation line hits the zero microvolt level) (Zemon et al., 1997).

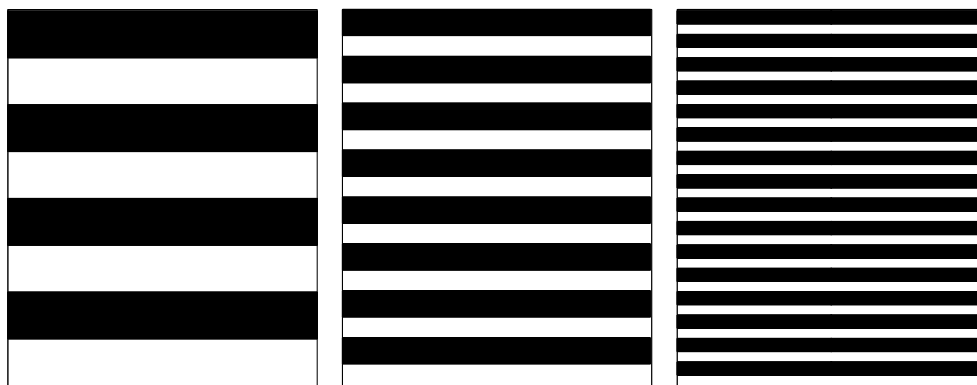


Figure 3. Example of a spatial frequency sweep used as stimulus.

CONTRAST SWEEP (15 CYCLES PER SCREEN). The stimulus consisted of horizontal square-wave gratings contrast reversed at 7.5 Hz (See Table 1 and Fig. 4). This stimulus contains 15 cycles of the stimulus per screen. One cycle is a pair of black and dark bars. The spatial frequency of the gratings was 0.75 c/deg, 1.5 c/deg and 3.0 c/deg at a distance of 57 cm, 114 cm and 228 cm respectively. Infants and children viewed these gratings monocularly at either 57 cm or 114 cm. Some adults viewed the stimuli at any of these distances; some adults viewed them at all three distances. The duration of a run was 8.5 seconds. Ten runs were collected from each participant. The contrast of the reversing gratings increased in 8 octave steps (0, 1, 2, 4, 8, 16, 32, 64 %). The amplitude and phase of the second harmonic were computed and plotted against depth of modulation. Response phase is defined as the initial phase of the second harmonic plus any contrast-dependent phase shift (Zemon & Gordon, 2006). The T^2_{circ} statistic (Victor & Mast, 1991) was used to obtain a measure of noise. A model that incorporates shunting inhibition developed by Zemon and Gordon (2006) was used to fit jointly the amplitude and phase of the responses to obtain estimates of electrical conductance, shunting inhibition and integrative time constants in the visual system.

According to the model, the total time constant of the system (τ) is determined by the following:

$$\tau = \frac{C}{g_0 + g_s} = \frac{C}{g_0 + m(D - d_0)}$$

where C = the capacitance of the membrane, g_0 = the initial conductance of the system, g_s = shunting conductance, D = the depth of modulation, d_0 = threshold depth of modulation and m = shunting inhibition coefficient.

Increasing the shunting conductance, decreases the time constant of the system which results in contrast gain control (amplitude compression and phase advance) with increases in contrast (Zemon & Gordon, 2006).

CONTRAST SWEEP (30 CYCLES PER SCREEN). The stimulus consisted of horizontal square-wave gratings contrast reversed at 7.5 Hz (See Table 1 and Fig. 4). This stimulus contains 30 cycles of the stimulus per screen. The spatial frequency of the gratings was 1.5 c/deg, 3.0 c/deg and 6.0 c/deg at a distance of 57cm, 114 cm and 228 cm respectively. Infants and children viewed these gratings monocularly at 57 cm only. Adults viewed them at all three distances. The duration of a single run was 8.5 seconds, and ten runs were collected. The contrast of the reversing gratings increased in 8 octave steps (0, 1, 2, 4, 8, 16, 32, 64%). The amplitude and phase of the second harmonic were computed and plotted versus depth of modulation. The T^2_{circ} statistic (Victor & Mast, 1991) was used to obtain a measure of noise. The model of shunting inhibition developed by Zemon and Gordon (2006) was also used to fit the data.

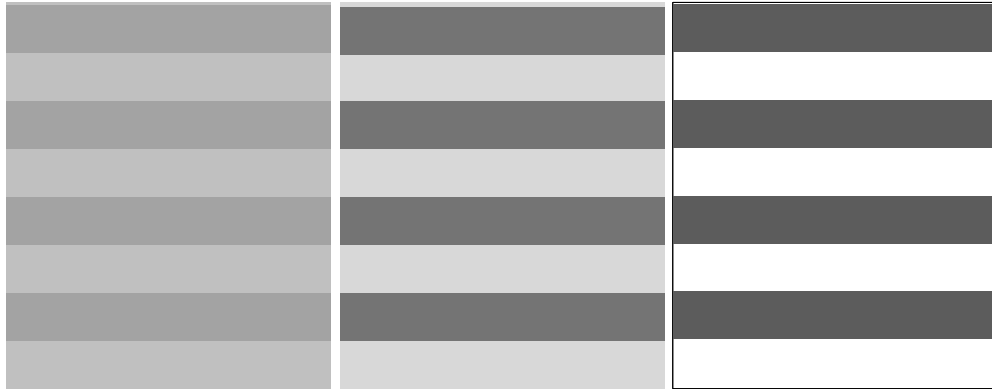


Figure 4. Example of a contrast sweep pattern used as stimuli.

STIMULI	TEMPORAL FREQ.	DURATION	DISTANCE	SPATIAL FREQUENCY	CONTRAST
Spatial Frequency Sweep	7.4976 Hz	6.40 s	114 CM	0.8, 1.6, 3.0, 6.0, 12, 24 c/d	100%
			228 CM	1.5, 3.0, 6.0, 12, 24, 48 c/d	100%
Contrast Sweep 15 cycles per screen	7.4976 Hz	8.50 s	57 CM	0.75 c/d	0,1, 2, 4, 8, 16, 32, 64%
			114 CM	1.5 c/d	0,1, 2, 4, 8, 16, 32, 64%
			228 CM	3.0 c/d	0,1, 2, 4, 8, 16, 32, 64%
Contrast Sweep 30 cycles per screen	7.4976 Hz	8.50 s	57 CM	1.5 c/d	0,1, 2, 4, 8, 16, 32, 64%
			114 CM	3.0 c/d	0,1, 2, 4, 8, 16, 32, 64%
			228 CM	6.0 c/d	0,1, 2, 4, 8, 16, 32, 64%

Table 1. Summary of parameters for the stimuli used in this study.

PARTICIPANTS

Sixty two normal male and female human infants ranging from 10 to 31 weeks of age were recruited for this study. Seven children, one adolescent and 17 adults were also tested. Most infants were recruited through The New York Presbyterian Hospital-Weill Medical College of Cornell University. Some infants, children and adults were also

recruited by word of mouth or through notices posted on bulletin boards near the Psychology Department Offices at Hunter College. This research was approved by the Institutional Review Boards at Hunter College and The New York Presbyterian Hospital-Weill Medical College of Cornell University. This project also complied with HIPAA (Health Insurance Portability and Accountability Act) privacy regulations. Written consent was obtained from all adults and parents of all infants and children tested. In addition, oral consent was obtained from children younger than 12 years of age, and written assent forms from children older than 12 years of age.

SPATIAL FREQUENCY SWEEP PARTICIPANTS

Forty two infants were tested with the spatial frequency sweep at 114 cm (See Table 2):

- 1) On 19 of these infants we tried to obtain 5 runs. On 17 of these 19 infants, we obtained 5 runs for each eye (OD = Oculus Dexter = right eye, and OS = Oculus Sinister = left eye), and on 13 of the 19 infants we also obtained 5 runs under binocular viewing (OU = Oculus Unitas = both eyes).
- 2) On 23 out of the 42 infants, we tried to obtain ten runs. On 19 of these 23 infants, we obtained ten runs for each eye (OD and OS) (on two infants we were only able to collect data for one eye, and on the other two we obtained 5 runs for one eye and ten runs for the other), and on 13 out of the 23 infants, we also obtained 10 runs under binocular viewing. Five children were tested: three at 114 cm and three at 228 cm. Seventeen adults were tested at 114 cm (n=4) and/or 228 cm (n=16). Ten trials were obtained from all children and adults.

CONTRAST SWEEP (15 CYCLES/ SCREEN) PARTICIPANTS

Twenty two infants, a 10-year old, a 14-year old and nine adults were tested with this contrast sweep at 57 cm (Table 2). We obtained monocular data (both OS and OD) from 20 of the infants and binocular data from 15 of the infants. No binocular data were obtained from the other participants. We also collected monocular data for one infant, three children, one adolescent and eleven adults and binocular data on 2 adults at 114 cm. One adolescent and 7 adults viewed the patterns monocularly at 228 cm.

CONTRAST SWEEP (30 CYCLES/ SCREEN) PARTICIPANTS

Monocular data were collected from six infants (out of seven), two children, one adolescent and 9 adults at 57 cm (Table 2). One infant only yielded binocular data. Ten adults and one adolescent were tested monocularly at 114 cm, and six adults and one adolescent at 228 cm.

STIMULI	DISTANCE	INFANTS		CHILDREN	ADOLESCENTS	ADULTS
Spatial Frequency	114 CM	42	5 RUNS: 19	3	0	4
			10 RUNS: 23			
	228 CM		0	3	1	16
Contrast 15 c/screen	57 CM		22	1	1	9
	114 CM		1	3	1	11
	228 CM		0	0	1	7
Contrast 30 c/screen	57 CM		7	2	1	9
	114 CM		0	0	1	10
	228 CM		0	0	1	6

Table 2. Number of participants recruited per stimulus condition and distance used.

RESULTS

SPATIAL FREQUENCY SWEEP

Of the 23 infants in whom we tried to obtain 10 runs, 21 yielded reliable data for the right eye and 19 for the left eye. Monocular second harmonic amplitude and phase data were obtained from these participants. There are noticeable differences between the responses obtained from infants and adults. In general, infant response amplitudes are larger than adult responses, and the peak of the function is shifted to lower spatial frequencies in infants. Many infants lack the low frequency fall-off characteristic of adult spatial functions. Infant phase plots are relatively flat or show a slight phase lag, whereas adults show steep phase lags with increases in spatial frequency. These observations agree with published results (Zemon et al., 1997).

Monocular vector means from ten sweeps for the amplitude and phase data of a 16-week old as a function of spatial frequency are displayed in Figure 5. The peak of the response is around 1.5 c/deg. Amplitude at the peak of the function is around 10 μ V for each eye. Response amplitudes to the last two spatial frequencies tested in this infant were not above the noise level. The lower confidence limits in the amplitude chart for the left eye have been plotted between the points of 6 c/deg and 12 c/deg in Figure 5 and Figure 6 to illustrate the method of interpolation used in this study. The point at which this line hits the zero microvolt level constitutes the acuity limit. Acuties for the right and left eyes were 6.63 c/deg and 8.28 c/deg respectively in this 16-week old. Phase error bars are not plotted when the corresponding error bars in the amplitude plot hit the zero microvolt level. The phase for the lowest spatial frequency tested (0.8 c/deg) is around

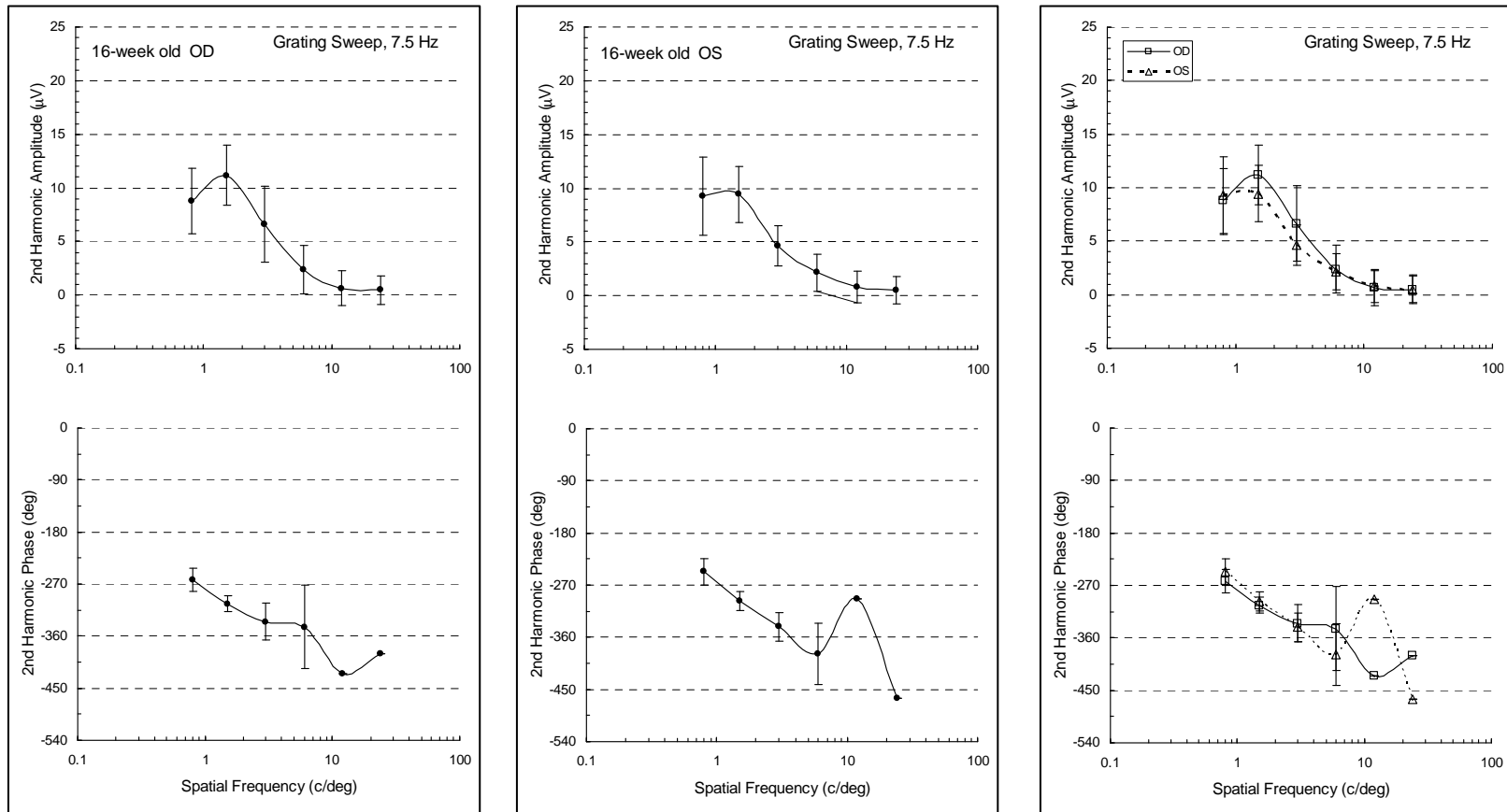


Figure 5. Monocular amplitude and phase of the second harmonic response versus spatial frequency for a 16-week old tested at a viewing distance of 114 cm. Symbols represent the vector means of the responses calculated from ten swept-parameter runs. Error bars indicate the 95% confidence intervals for the vector-averaged responses. The last panel shows responses from the right and left eye superimposed. (OD=right eye; OS=left eye).

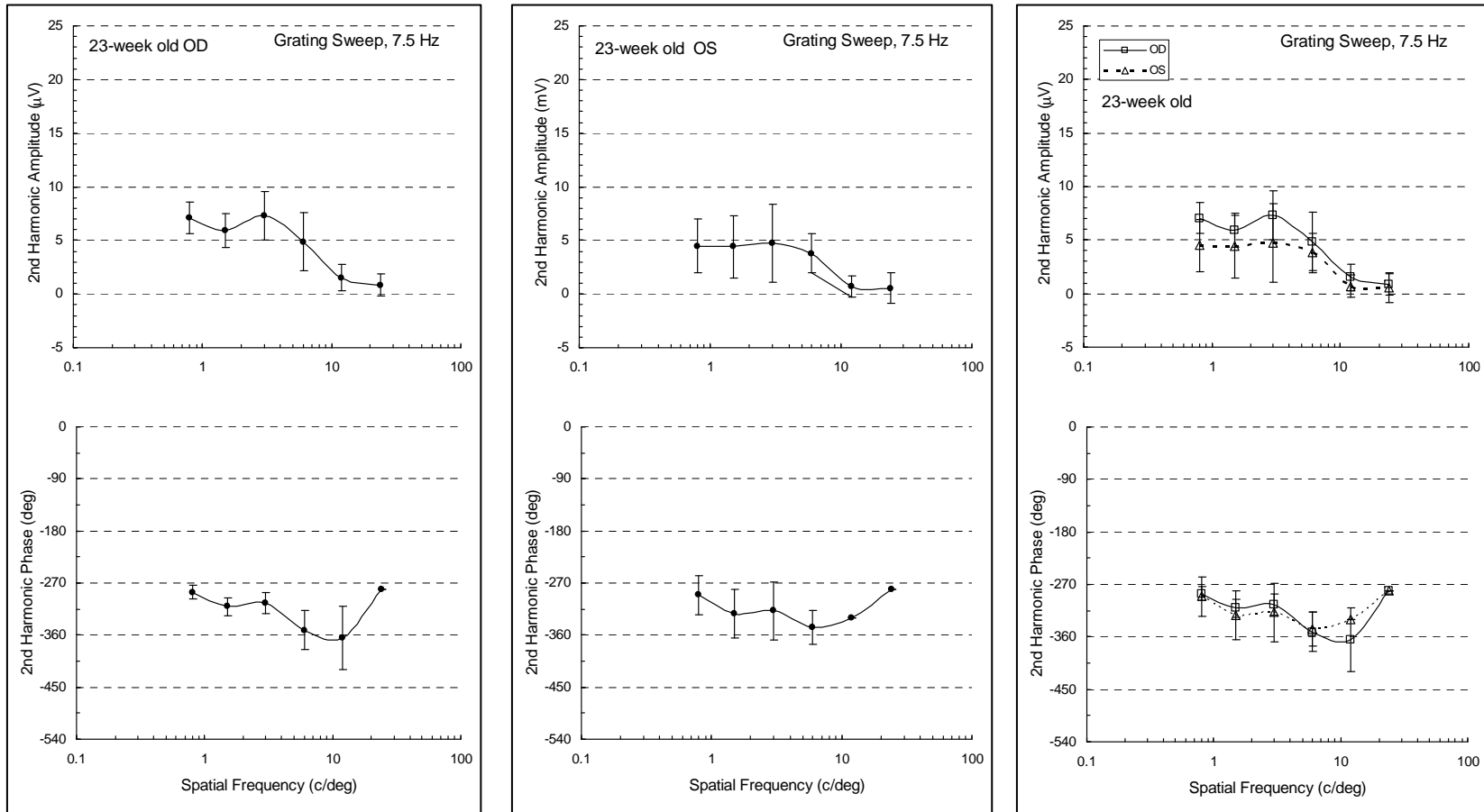


Figure 6. Monocular amplitude and phase of the second harmonic response versus spatial frequency for a 23-week old tested at a viewing distance of 114 cm (For details see text and legend in Figure 5).

-270° in both eyes. The phase plot is relatively flat with a slight phase lag that spans approximately a 90° range when taking into account only the significant phases. There were no significant differences between the eyes as assessed by the two-sample T^2_{circ} statistic.

Data from a 23-week old are illustrated in Figure 6. The peak of the response occurs at about 3.0 c/deg. Amplitude at the peak of the function is around 7 μV and 5 μV for the right and left eyes respectively. There were no significant differences between the eyes. Acuities for the right and left eyes were 19.54 c/deg and 11.21 c/deg respectively. The phase plot again is relatively flat and ranges from -270° to -360°.

Figure 7 shows data from a 4-year old. Peak amplitude is around 5 μV and occurs at about 3 c/deg. The phase of the response to the lowest spatial frequency tested (0.8 c/deg) is close to or at -180°. Acuities were 10.35 c/deg and 11.41 c/deg for the right and left eyes. The 6 c/deg data point was significantly different between the eyes at the 0.01 level. A significance level of 0.01 was selected for all comparison tests between the eyes to avoid a magnified Type I error rate associated with multiple significance tests.

The responses of an adult 30 years of age are illustrated in Figure 8. The peak amplitudes are around 4 and 2 μV for the right and left eye respectively, and they occur at about 6 c/deg. There were no significant differences between the eyes. The phases of the responses to the four lowest spatial frequencies tested were in the -90° to -360° range. There is a steep phase lag with increasing spatial frequency. The data yielded acuity estimates of 22.19 c/deg (right eye) and 17.61 c/deg (left eye).

Figure 9 shows monocular data for a 24-week old, a 2-year old and a 23-year old. The response amplitudes as well as the response variability in the 24 week-old infant are

larger than in the 2-year old or the 23-year old. The phase plots for the infant and the 2-year old are relatively flat compared to the steep phase lag displayed by the adult as spatial frequency increases. There is a relative phase advance which is clearly observed in the two older observers when compared with the infant data. Amplitude at the peak was 7.38 μV , 3.18 μV and 3.59 μV in the 24-week old, the 2-year old and the 23-year old respectively.

	Spatial Frequency	OD			OS		
		n	r	P	n	r	p
10 RUNS	0.8	16	0.4475	*	14	0.3393	NS
	1.5	18	0.5602	***	14	0.4453	NS
	3	16	0.5917	***	15	0.6552	****
	6	16	0.4973	**	10	0.3129	NS
	12	4	0.5953	NS	1		
	24	2			2		
5 RUNS	0.8	23	0.4579	**	23	0.3432	NS
	1.5	24	0.5976	****	29	0.5469	****
	3	25	0.5228	****	26	0.6601	****
	6	19	0.5299	***	19	0.3677	NS
	12	4	0.7612	NS	3		
	24	2			1		

* $p < .05$, ** $p < .025$, *** $p < .01$, **** $p < .005$, one tail, NS=not significant

Table 3. Pearson correlations between phase and age for the right (OD) and left (OS) eyes by each spatial frequency tested at 114 cm. Correlations were not obtained in cases where the value of n was 3 or less.

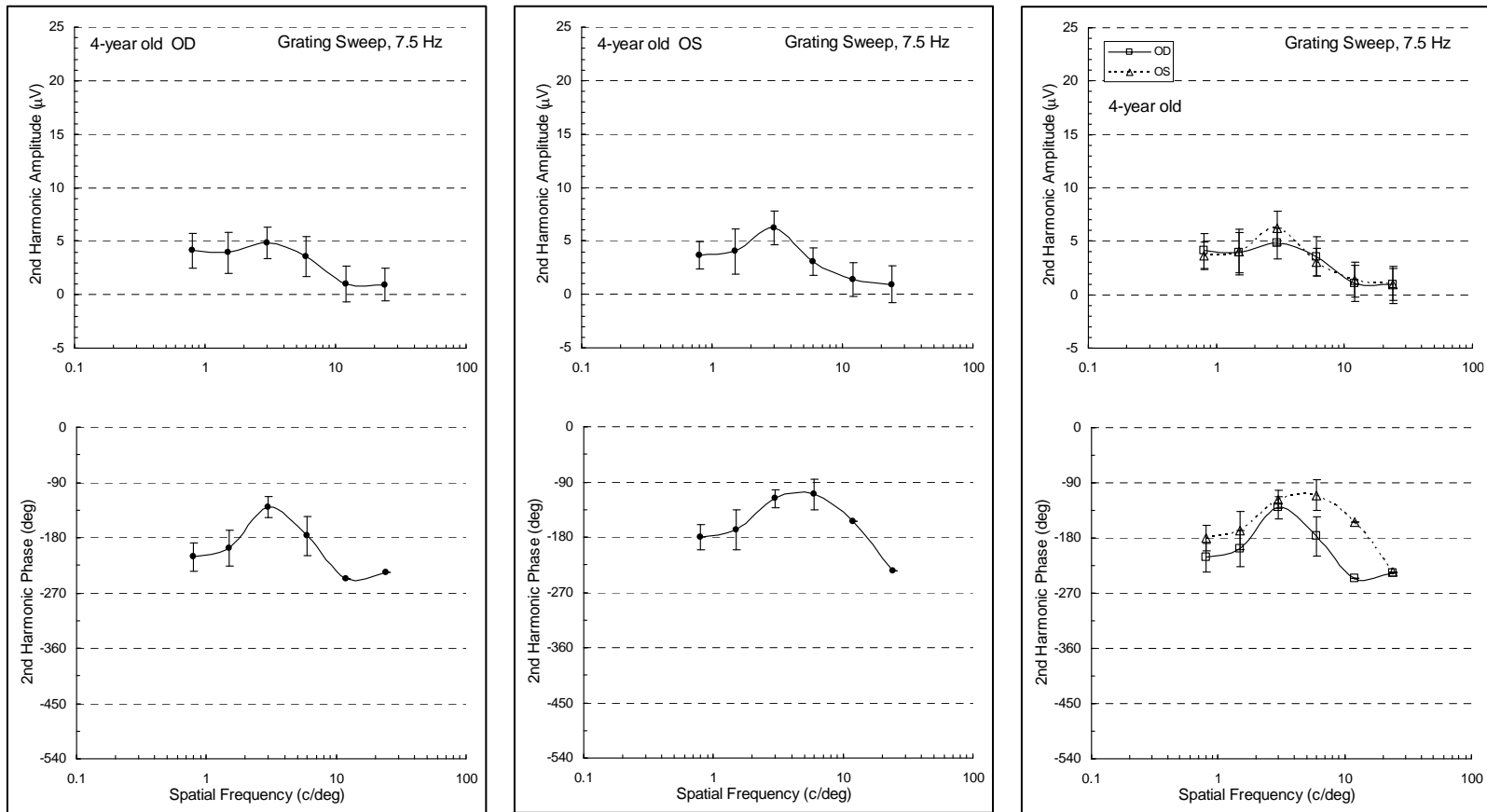


Figure 7. Monocular amplitude and phase of the second harmonic response from a 4-year old tested at a viewing distance of 114 cm. (For details see text and legend in Figure 5).

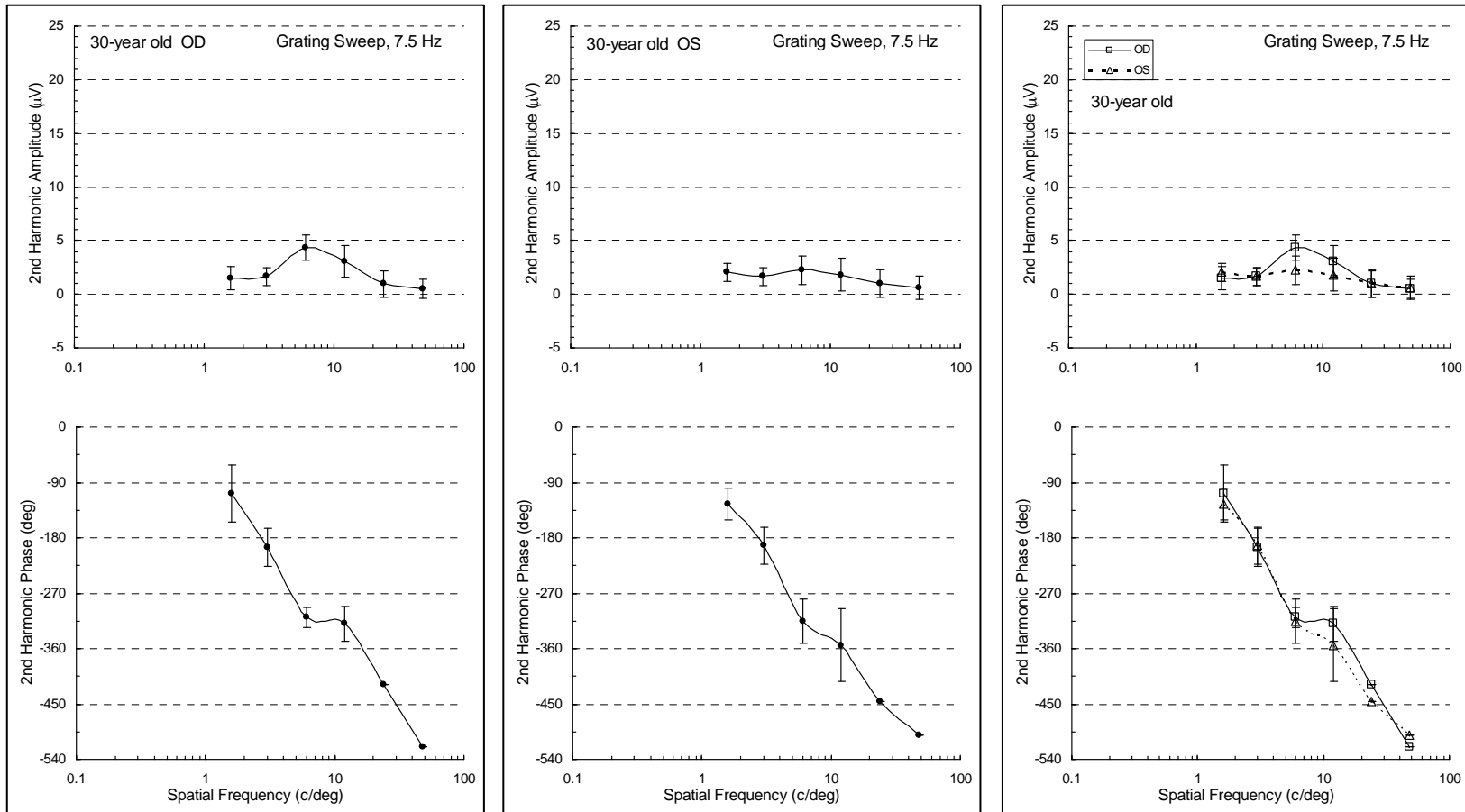


Figure 8. Amplitude and phase of the second harmonic response from a 30-year old adult tested at a viewing distance of 228 cm (For details see text and legend in Figure 5).

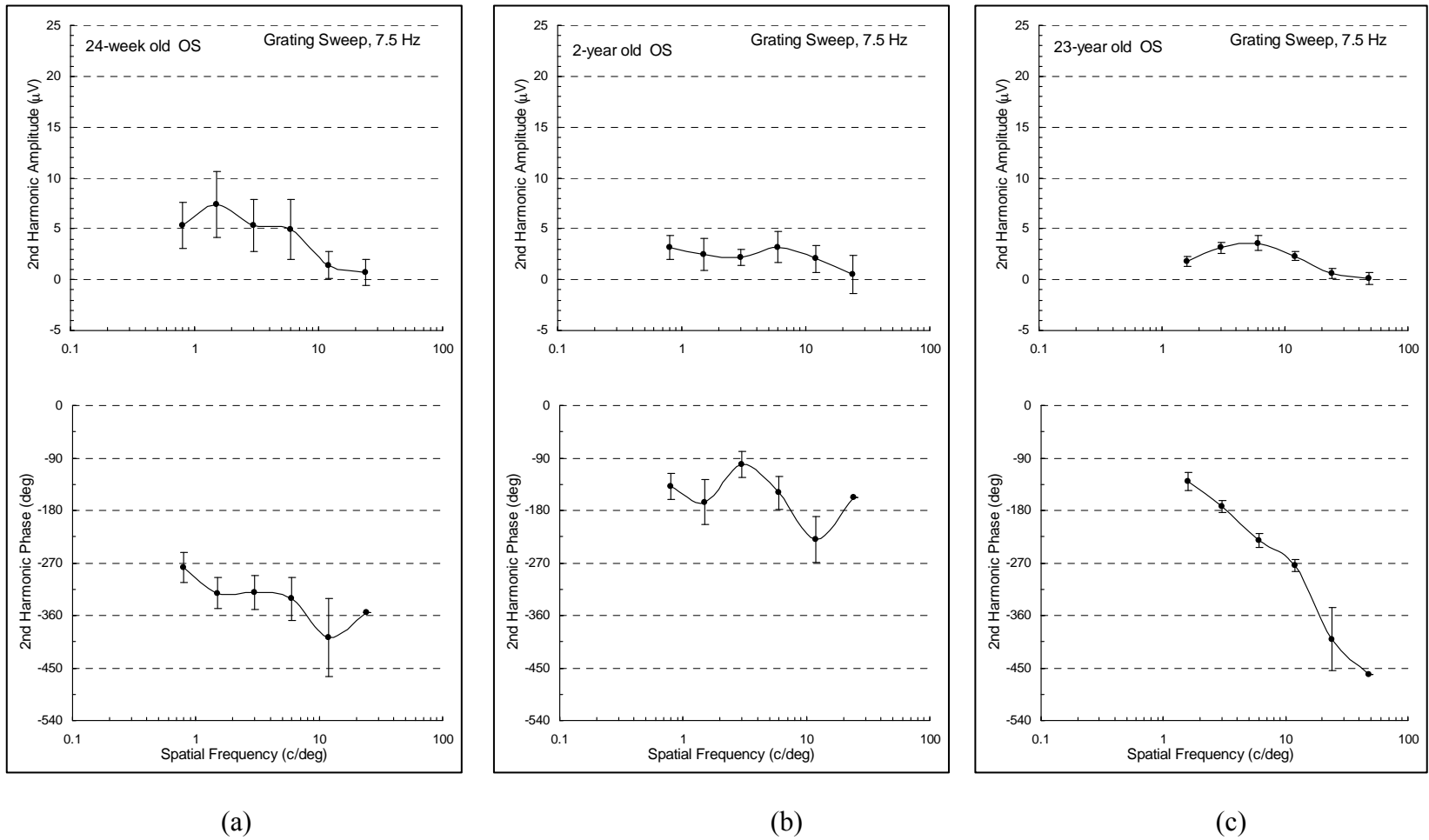


Figure 9. Monocular amplitude and phase of the second harmonic response from a (a) 24-week old tested at a viewing distance of 114 cm, a (b) 2-year old tested at 114 cm, and a (c) 23-year old adult tested at 228 cm. (See legend in Figure 5)

The peak occurred at 1.5 c/deg in the 24-week old and at 6 c/deg in the 2- and 23-year olds. The estimated acuities were 14.04 c/deg in the 24-week old, 16.13 c/deg in the 2-year old and 29.08 c/deg in the 23-year old.

Figure 10 and Figure 11 display scatter plots of phase of the response to the contrast-reversing gratings for the right eye (OD) and left eye (OS) respectively as a function of age for each of the spatial frequencies tested. Participants were tested at 114 cm, and each point represents the mean phase calculated from ten runs. Only phases of responses that were above the noise level were plotted. In column (a), data for infants, children and adults is presented on a logarithmic scale. Infant phases are around -300° whereas adult phases are around -180° at 0.8 c/deg, the spatial frequency at which the difference between adult and infant phases is more pronounced (see also Figures 15a and 15b). As spatial frequency increases, the difference between adult and infant mean phase values decreases, and the number of reliable data points from infants and adults also decreases. The children have similar phases as the adults at the two lowest spatial frequencies. In Figures 10 and 11, column (b), infant phases are plotted on a linear scale. The range of ages is 16 through 31 weeks. There is a positive correlation between phase and age, which is significant for the lowest four spatial frequencies tested in the right eye, but significant only for the 3.0 c/deg in the left eye (see Table 3). Nonetheless, there is a general trend of increasing phase values with increasing age.

Figures 12 and 13 display scatter plots of phase of the response (for the right and left eye respectively) as a function of age for participants in whom only five as well as participants in whom ten runs were obtained. In these figures, however, each point represents the mean phase calculated from the first five runs only. Testing distance was

also 114 cm. The pattern of the scatter plots is similar to the pattern in Figures 10 and 11. Phase values decrease with increasing spatial frequency. There are positive significant correlations between phase and age 16 through 31 weeks for the 0.8, 1.5, 3.0 and 6.0 c/deg spatial frequencies in the right eye and for 1.5 and 3.0 c/deg in the left eye (see Table 3). Figure 14 shows the scatter plots of phase versus age for children and adults tested at 228 cm. Plots in column (a) display data for the right eye, and plots in column (b) data for the left eye. The data for both eyes are very similar. Adult mean phases decrease from about -138° at 1.6 c/deg to about -362° at 24 c/deg (Figure 15). At 48 c/deg, there are no phase data points for the adults because they did not have significant responses at that high spatial frequency.

In Figure 15, a missing graph bar indicates that no significant data were obtained for that condition. A graph bar without an error bar indicates significant phase data for a single observer. The decrease in phase values with increasing spatial frequency is steeper in adults than in infants, particularly in the lowest four spatial frequencies (Figure 15 a, b, c, d). In general, adult phases start around -180° at 0.8 c/deg and run to about -300° at 6 c/deg, infant phases start around -300° at 0.8 c/deg and end about -360° at 6 c/deg. Adults show a relative phase advance with respect to the infants which can be inferred from the less negative phase values seen in adults. Figure 15 (panels e and f) shows right eye and left eye data for adults tested at 228 cm. In these figures, there is an appreciable decrease in phase value with increasing spatial frequency.

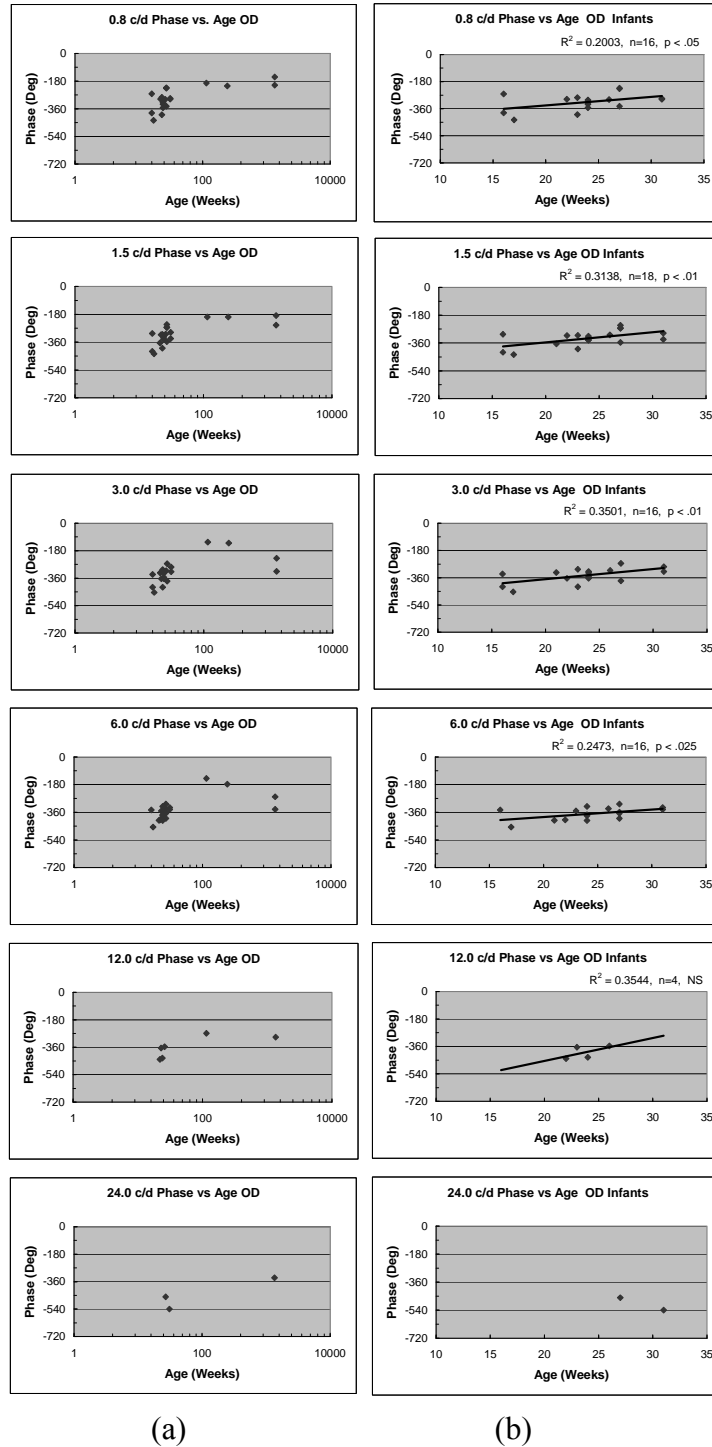


Figure 10. Scatter plots of phase (in degrees) versus age (in weeks) for the right eye (OD) by each of the spatial frequencies tested at 114 cm (ten-runs analysis). Plots in column (a) include infants and adults. Plots in column (b) display data for the same infants only. Symbols represent the mean phases calculated from ten swept-parameter runs (NS=not significant). Regression lines are drawn for infant plots in column (b).

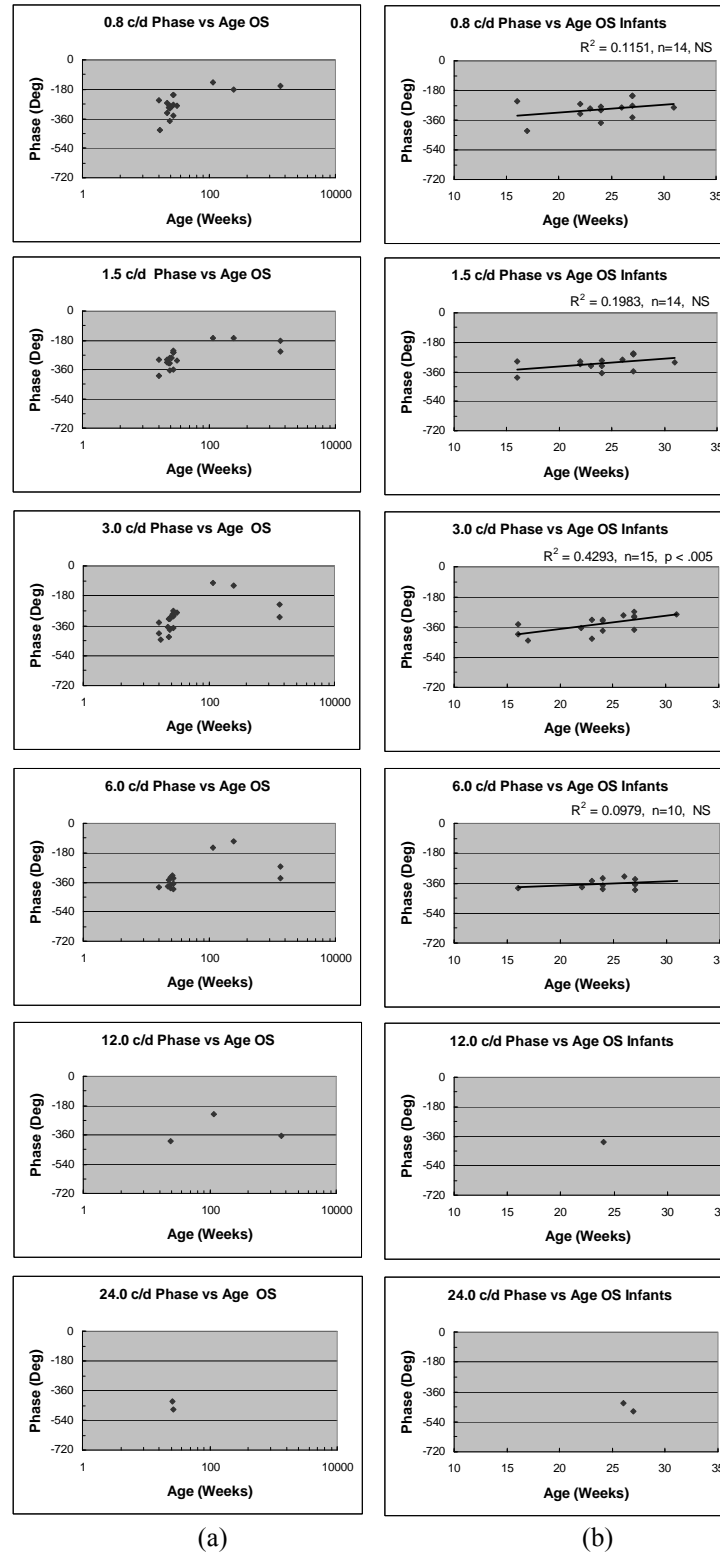


Figure 11. Scatter plots of phase (in degrees) versus age (in weeks) for the left eye (OS) by each of the spatial frequencies tested at 114 cm (ten-runs analysis). (For details see text and legend in Figure 10).

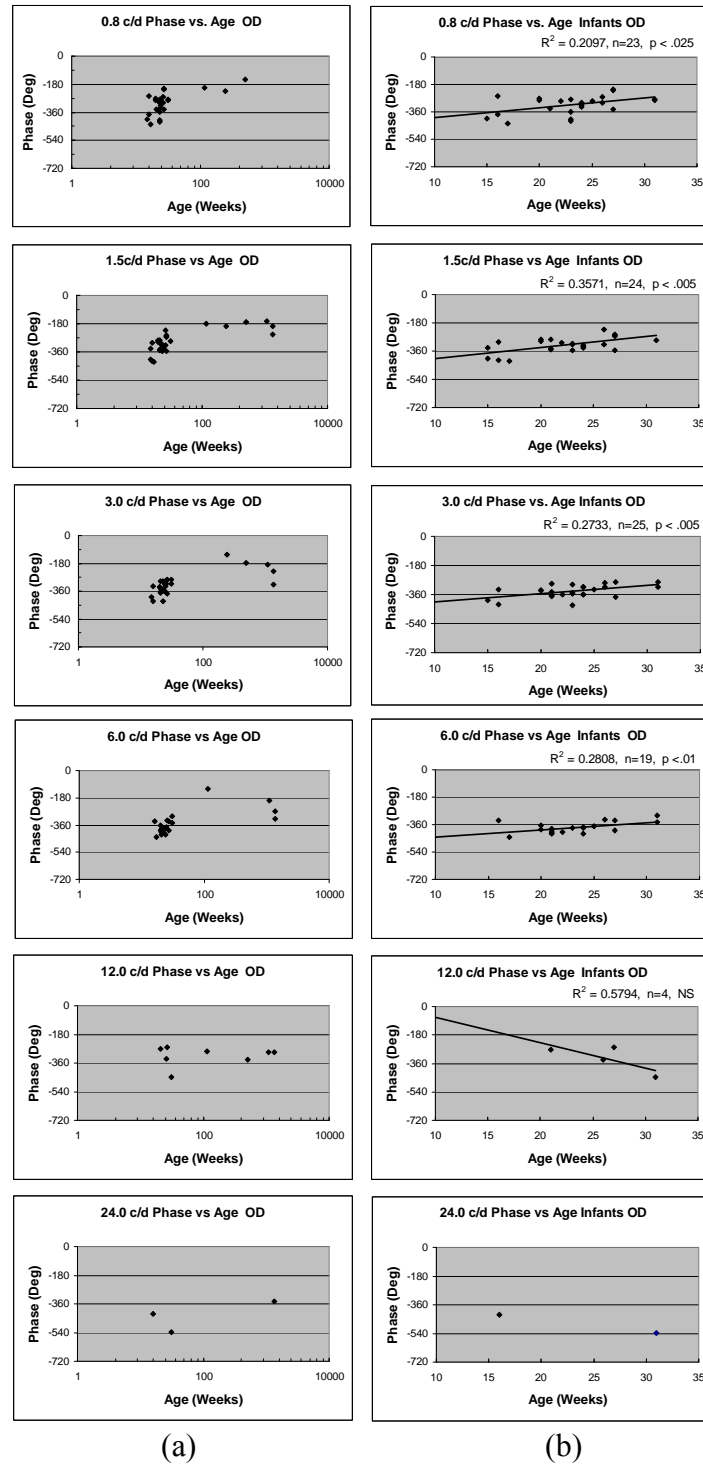


Figure 12. Scatter plots of phase (in degrees) versus age (in weeks) for the right eye by each of the spatial frequencies tested at 114 cm (five-runs analysis). Plots in column (a) include infants and adults. Plots in column (b) display data for infants only. Symbols represent the mean phases calculated from five swept-parameter runs. Regression lines are drawn for infant plots in column (b).

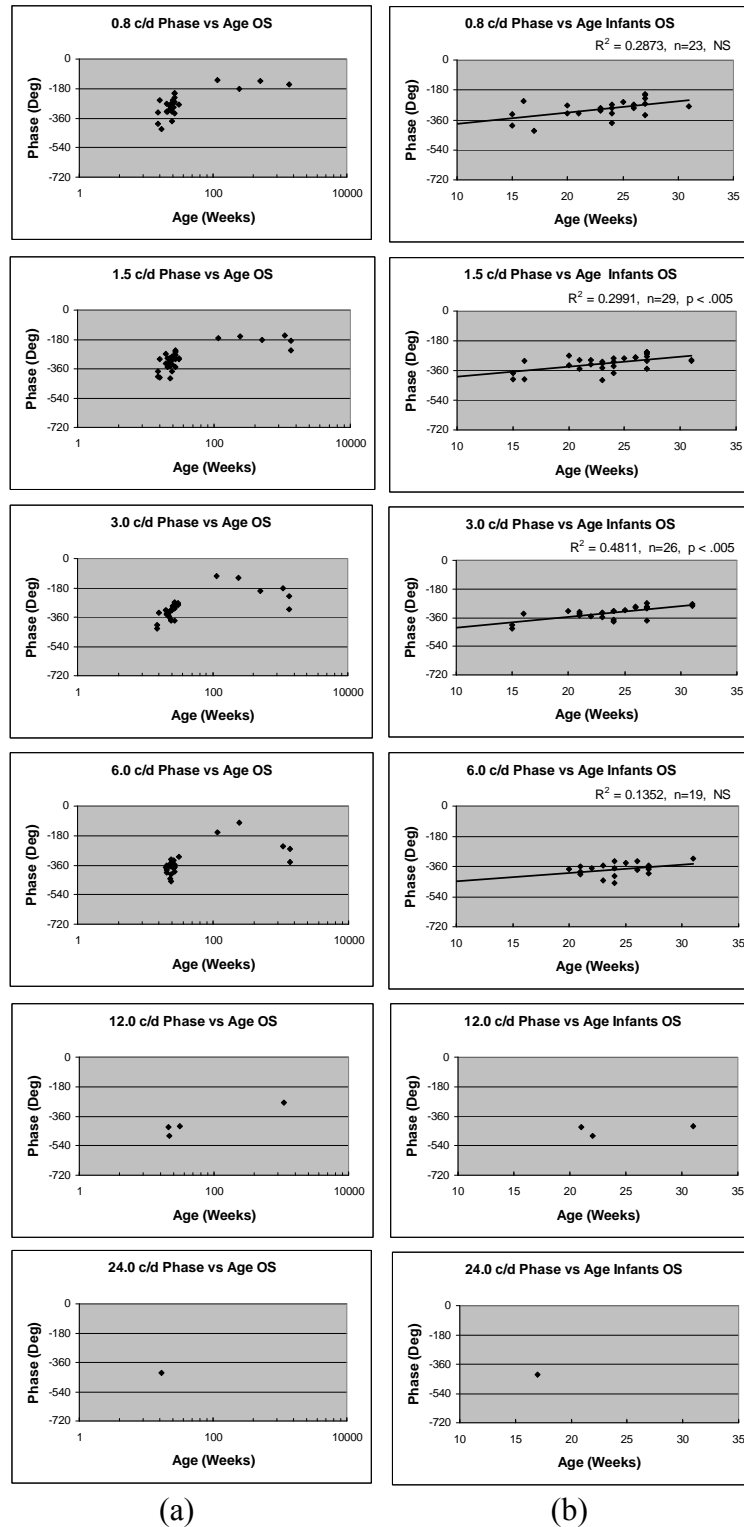


Figure 13. Scatter plots of phase (in degrees) versus age (in weeks) for the left eye by each of the spatial frequencies tested at 114 cm (five-runs analysis). (For details see text and legend in Figure 12).

Figures 16 and 17 show scatter plots of acuity versus age. Figure 16 displays results obtained from vector averaging of ten swept parameter runs whereas figure 17 shows results from the five-runs analysis. There is considerable inter-individual variability in the measure of acuity. Slightly better acuities are observed for the right eye and for binocular testing than for the left eye. There is a trend of higher acuity with increasing age in the 15 through 31 week range which is significant only for the right eye in the five-runs analysis ($r=0.446$, $n=29$, $p < .01$, one tail).

Figure 18 shows scatter plots of acuity versus age in children and adults. There is a lot of inter-individual variability in adults as well. In general, adult acuities are better than in the infants (Figures 16 and 17). Binocular acuity is better than monocular acuity. Table 4 shows binocular and monocular mean acuities in infants and adults for the five- and ten-runs analyses only for participants in which both monocular and binocular data was obtained. Table 5 shows monocular mean acuities in infants and adults for the five- and ten-runs analyses for all participants regardless of whether binocular acuity was obtained or not.

In the ten-runs analysis, mean acuity in infants is about 11 c/deg and 8 c/deg for the right and left eye respectively; mean acuity for the right and left eye is around 20 c/deg in adults (Figures 19 and 20, panels a and c; Tables 4 and 5). Binocular mean acuity in infants is $10.73 (\pm 0.71 \text{ SEM})$ and $11.8 \text{ c/deg} (\pm 1.25 \text{ SEM})$ in the five- and ten-runs analyses respectively (Table 4). In adults, binocular mean acuity is $29.79 \text{ c/deg} (\pm 3.74 \text{ SEM})$ and $40.37 \text{ c/deg} (\pm 1.49 \text{ SEM})$ in the five- and ten-runs analyses respectively (Table 4). There is a small significant difference between the eyes in infants only in the ten-runs analysis (Table 6: $t=3.05$, $n=15$, $p < .005$, one tail). There are also significant

differences between left eye and binocular acuity in the five- and ten-runs analysis (five runs: $t=2.57$, $n=18$, $p=.01$, one tail; ten runs: $t=2.74$, $n=8$, $p=.016$, one tail). A significant difference is also observed between the right eye and binocular acuity but only in the five- runs analysis ($t=1.95$, $n=17$, $p=.035$, one tail) (Figure 19 and Table 6). In adults, there are no significant differences between the eyes. There are significant differences between monocular and binocular acuity in the ten-runs analysis (right eye versus binocular acuity: $t=11.92$, $n=5$, $p=.00014$, one tail; left eye versus binocular acuity: $t=8.10$, $n=5$, $p=.00064$, one tail) and the five-runs analysis (only left eye vs. binocular acuity: $t=2.494$, $n=6$, $p < 0.05$, one tail) (Figure 20 and Table 6).

A measure of low spatial frequency fall-off was calculated by obtaining the log value of the ratio of the signal to noise (S/N) value at the 0.8 c/deg spatial frequency and the S/N value at the peak of the response. A zero value in this measure indicates the peak is at the lowest spatial frequency tested (no low spatial frequency fall-off). The more negative the log value, the higher the gap between the S/N value at the 0.8 c/deg spatial frequency and the S/N at the peak indicating a more bandpass spatial tuning characteristic. Figure 21 shows scatter plots of the log value of this ratio as a function of age. Figure 23 displays bar graphs of the mean log value of the ratio in infants and adults. Mean infant values ranged from -0.16 to -0.25, whereas adult mean values ranged from -0.44 to -0.70 depending on the number of runs and eye tested. The log of the ratio of the S/N value at 1.5 c/deg (1.6 c/deg) to the S/N value at the peak was also calculated because for most of the adults this was the lowest spatial frequency tested. Scatter plots (Figure 22) as well as bar graphs (Figure 24) for this measure were also obtained.

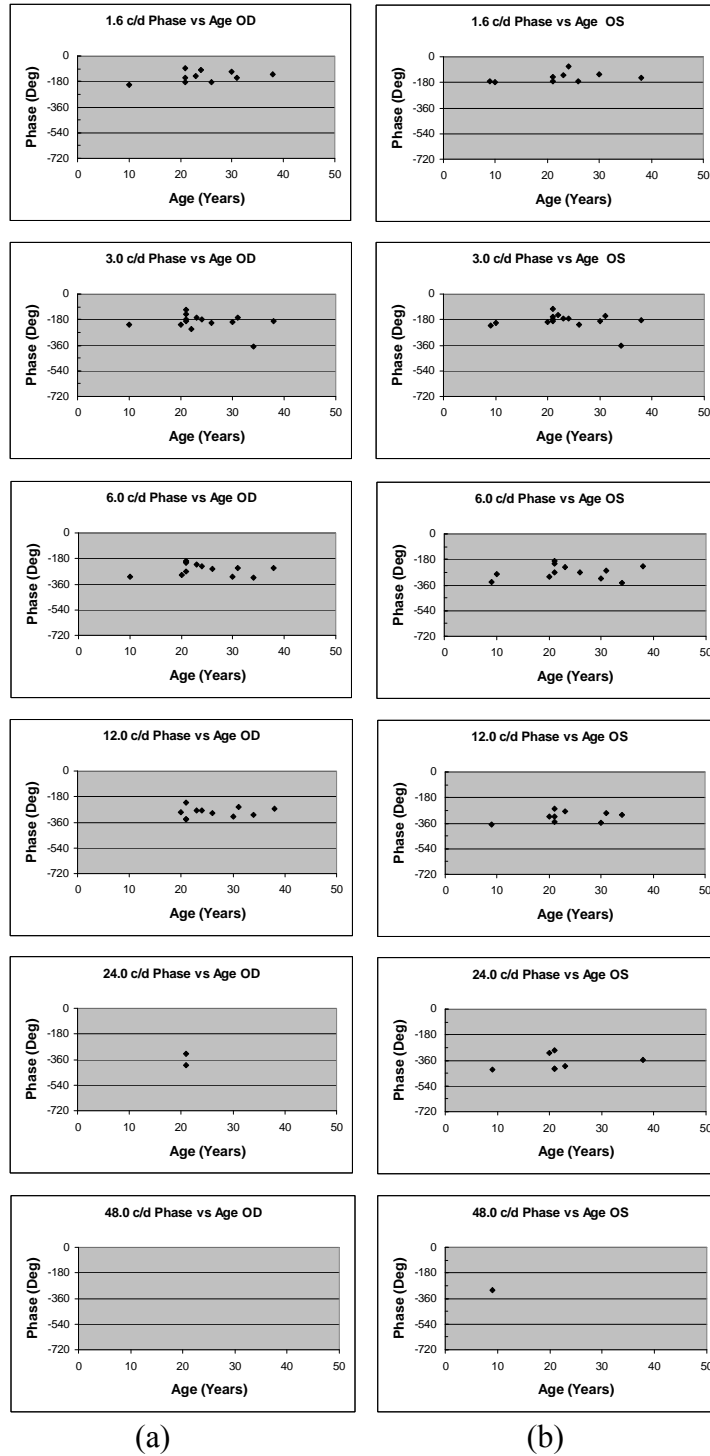


Figure 14. Scatter plots of phase (in degrees) versus age (in years) for the right (column a) and left eye (column b) by each of the spatial frequencies tested at 228 cm. Plots include data for children and adults. No infants were tested at this distance. Symbols represent the mean phases calculated from ten swept-parameter runs.

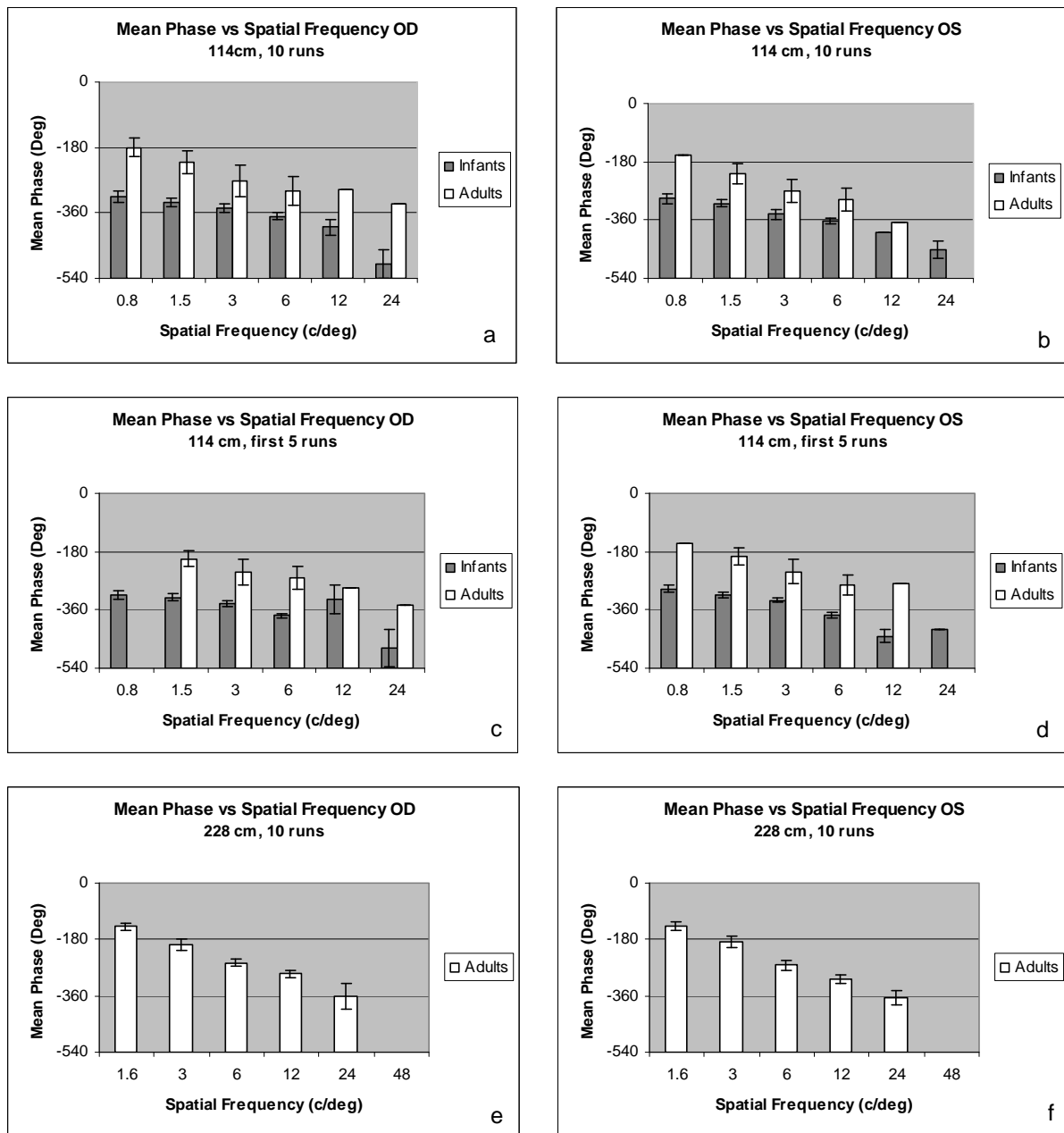


Figure 15. Mean phase versus spatial frequency bar graphs. White bars represent adults; gray bars correspond to infants. Panels a, c and e show results obtained for the right eye, and panels b, d and f show results from the left eye. Testing distance and number of runs is indicated in each panel.

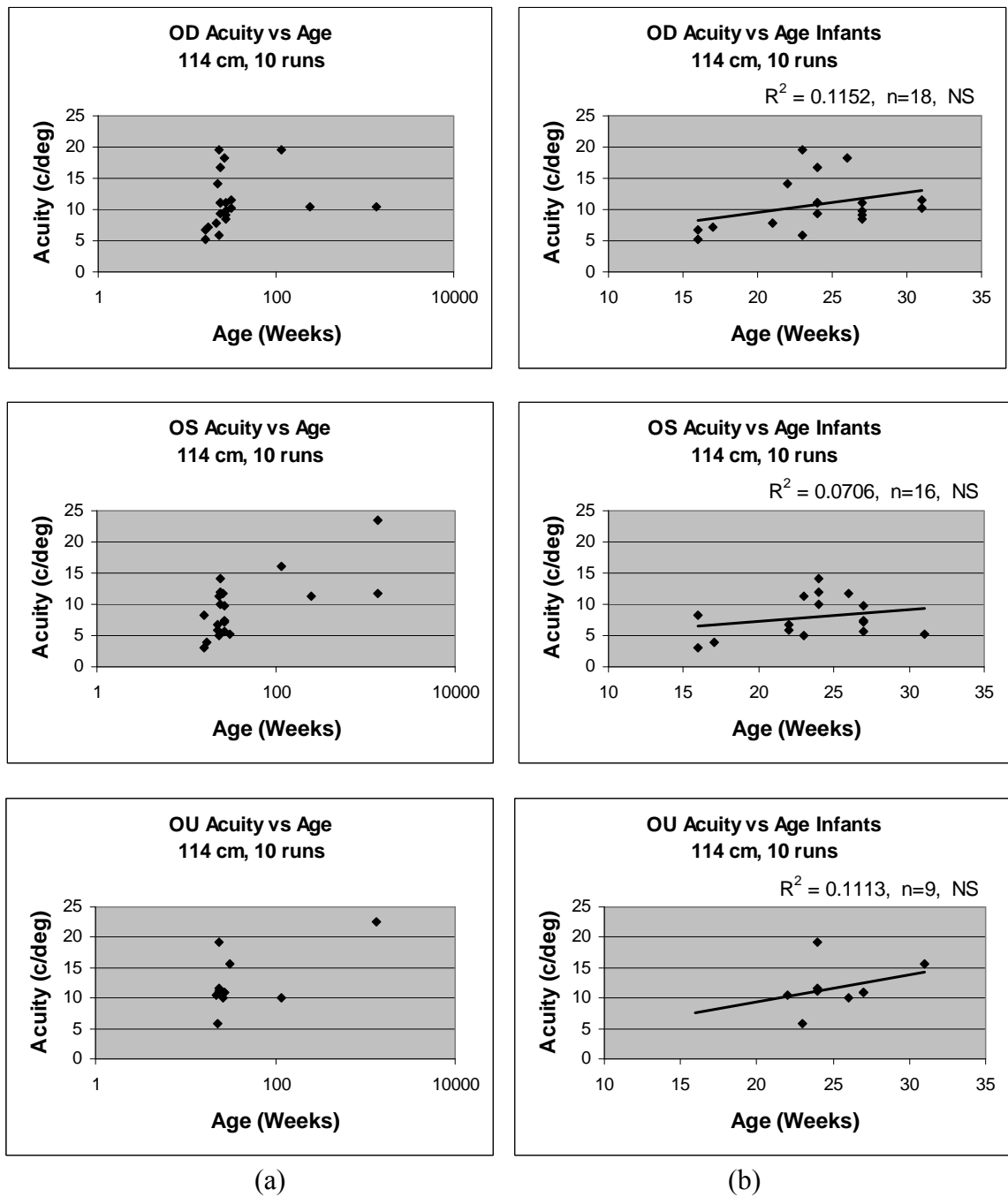
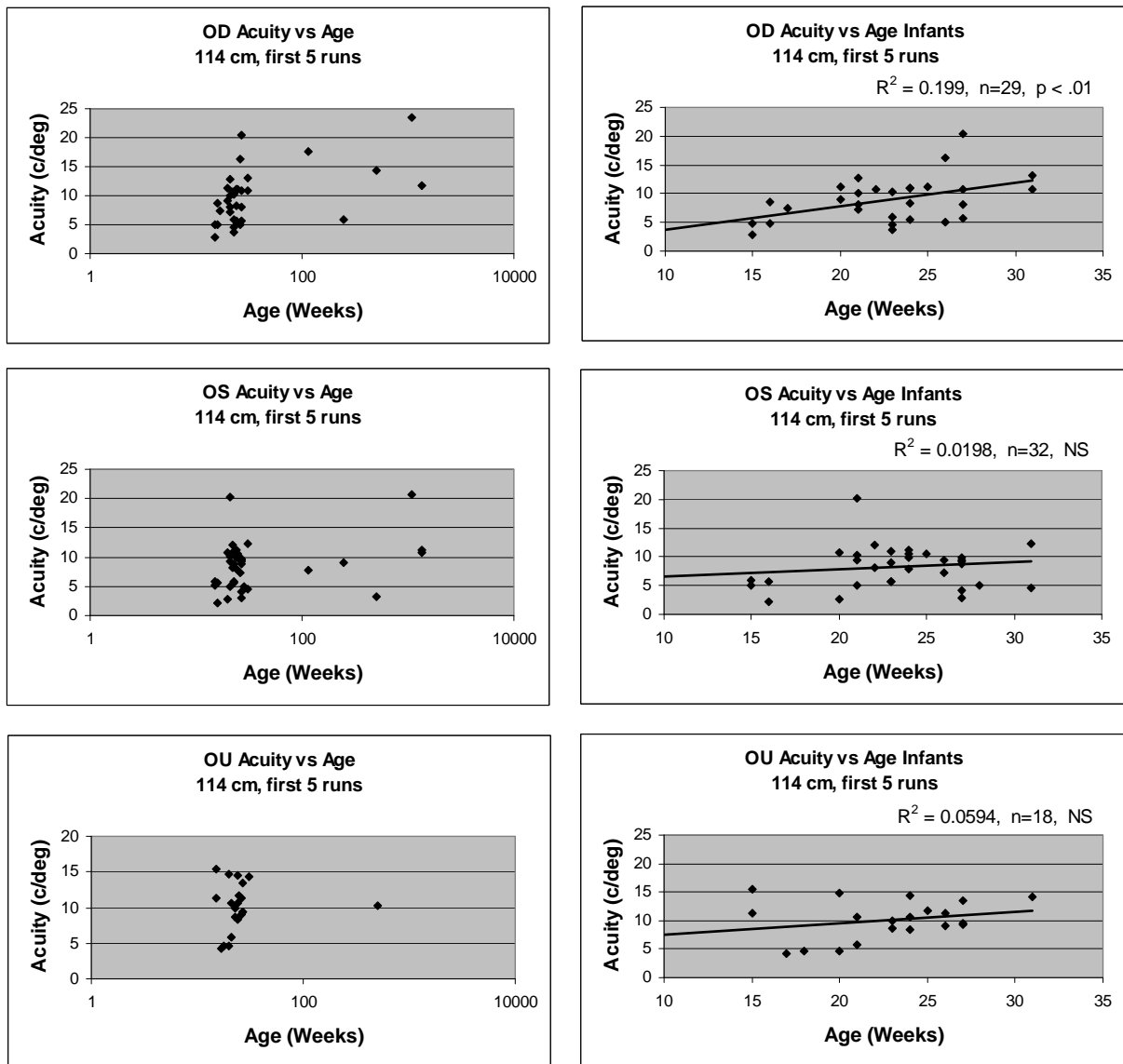


Figure 16. Scatter plots of acuity versus age (ten runs). Column (a) displays acuity for all participants on a logarithmic scale for the right eye (top), left eye (middle), and binocular condition (bottom). Column (b) shows acuity data for infants on a linear scale. Each symbol represents monocular mean acuity for a single observer calculated from ten swept-parameter runs. Regression lines are drawn for infant plots in column (b).



(a)

(b)

Figure 17. Scatter plots of acuity versus age (five runs). Column (a) displays acuity for all participants on a logarithmic scale for the right eye (top), left eye (middle), and binocular condition (bottom). Column (b) shows acuity data for infants on a linear scale. Each symbol represents monocular mean acuity for a single observer calculated from five swept-parameter runs. Regression lines are drawn for infant plots in column (b).

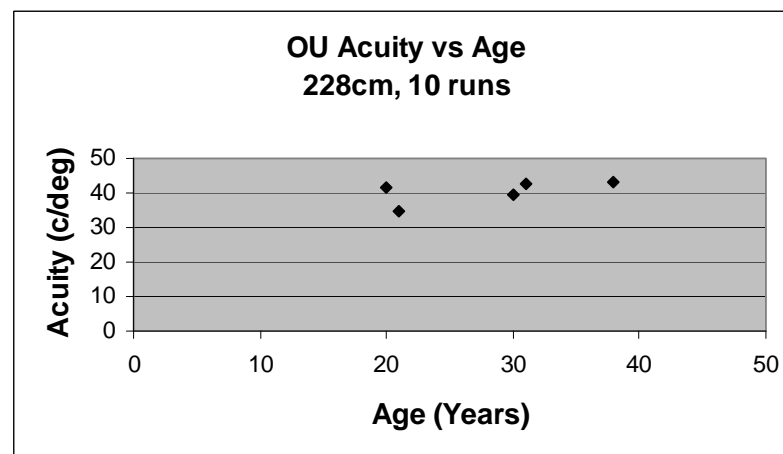
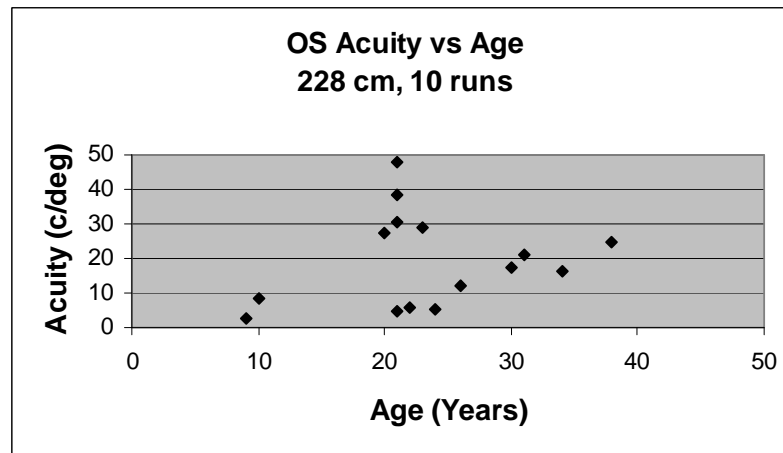
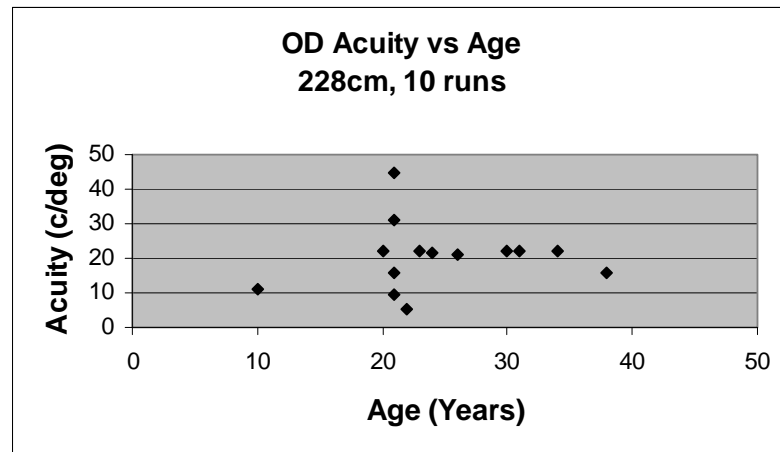


Figure 18. Scatter plots of acuity versus age for the right eye (top), left eye (middle) and both eyes (bottom) in children and adults tested at 228 cm.

		BINOCULAR VERSUS MONOCULAR MEAN ACUITIES					
		INFANTS			ADULTS		
		OD	OS	OU	OD	OS	OU
5 runs	n	17	18	18	6	6	6
	Acuity	8.55	8.46	10.73	19.32	16.79	29.79
	SEM	± 0.86	± 0.57	± 0.71	± 3.56	± 3.18	± 3.74
10 runs	n	9	8	9	5	5	5
	Acuity	11.05	8.31	11.80	18.38	19.16	40.37
	SEM	± 1.17	± 1.17	± 1.25	± 2.52	± 3.94	± 1.49

Table 4. Binocular and monocular mean acuities in infants and adults for the 5-runs and 10-runs analyses only for participants in which binocular data was obtained.

		MONOCULAR MEAN ACUITIES			
		INFANTS		ADULTS	
		OD	OS	OD	OS
5 runs	n	29	32	14	13
	Acuity	8.94	8.17	20.04	18.12
	SEM	± 0.72	± 0.64	± 2.85	± 1.70
10 runs	n	18	16	12	12
	Acuity	10.72	7.93	22.52	22.94
	SEM	± 0.97	± 0.80	± 2.49	± 3.72

Table 5. Monocular mean acuities in all infants and adults for the 5-runs and 10-runs analyses.

		COMPARISONS					
		INFANTS			ADULTS		
		OD-OS	OU-OD	OU-OS	OD-OS	OU-OD	OU-OS
5 runs	n	27	17	18	13	6	6
	t	0.27	1.95	2.57	0.9	1.86	2.49
	p	0.4	0.035	0.01	0.19	< 0.1	< 0.05
10 runs	n	15	9	8	12	5	5
	t	3.05	0.44	2.74	-0.16	11.92	8.1
	p	< 0.005	0.34	0.016	0.44	< 0.00014	< 0.00064

Table 6. Number of participants (n), t values (t), and probabilities (p) for monocular and binocular comparisons (one tail) in infants and adults. (OD: right eye, OS: left eye, OU: both eyes)

In this case, mean infant values ranged from -0.08 to -0.12, and adult values ranged from -0.16 to -0.35 at 114 cm. Mean adult values at 228 cm were around -0.4. In every condition, adults have more negative log values of the S/N ratio than infants which indicates adults have a more pronounced low spatial frequency fall-off.

Figure 25 displays frequency distribution plots showing where the peak of the function occurs based on amplitude values (left column) and on signal to noise values (left column). In general, in infants, the peak of the spatial tuning function occurs more often at 1.5 and at 3 c/deg. In adults, the peak of the function occurs more often at 3 or 6 c/deg. In some infants the peak occurred at 0.8 c/deg; no adults had a peak at this low spatial frequency.

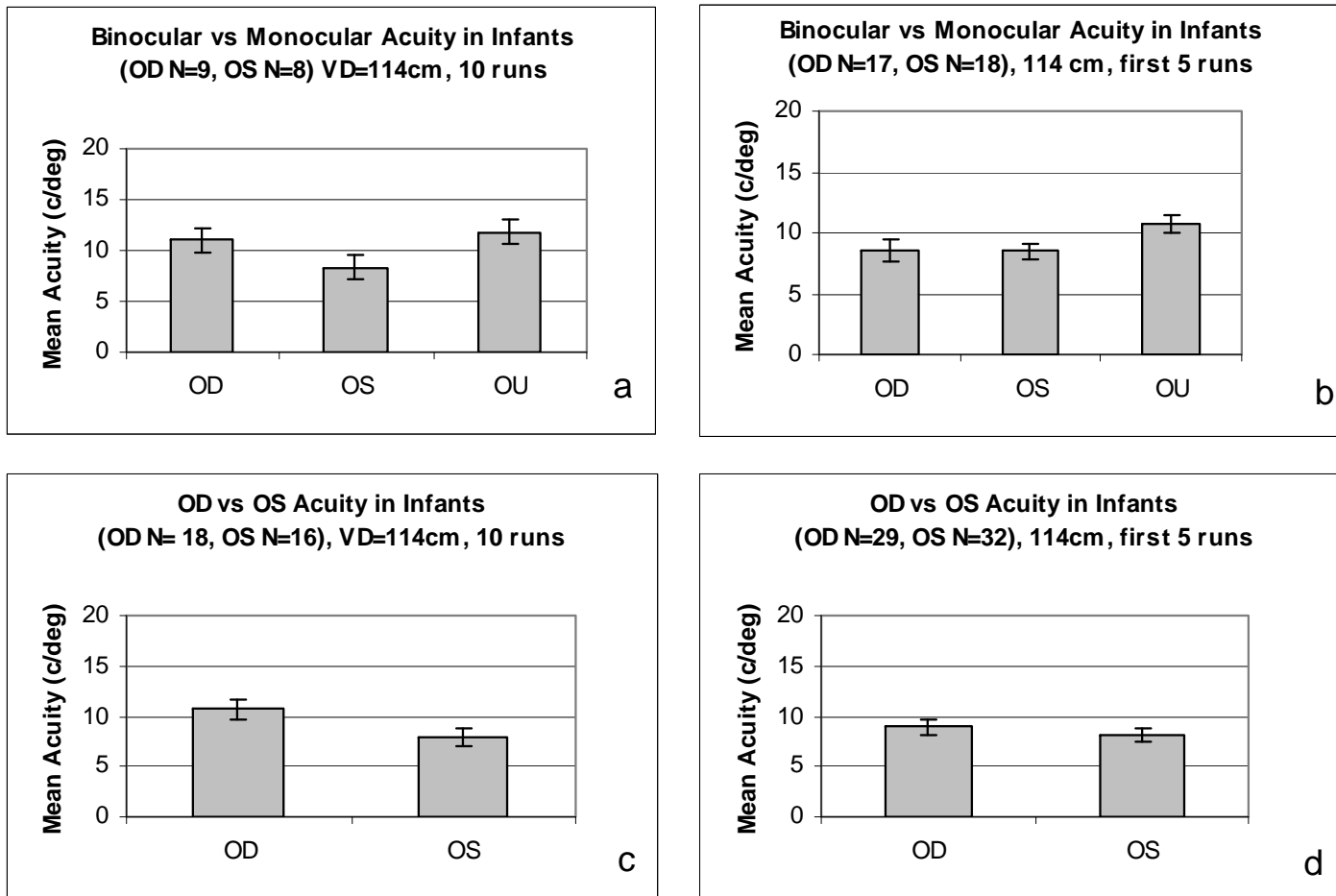


Figure 19. Bar graphs of mean monocular and binocular acuity in infants. Panels (a) and (b) show results from participants in whom binocular vision (OU) responses were available for comparison with monocular results. Panels (c) and (d) display results for participants in whom only OD and OS results were considered. Number of runs averaged is indicated in each panel.

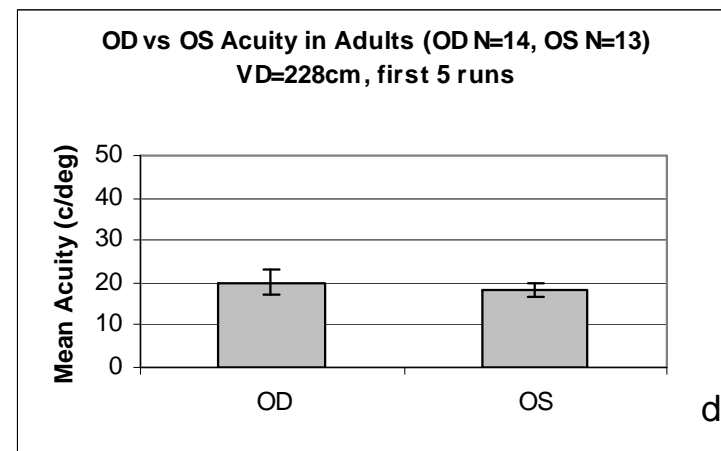
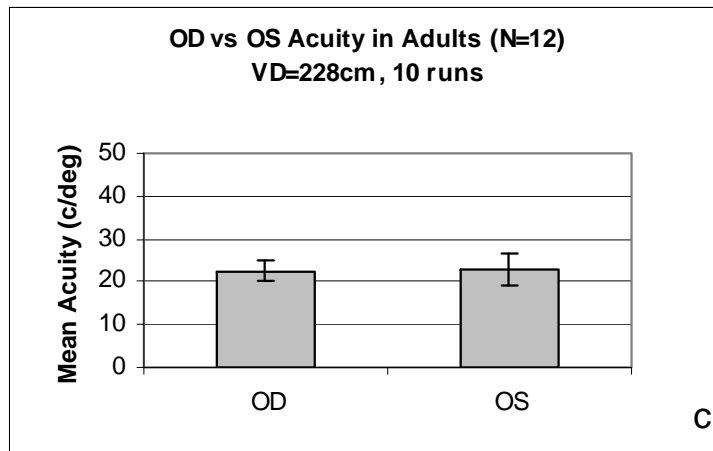
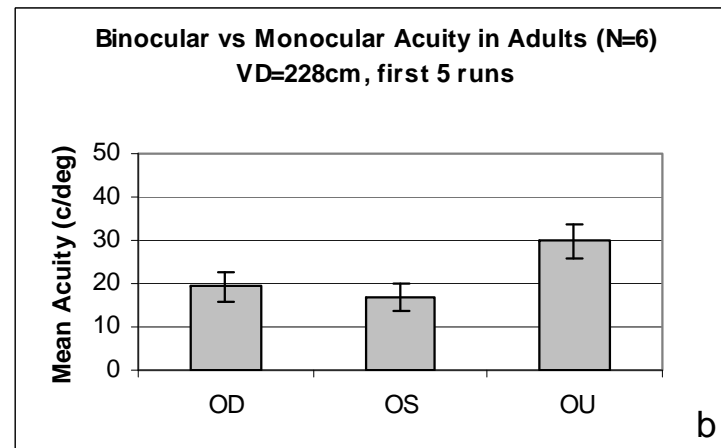
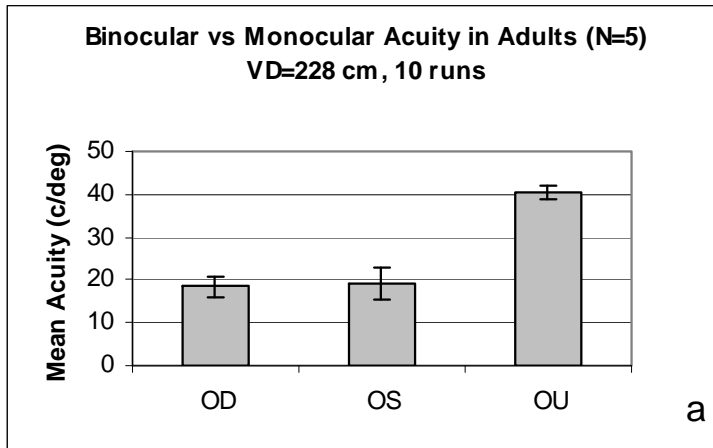


Figure 20. Bar graphs of mean monocular and binocular acuity in adults. For details, see text and legend in Figure 19.

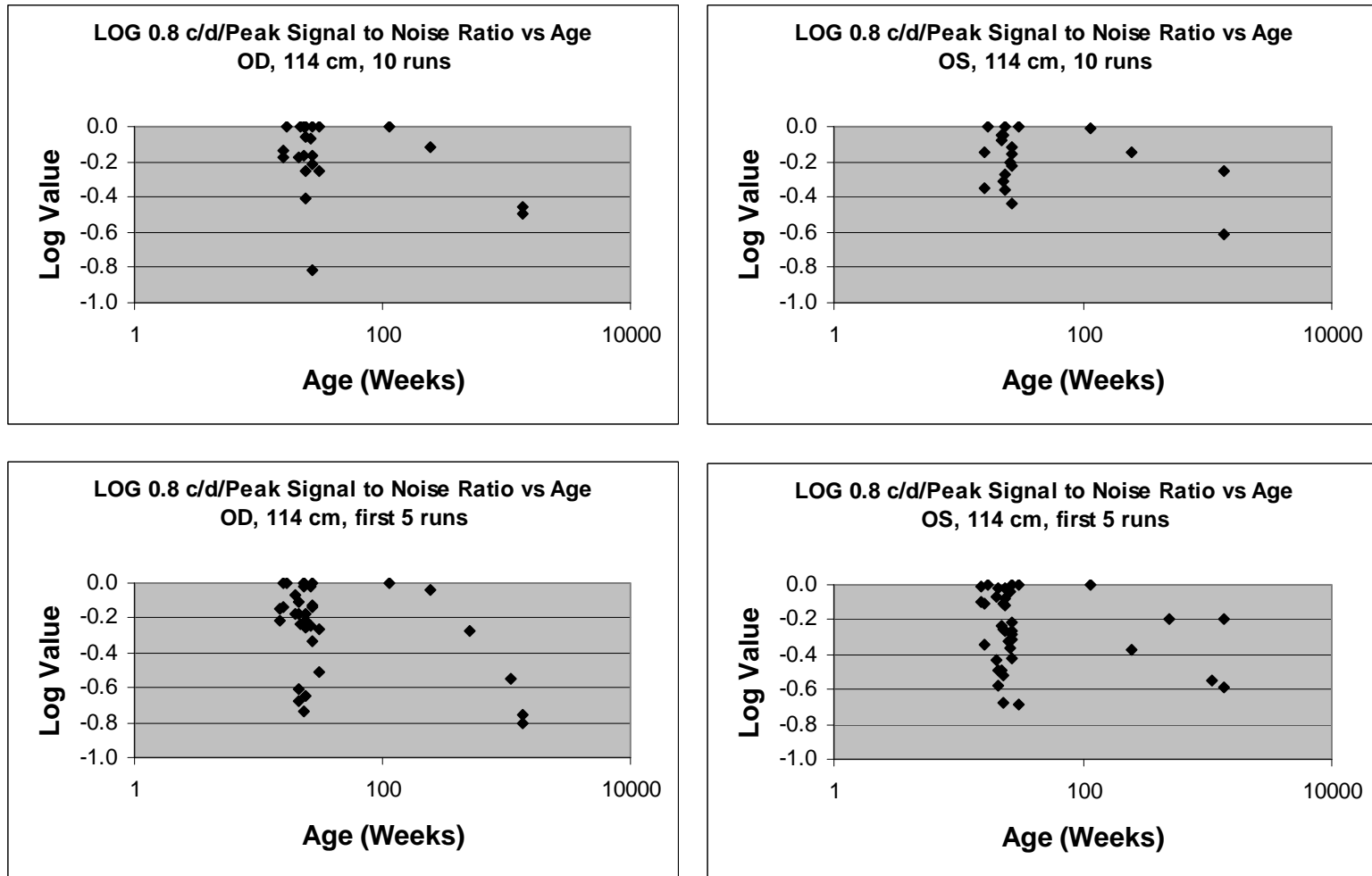


Figure 21. Scatter plots of the LOG value of the ratio of the signal to noise value at 0.8 c/deg and the signal to noise value at the peak spatial frequency as a function of age. Eye tested, distance used and number of runs is indicated in each panel.

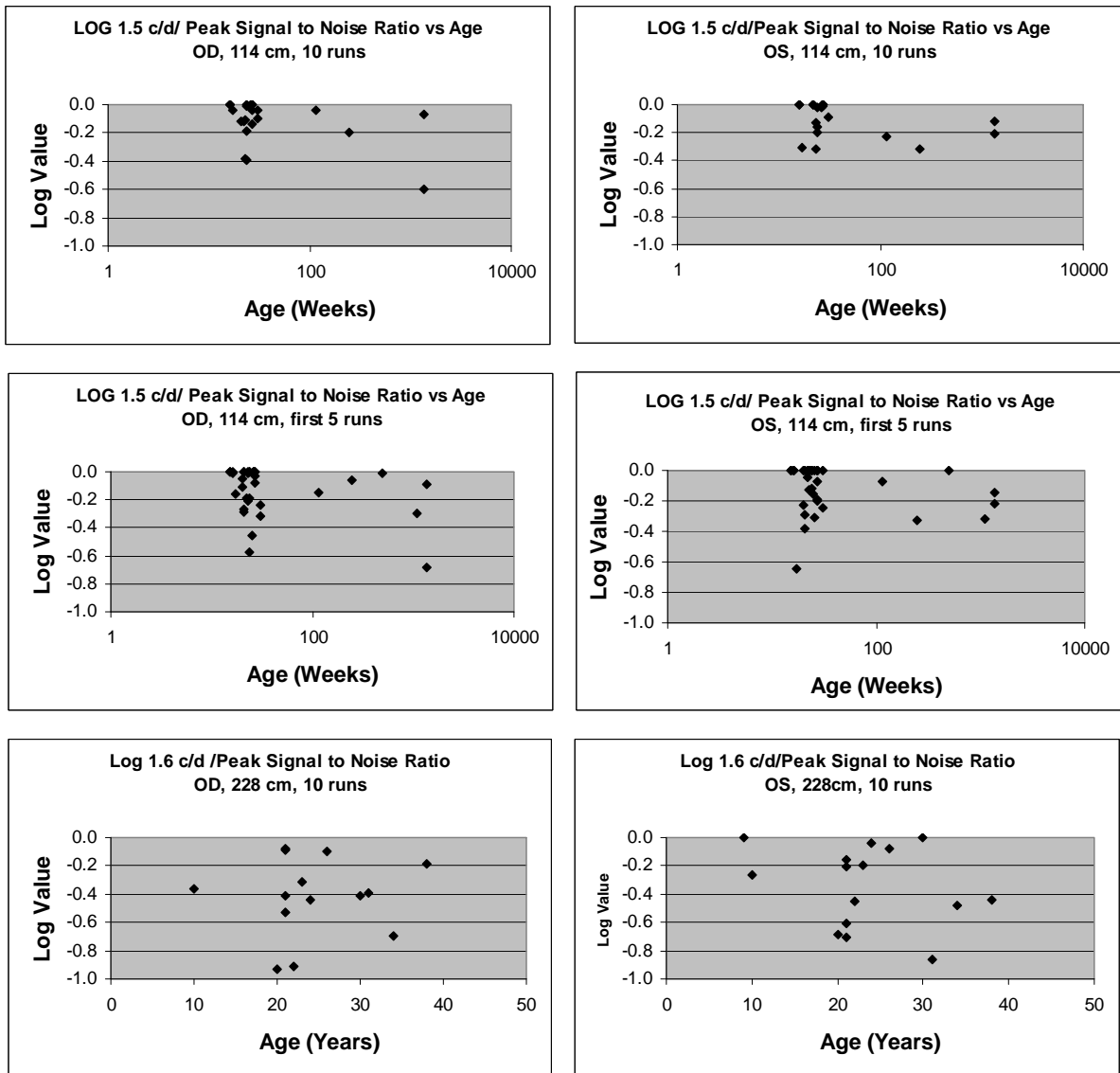


Figure 22. Scatter plots of the LOG value of the ratio of the signal to noise value at 1.5 c/deg (1.6 c/deg) and the signal to noise value at the peak spatial frequency as a function of age. Eye tested, distance used and number of runs is indicated in each panel.

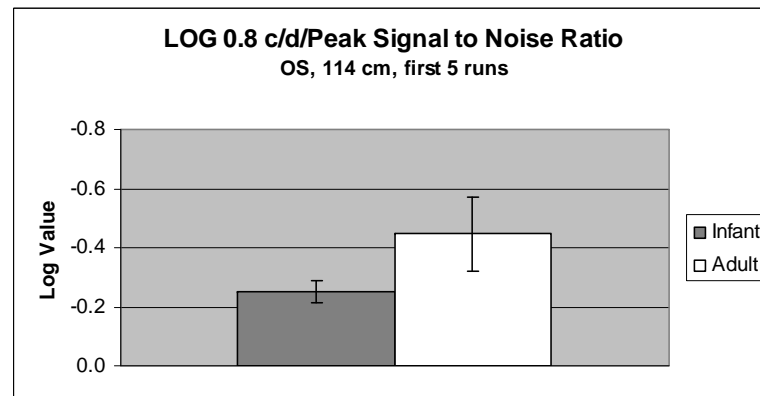
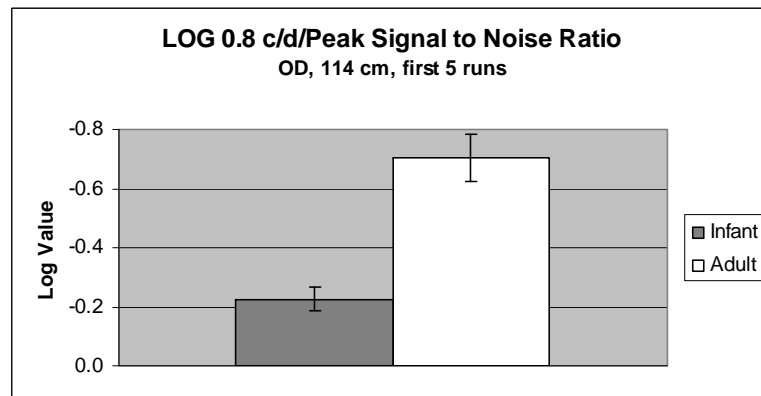
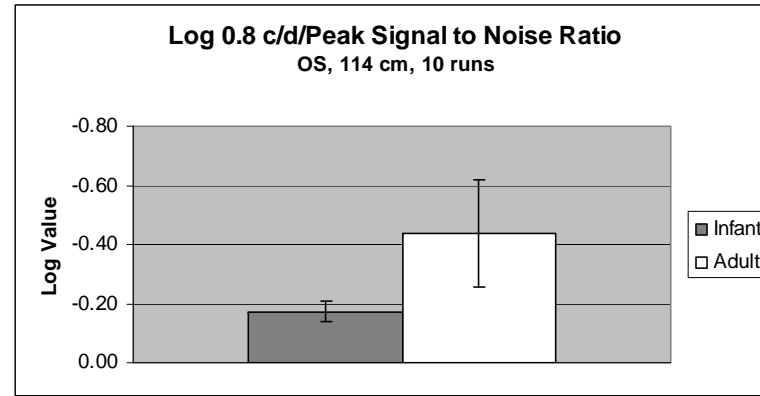
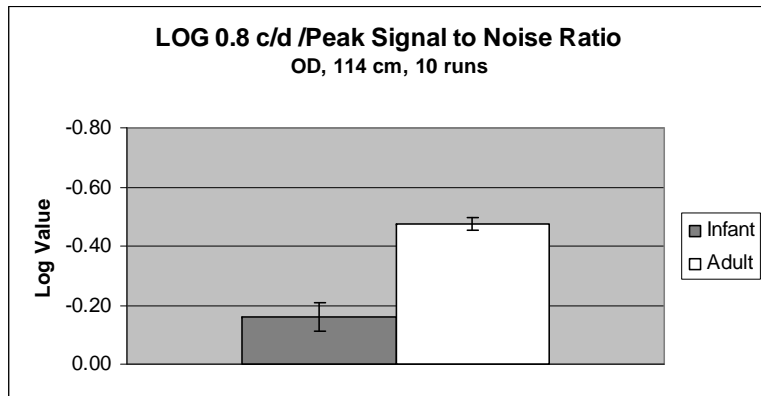


Figure 23. Bar graph of mean log value of the ratio of the S/N value at 0.8 c/deg and S/N value at the peak of the response in infants and adults. Eye tested, distance used and number of runs is indicated in each panel.

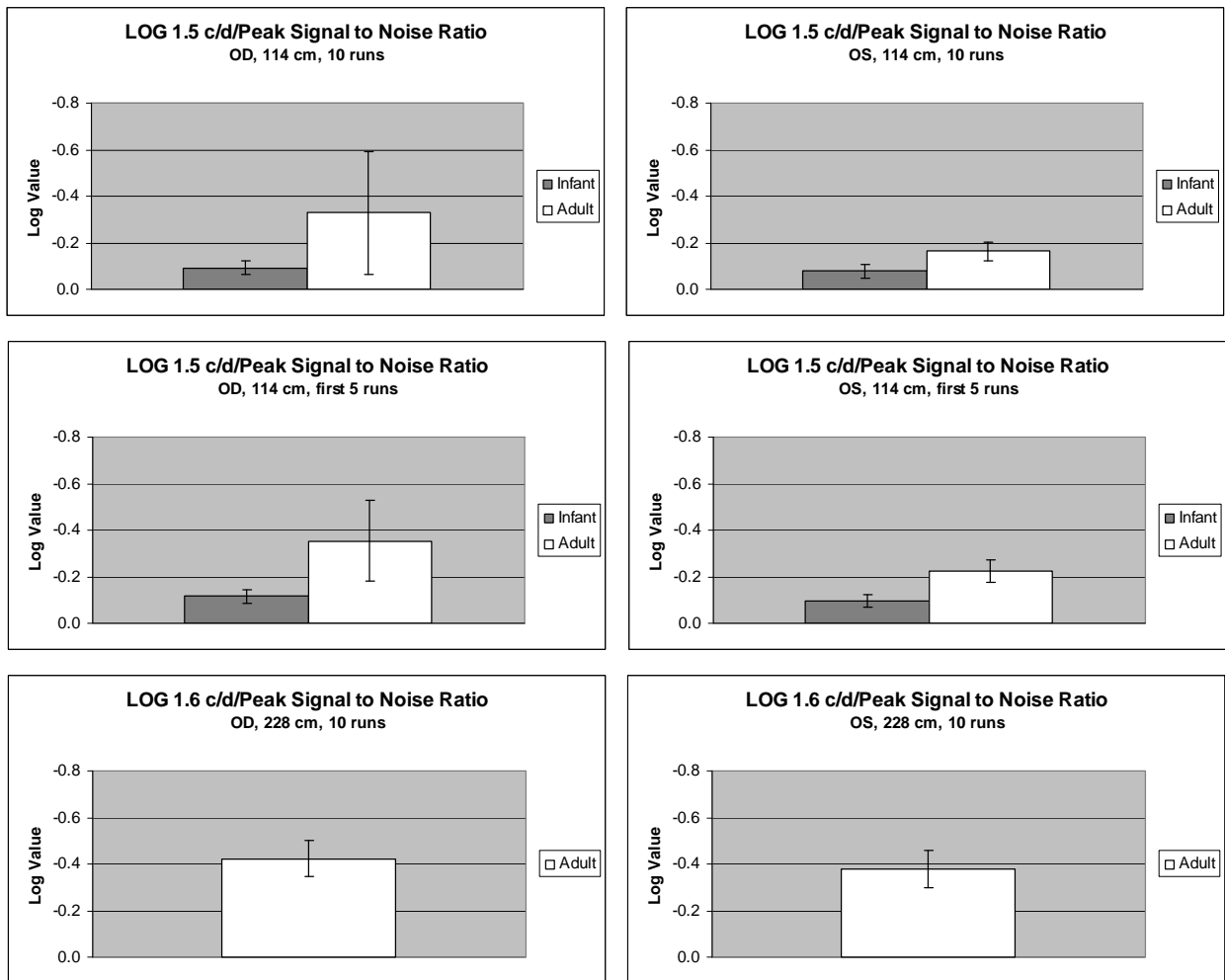


Figure 24. Bar graph of log value of the ratio of the S/N value at 1.5 c/deg and S/N value at the peak of the response. For details see text and legend Figure 23.

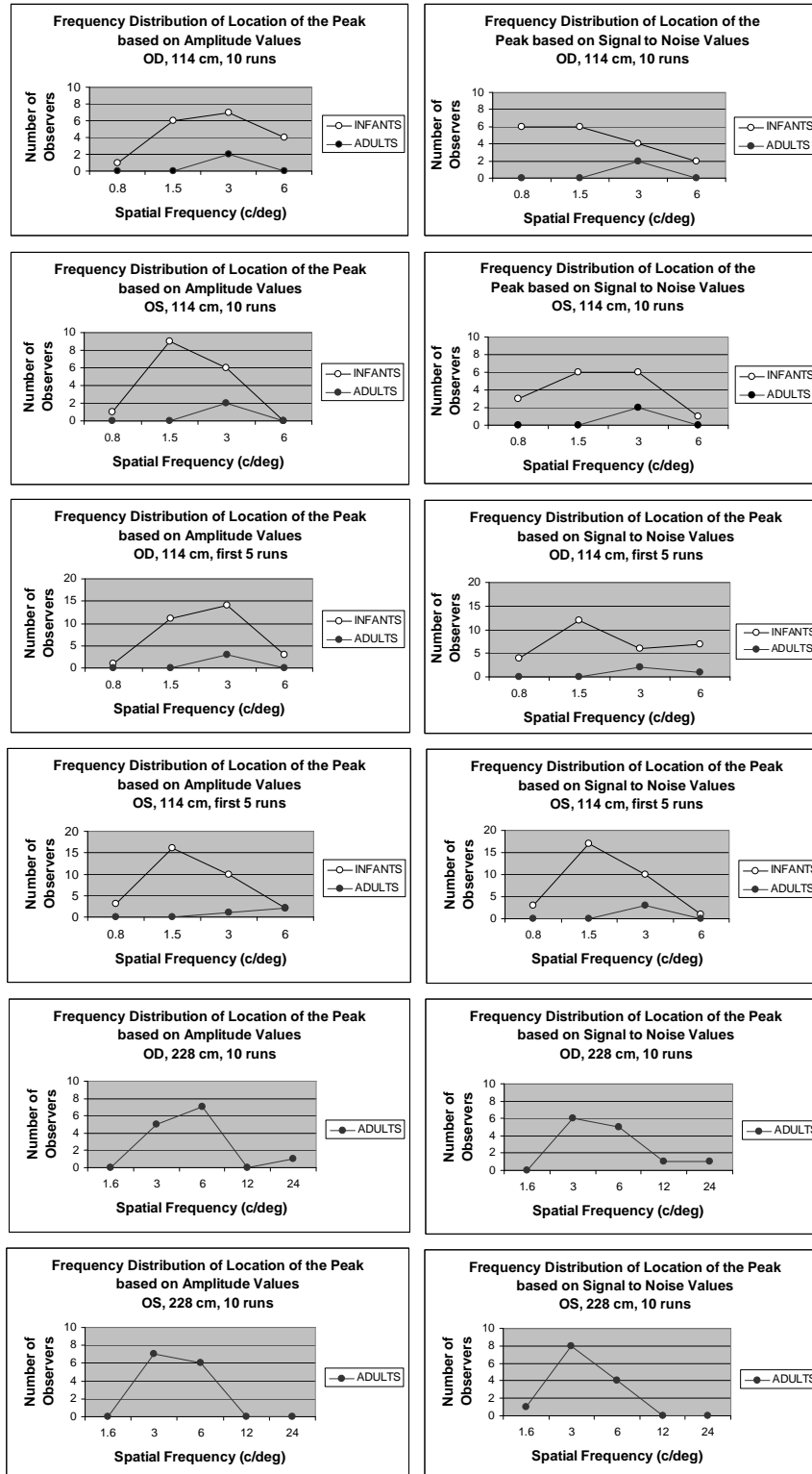


Figure 25. Frequency distribution plots of location of peak of response based on amplitude values and signal to noise ratios. Eye tested, distance used and number of runs is specified in each panel.

Gender differences in the responses to visual tests have been explored in the past. Abramov et al. (2006) found gender differences in adults for some visual tasks (ie. higher contrast sensitivity in males versus females at high spatial frequencies for five temporal rates). Moreover, in a later analysis of the infant data from the study by Hainline and Abramov (1997), the authors found that acuity estimates were superior in males versus females (I. Abramov, personal communication, 2006). In the present study, mean acuity estimates for males and females were very similar (see Figure 26). Mean acuity in the ten- runs analysis is 10.71 c/deg (± 1.14 , n=9) in males and 10.72 c/deg (± 1.63 , n=9) in females for the right eye. Mean acuity for the left eye is 7.29 c/deg (± 1.27 , n=6) and 8.32 c/deg (± 1.07 , n=10) in males and females respectively.

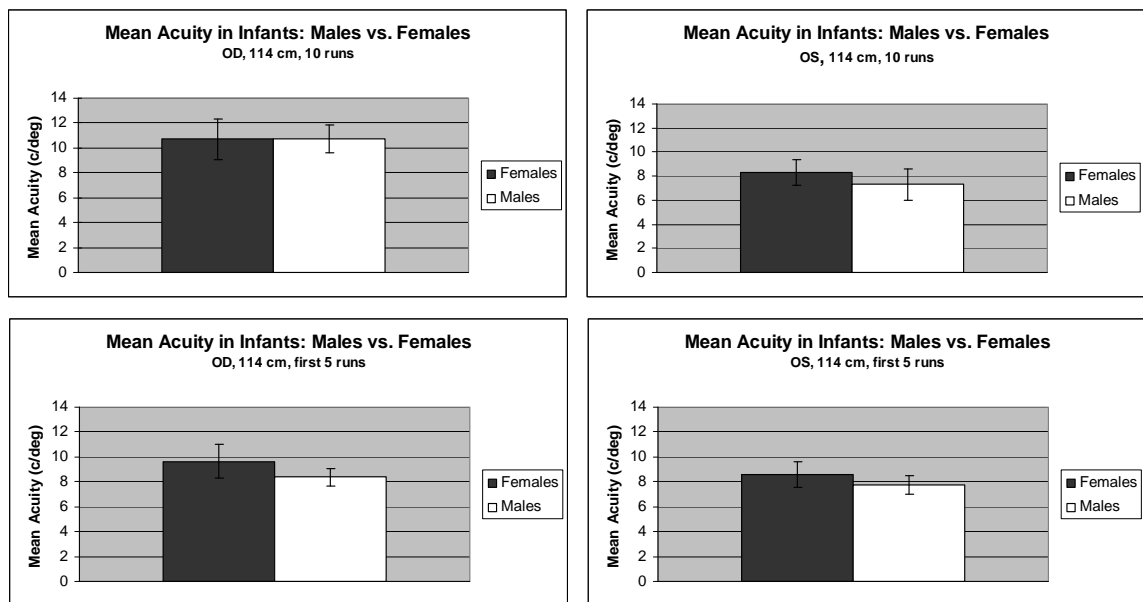


Figure 26. Bar graphs of mean acuity in infants by gender.

MONOCULAR DIFFERENCES

Most participants had well matched right and left eye spatial functions with none or just one point of interocular difference as measured with the T^2 circ statistic. Some participants had two or more points that were significantly different on the spatial functions from the right and left eye. These participants were not included in the analyses described above. From the five-runs analysis, four infants and one adult were excluded, and in the ten-runs analysis, three infants, one child and two adults were excluded.

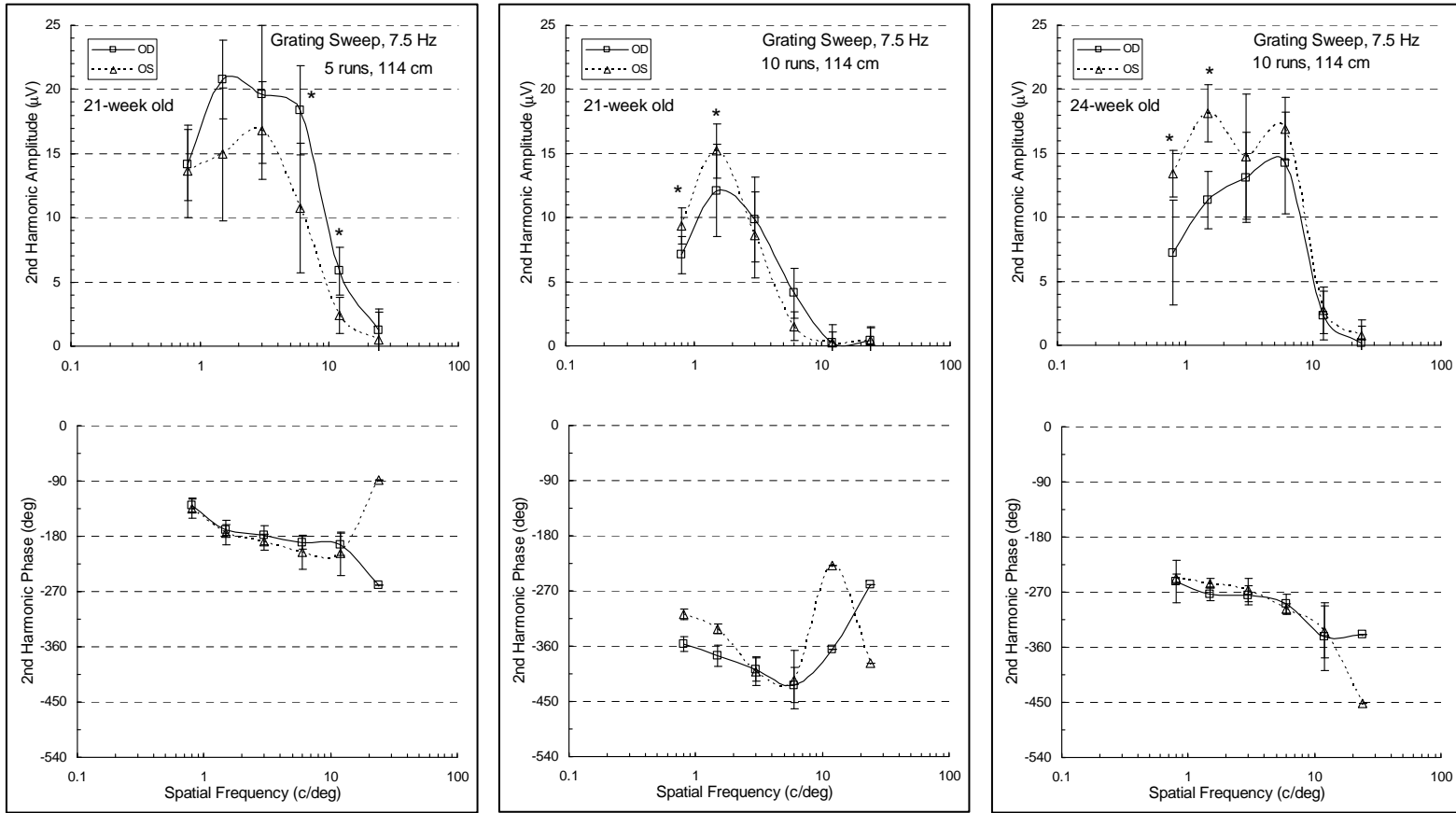
Figure 27 displays the responses of two 21-week olds (panels a and b) and a 24-week old (panel c) which had at least two points significantly different between the right and left eyes. The 21-week old in panel (a) has very similar right and left eye phase plots. Response amplitudes for the right eye are larger than for the left eye, and the third and fourth points on the plots were significantly different. Acuities for the right and left eye were 22.84 c/deg and 16.38 c/deg respectively. This particular infant shows a relative phase advance with respect to other infants of similar age. Note that the amplitude scale from panel (a) differs from the scale of panels (b) and (c). The 21-week old in panel (b) has asterisks in the first two points of the response function indicating significant differences between the eyes at the lowest spatial frequencies. The difference is particularly visible as a phase shift between those points. Acuity for the right eye was 10.7 c/deg and 7.60 c/deg for the left eye. The 24-week old in panel (c) shows significant differences in the first two points in the amplitude plots; the phase plots are virtually the same. Acuities for this infant were 15.06 c/deg for the right eye and 19.4 c/deg for the left eye.

Figures 28 and 29 show plots for children (9-, 11- and 14-year old participants) and adults (21-, 23- and 36-year olds) with two or more points of interocular difference. As in Figure 27, all differences are indicated by asterisks. Although there are differences between the eyes for these participants, the general trends described in previous sections apply to these plots. Namely, infant responses are larger than adult responses, infant phases show a slight phase lag with increasing spatial frequency whereas adults show a very steep phase lag, and there is a relative phase advance with increasing age. Acuties for the right and left eyes in the 9-year old and the 14-year old were not matched (9-year old: OD: 17.2 c/deg, OS: 6.49 c/deg; 14-year old: OD: 22.93 c/deg, OS: 41 c/deg). The other participants had similar right/left eye acuities. Acuties could not be obtained for the 21-year old because all points were significantly different from the noise. The 23- and the 36-year olds clearly show phase shifts between the right and left eyes.

What exactly each of these differences means remains to be elucidated. These differences, however, may indicate the presence of some deficit in the visual system, and may warrant further exploration by an eye care physician. Some insight to the meaning of these differences may come from the study of amblyopes with the stimuli and instrumentation used in this study.

Figure 30 shows spatial tuning functions of a 46-year-old diagnosed amblyope (left esotropia). This participant had patching treatment 17 years before present VEP testing. Reported Snellen acuities were 20/20 for the right eye and 20/80 for the left eye. Panels (a) and (b) show responses from the right and left eyes respectively. Panel (c) shows both eyes superimposed. Responses to the first four spatial frequency values were significantly different (marked with asterisks in the figure) between the eyes by the two-

sample T^2 statistic at the 0.01 level. Response amplitudes from the left eye are smaller than the ones for the right eye. However, estimated acuities were very similar. The VEP interpolated acuities were 21.38 c/deg for the right eye and 20.81 c/deg for the left eye. Phase responses for the points that were significantly different from noise were lagging in the range of -90° to -270° in the right eye. The three significant phase points in the left eye were slightly leading between -180° and -270° .



(a)

(b)

(c)

Figure 27. Monocular responses from two 21-week olds (a and b) and a 24-week old (c) showing significant differences between the eyes.

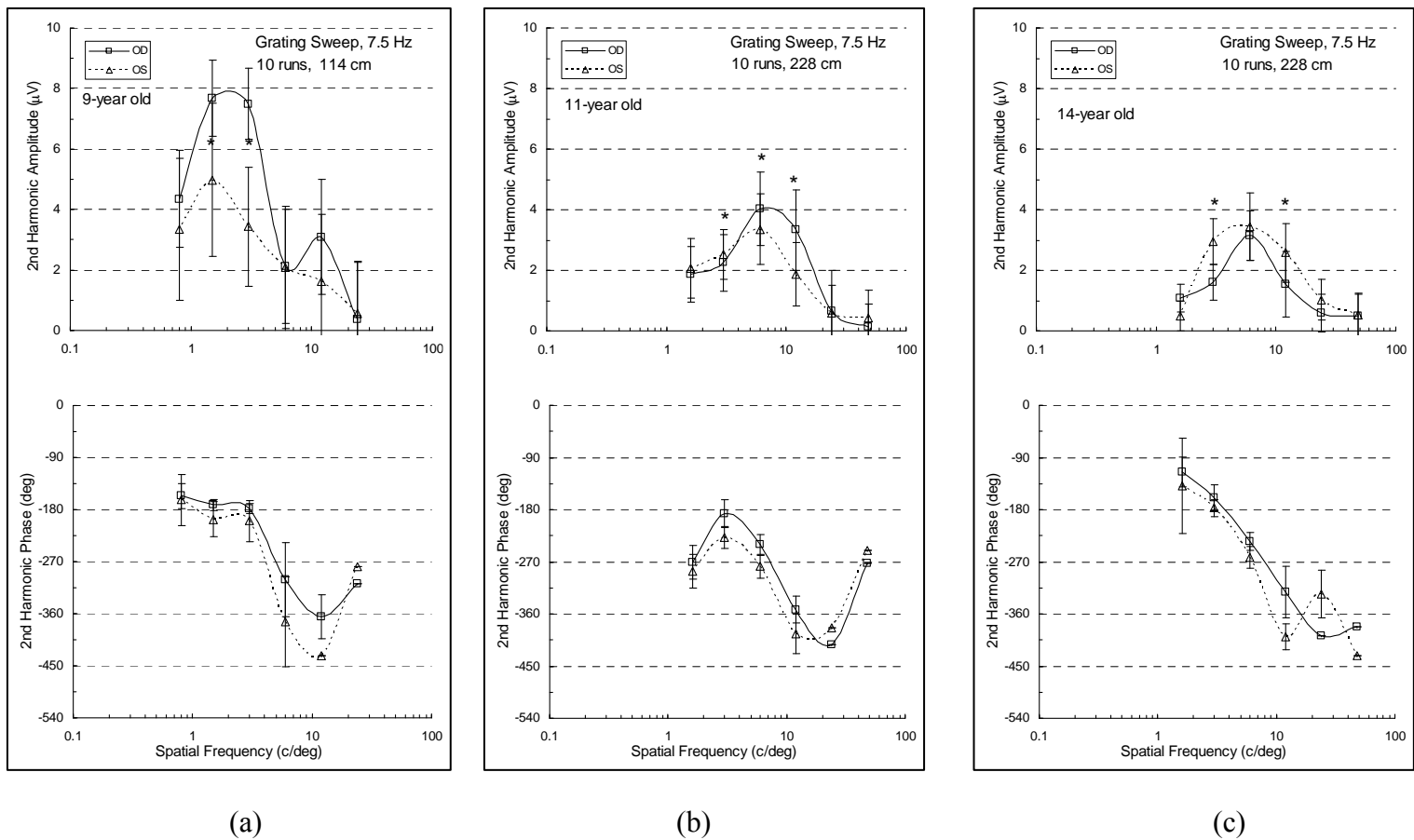
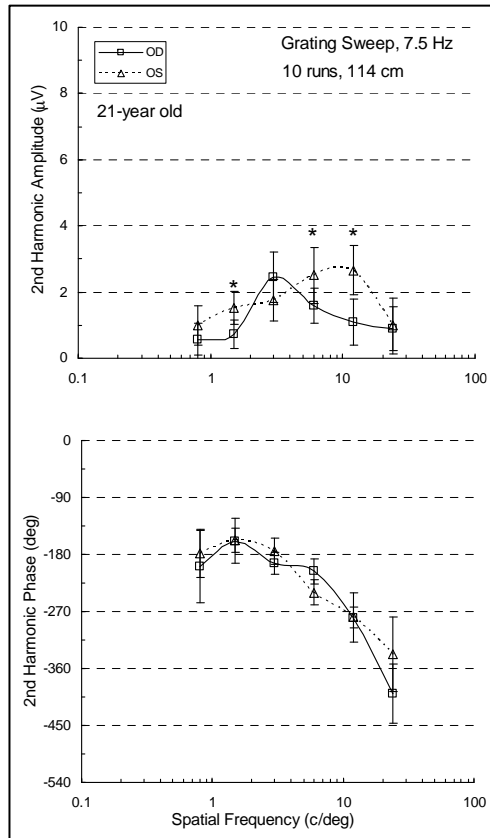
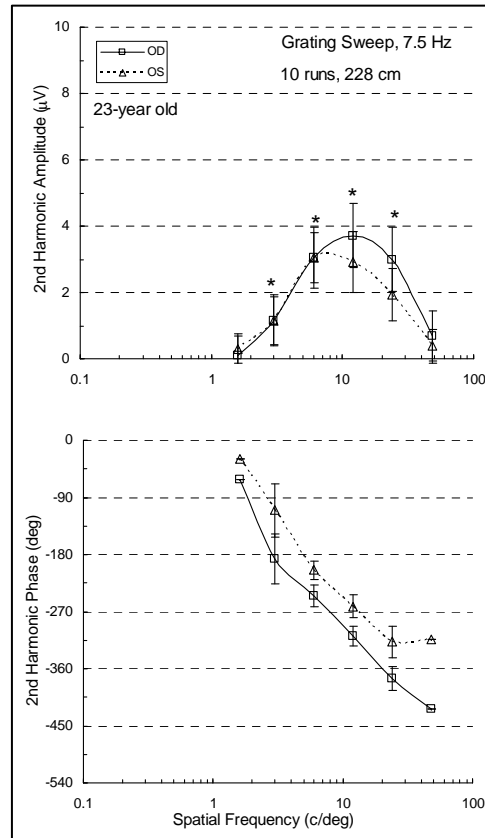


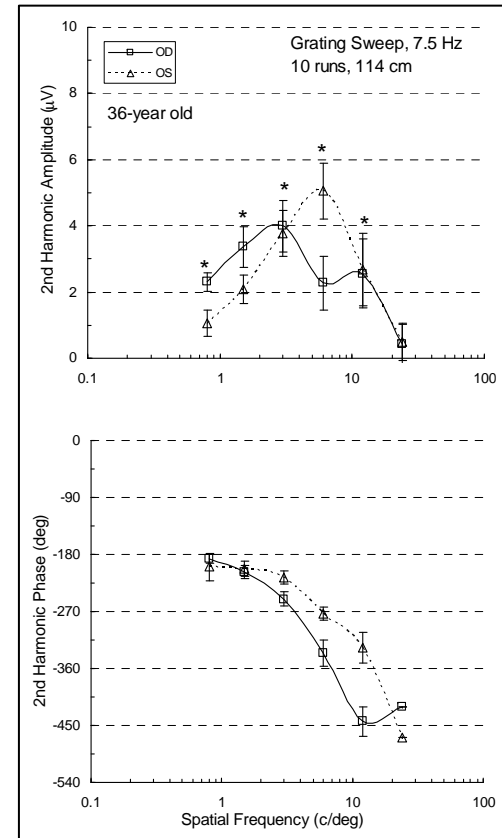
Figure 28. Monocular responses from a 9-year old (a), an 11-year old (b) and a 14-year old (c) showing significant differences between the eyes.



(a)



(b)



(c)

Figure 29. Monocular responses from a 21-year old (a), a 23-year old (b) and a 36-year old (c) showing significant differences between the eyes.

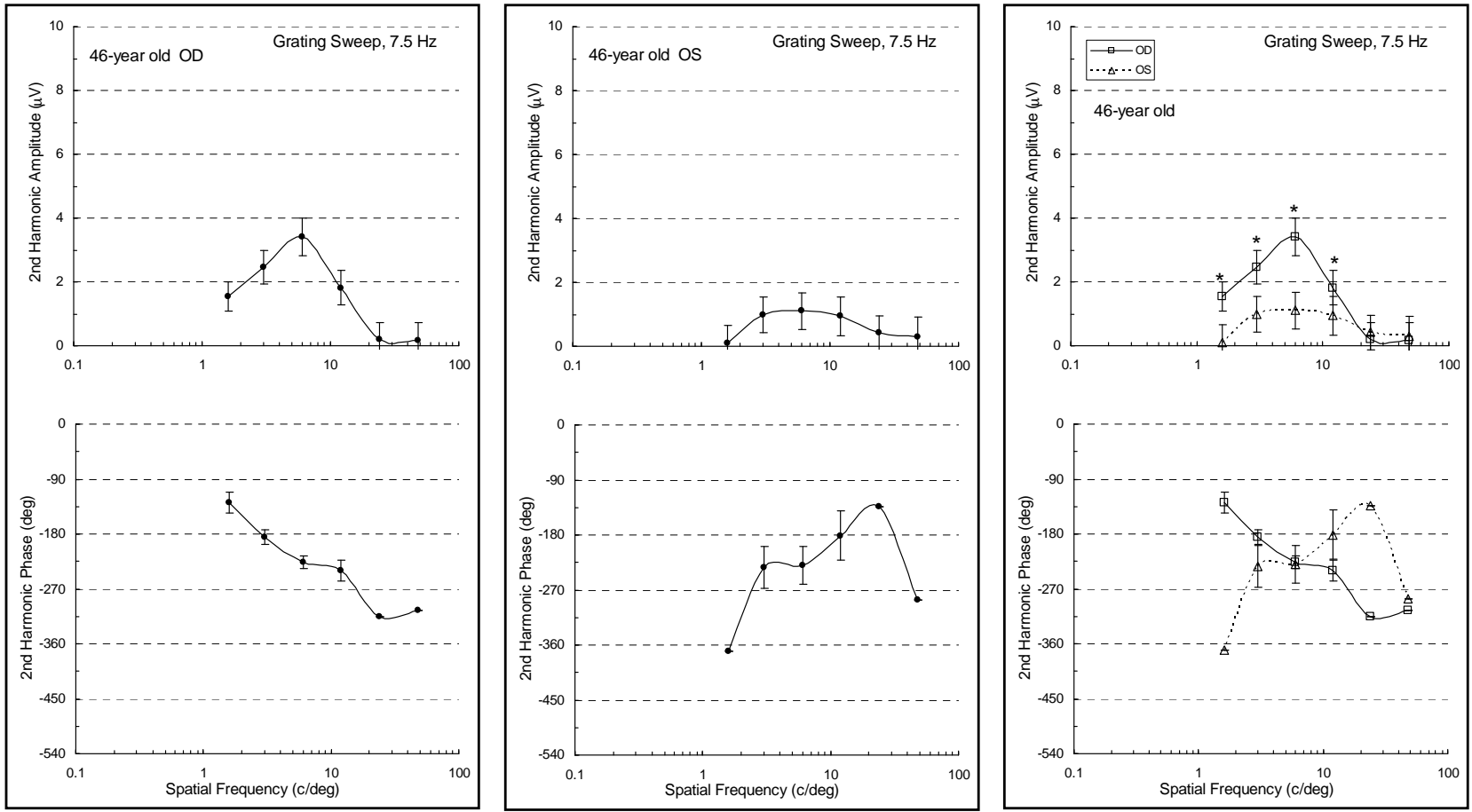


Figure 30. Spatial tuning functions for a 46-year-old diagnosed amblyope. Significant differences between the eyes are marked with asterisks. For details see text and legend in Figure 5.

CONTRAST SWEEP (15 CYCLES PER SCREEN)

Of the 22 infants tested with this contrast stimulus at 57 cm (0.75 c/deg contrast sweep), 19 yielded reliable data for the right eye and 20 for the left eye. Data for the right eye were not collected for one infant and for the left eye for another. Noisy data for either one or both eyes from two other infants were not included in the analysis. Monocular second harmonic amplitude and phase data as a function of depth of modulation for a 19-week old, a 23-week old, a 28-week old, a 10-year old and a 26-year old are displayed in Figure 31. Amplitude and phase data for each participant are displayed side by side, and the model's parameter estimates, R^2 values and time constants are shown below each data set (for more details, read model description in Methods section).

There are striking differences between the contrast functions of infants and the functions of the 10- and 26-year olds. The functions from infants are in general very linear; they show very little amplitude compression and the phases are very flat. Note that the amplitude scales differ from panel to panel. In general, infant response amplitudes are larger than adult responses. Both the 10-year old and the 26-year old display amplitude compression and phase advance with increases in contrast.

In Figure 31, K is a gain constant set at a value of 10 for all fits, G_0 is the initial conductance of the system, ϕ_0 is the initial phase of the second harmonic response, d_0 is the threshold depth of modulation, m is the shunting coefficient, R -sq is the R^2 value for the model's fit, $\tau_{1\%}$ is the time constant at 1% contrast and $\tau_{32\%}$ is the time constant at 32% contrast (Zemon & Gordon, 2006). The shunting coefficients (m) for the three infants are below one whereas the coefficients for the 10-year old and the 26-year old are

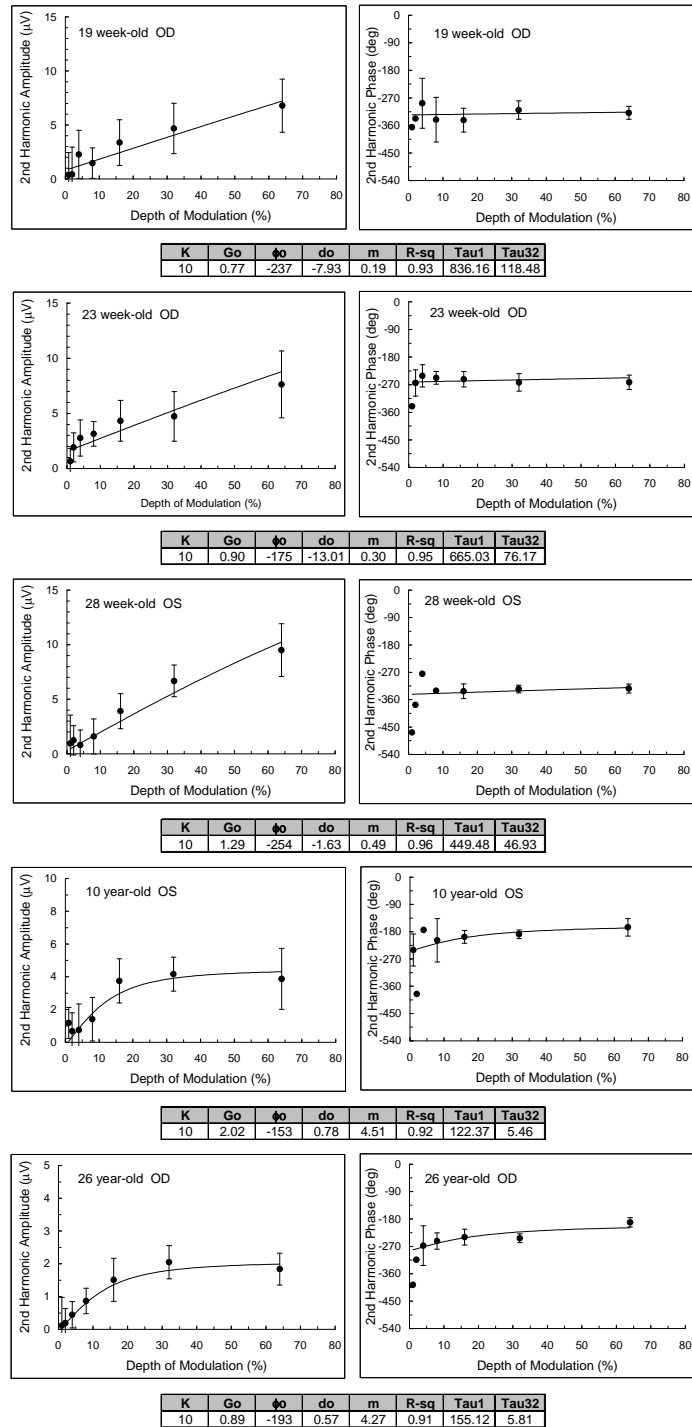


Figure 31. Monocular amplitude and phase of the second harmonic response to the 0.75 c/deg contrast grating sweep from a 19-week old, a 23-week old, a 28-week old, a 10-year old and a 26-year old. Participant's age and eye used is displayed in each panel. The model's parameter values are displayed below each set of graphs.

around four. Time constant values decreased with increasing contrast from 1-32%. In the 10- and the 26-year olds, there is a more than 20-fold decrease in the time constant. In the infants, there is a less than ten-fold decrease.

Figure 32 shows examples of observers who display negative shunting coefficients which are associated with slightly negative phase slopes. The time constants either decrease to negative values or are already negative and decrease in negativity in the 1-32% contrast range. Negative time constants reflect negative conductance in the visual system. Again, the responses of infants are very linear with very flat slightly lagging phase plots. The 20-year old, shows amplitude compression and a more pronounced phase lag than the infants.

Figure 33 displays scatter plots of the model's parameters and time constants as a function of age. These plots include data from the best eye from a group of participants who yielded good representative data. There were significant positive correlations with age for the absolute value of m ($r=0.95$, $n=15$, $p < 0.005$), the initial phase ($r=0.72$, $n=15$, $p < 0.005$) and threshold depth of modulation ($r=0.68$, $n=15$, $p < 0.005$). There was a significant negative correlation between the time constant at 1% DOM (Tau1) and age ($r=0.5$, $n=15$, $p < 0.05$). The positive correlation between age and m remained significant even when the signed value of m was used ($r=.57$, $n=15$, $p < 0.025$).

In a similar analysis which included all participants with reliable data separately by eye, similar trends were observed with age; however, only the shunting coefficient (both absolute and signed) and the initial phase reached significance in the right and left eyes. There was a significant positive correlation between Tau1 and age in the left eye only.

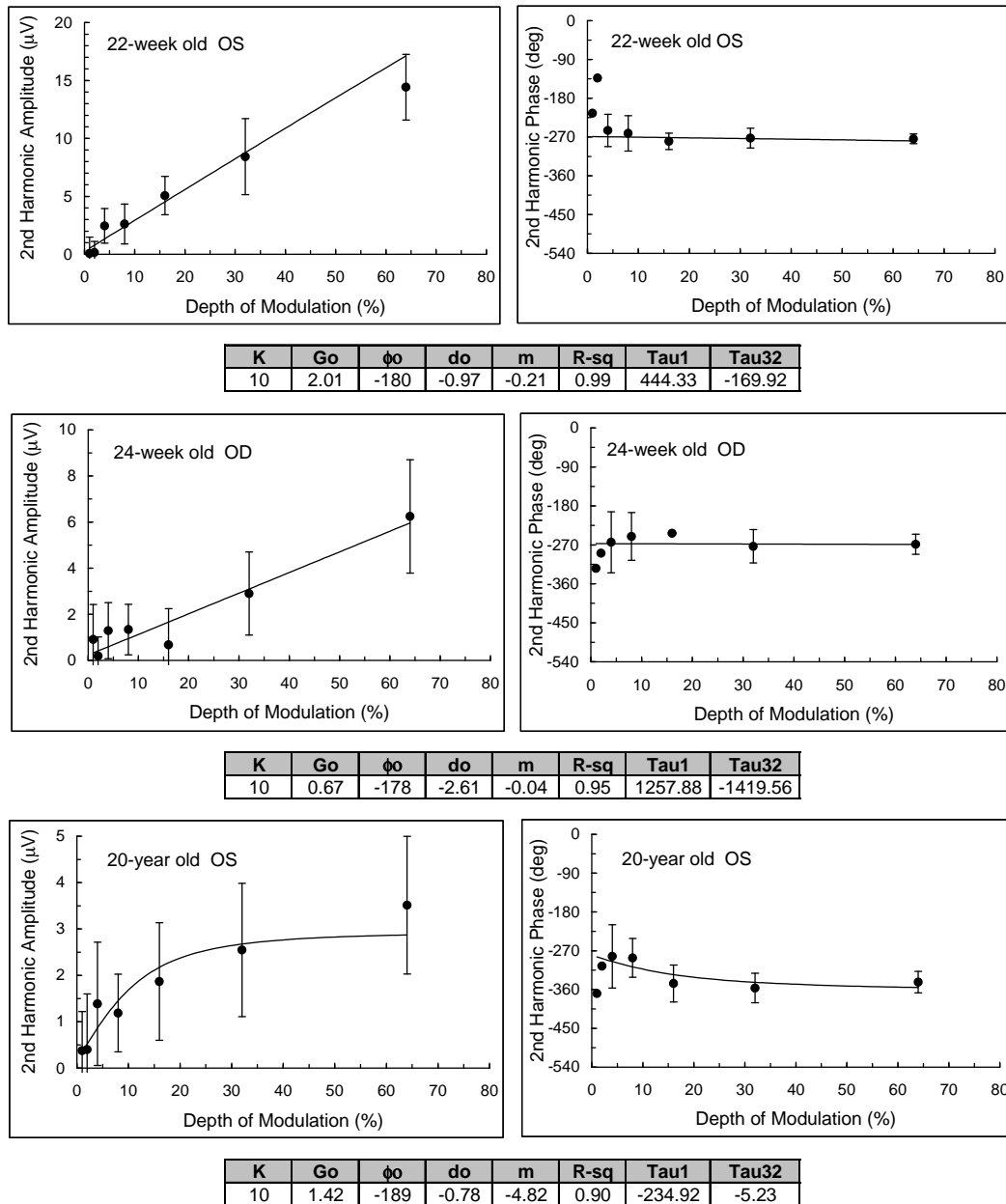


Figure 32. Monocular amplitude and phase of the second harmonic response to the 0.75 c/deg contrast grating sweep from a 22-week old, a 24-week old and a 20-year old showing negative shunting coefficients. Participant's age and eye used is displayed in each panel. The model's parameter values are displayed below each set of graphs.

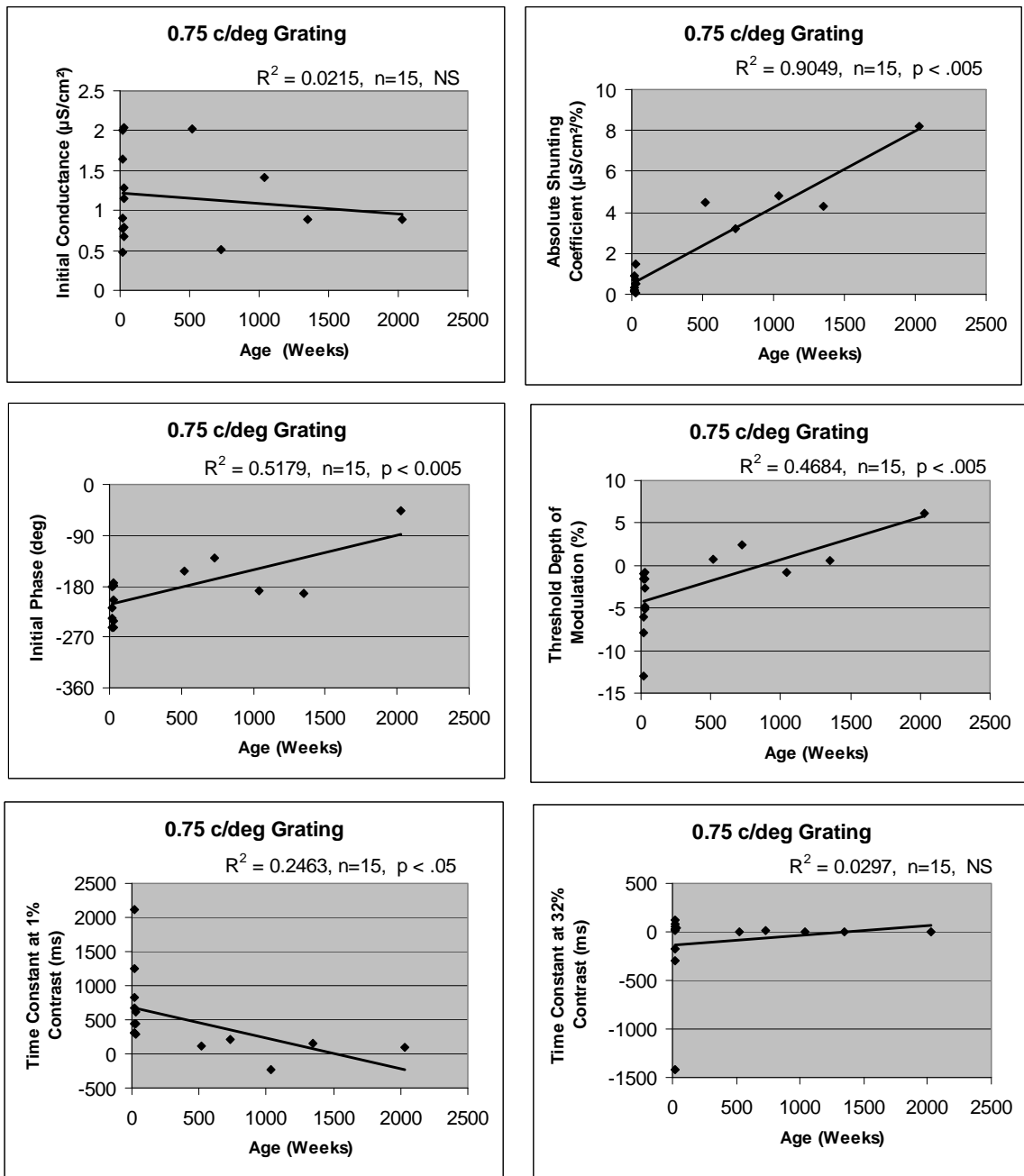


Figure 33. Scatter plots of each of the model's parameters versus age for the 0.75 c/deg contrast sweep responses. Monocular representative data were included in these plots. Regression lines were drawn.

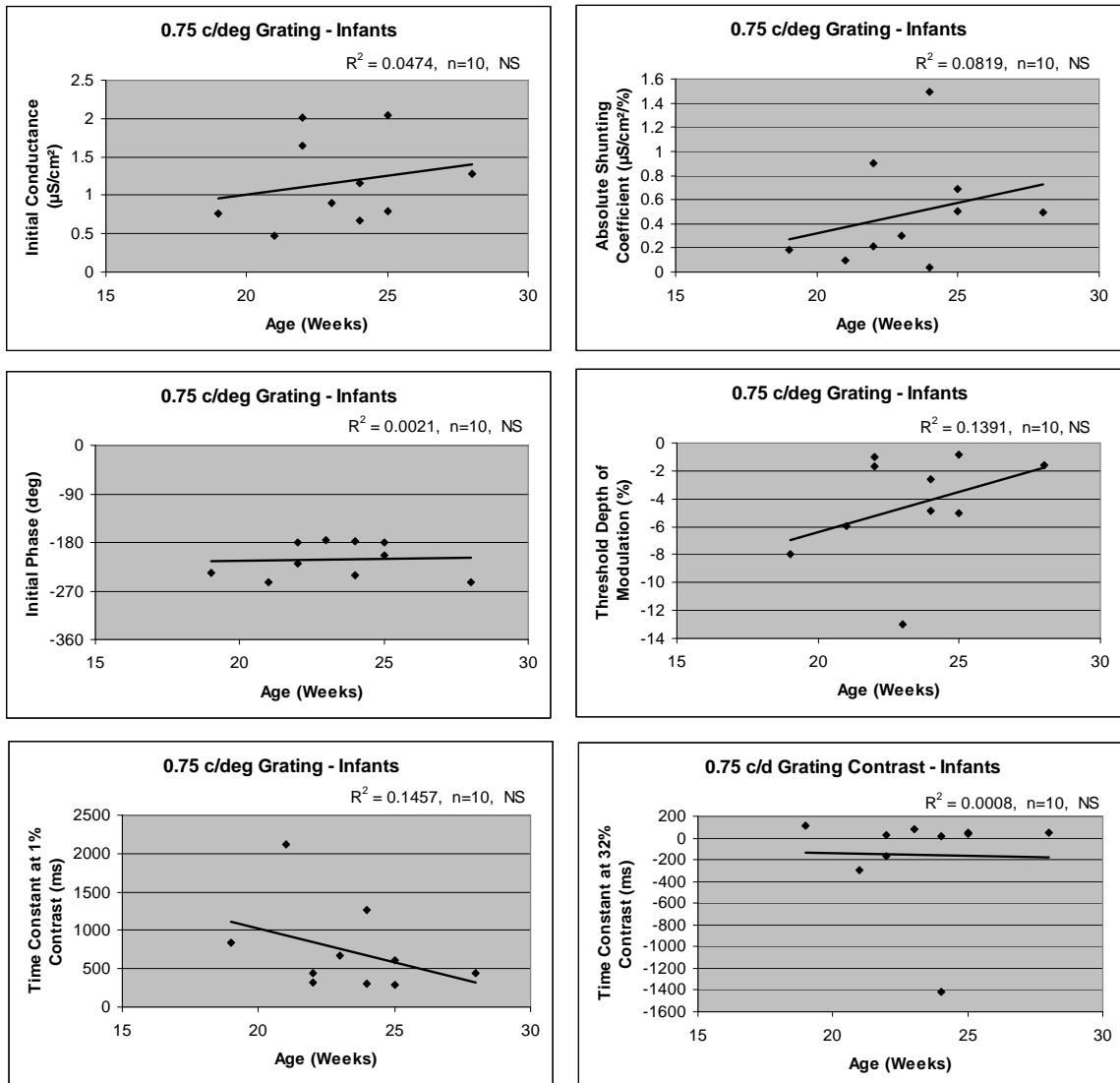


Figure 34. Scatter plots of each of the model's parameters versus age showing only the infants from Figure 33 (0.75 c/deg contrast sweep responses). Regression lines were drawn.

Figure 34 presents scatter plots of the model's parameters and time constants as a function of age for the infants shown in Figure 33. Regression lines were drawn in these plots. There was a trend of increasing initial conductance, increasing shunting coefficient and increasing threshold depth of modulation with increasing age in these infants;

however, none of the trends were significant. There was a negative correlation between the time constant at 1% contrast and age, but it was not significant either.

Figure 35 shows bar graphs of the parameters' mean values and time constants in adults and infants for best eye data. There are marked differences between adults and infants, particularly for the shunting coefficient, the initial phase, the threshold depth of modulation and Tau1. The absolute mean shunting coefficient was 0.49 (± 0.14 SEM, n=10) in infants and 5.76 (± 1.22 SEM, n=3) in adults. Mean initial phase was -212° (± 10.39 SEM, n=10) in infants, and -143° (± 48.16 SEM, n=3) in adults. Mean threshold DOM was -4.45% (± 1.21 SEM, n=10) and 1.96% (± 2.1 SEM, n=3) in infants and adults respectively. Infants had a mean Tau1 value of 730 ms (± 181 SEM, n=10) whereas adults had a mean of 277 ms (± 120 SEM, n=3).

In the analysis which included all infants and adults who yielded reliable data, similar results were observed with the shunting coefficient and Tau1 showing the most marked differences between infants and adults. The absolute mean shunting coefficient in infants was 0.72 (± 0.14 SEM, n=19) and 0.94 (± 0.27 SEM, n=20) for the right and left eye respectively. In adults, it was 5.88 (± 1.97 SEM, n=7) and 5.66 (± 1.46 SEM, n=7) for the right and left eye respectively. Tau1 in infants was 765 ms and 875 ms for the right and left eyes as compared to 315 ms and 143 ms in adults.

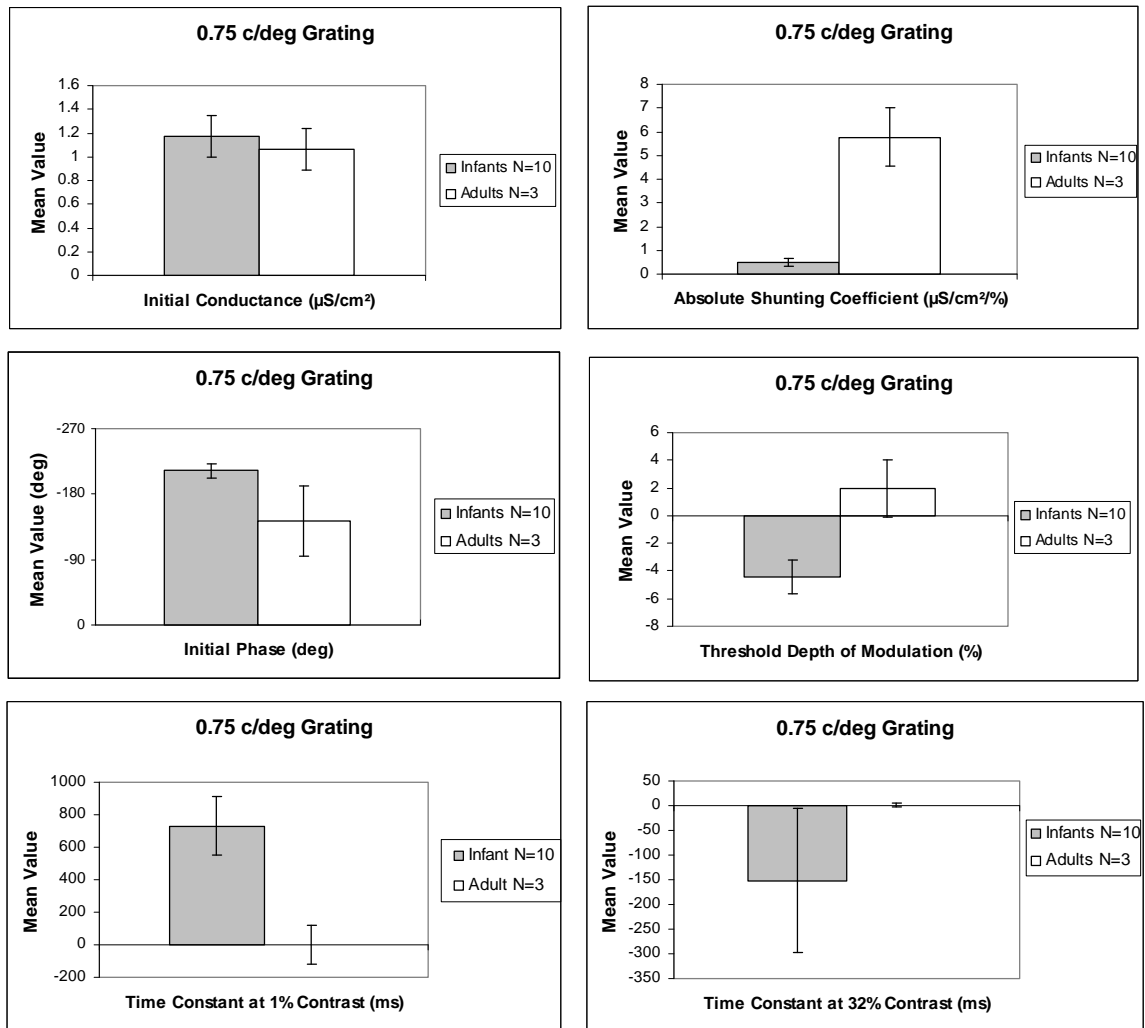


Figure 35. Bar graphs of each of the parameters mean values for adults and infants corresponding to the data shown in Figure 33.

CONTRAST SWEEP (30 CYCLES PER SCREEN)

Figure 36 shows data for a 16-week old, a 21-week old, a 3-, a 14- and a 26-year old tested with the 1.5 c/deg contrast sweep. The pattern observed in this set of figures is similar to the one seen when participants were tested with the 0.75 c/deg contrast sweep

(Figure 31). Again, there are striking differences between the contrast functions of infants and the functions of older observers, particularly the 14- and 26-year olds. Infant responses are very linear (no amplitude compression) with very flat phase plots. Amplitude scales in this figure also differ from panel to panel. There is a relative phase advance in the 3-year old with respect to the infant phases, but the phase plot in this child is still relatively flat. The amplitude plot shows a weak indication of amplitude compression which is associated with a higher shunting coefficient ($m=1.17$). The 14-year old and the 26-year old both show increasing response amplitudes with increasing contrast to about 16% contrast where they begin to reach saturation. The last point in the 14-year old plot cannot be fit with the model. This decrease in the response amplitude at high contrasts may be related to hyperpolarizing inhibition (Borg-Graham et al., 1998; Zemon & Gordon, 2006). The 14- and the 26-year olds show a very steep phase advance with increasing contrast with their phase plots ending around the same level as the phase plot of the 3-year old (between the -180° and -270° range). The time constants decrease with increasing contrast in the range of 1-32%. In this case, there is approximately a 10-fold decrease in the infants. The decrease is more than 20-fold in the 3-, the 14- and the 26-year olds. The shunting coefficients range from 0.16 in the 16-week old to 14.72 in the 26-year old.

Scatter plots of the parameters and time constants obtained with the model as a function of age are displayed in Figure 37. These plots include monocular data from the best eye from a group of participants who yielded good representative data. There are significant positive correlations between age and the following: initial conductance ($r=0.77$, $n=8$, $p < .025$, one tail), shunting coefficient ($r=0.89$, $n=8$, $p < .005$, one tail),

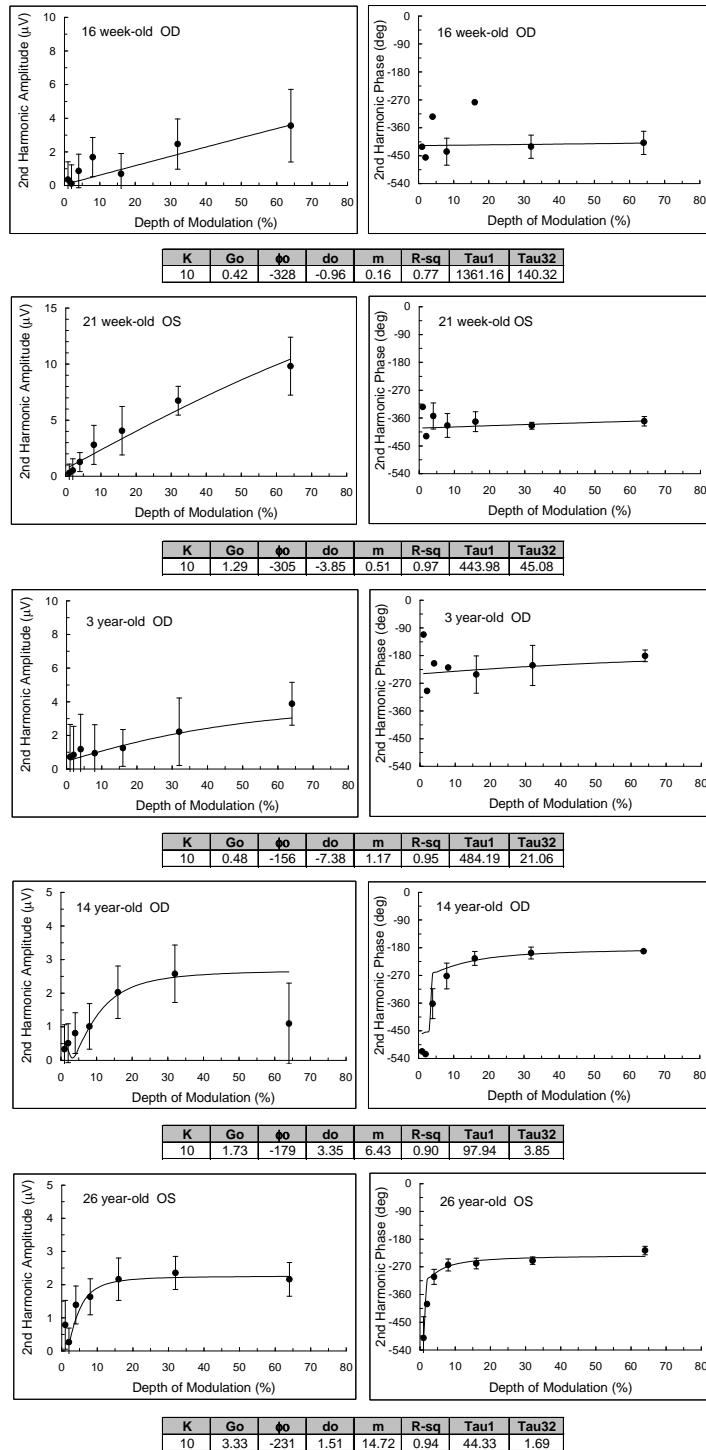


Figure 36. Monocular amplitude and phase of the second harmonic response to the 1.5 c/deg contrast grating sweep from a 16-week old, a 21-week old, a 3-year old, a 14-year old and a 26-year old. Participant's age and eye used is displayed in each panel. The model's parameter values are displayed below each set of graphs.

and threshold depth of modulation ($r=0.67$, $n=8$, $p < .05$, one tail). There is also a negative correlation between Tau1 and age ($r=0.71$, $n=8$, $p < .025$, one tail).

Similar trends were observed when all participants with reliable data were included in the analysis and the data were separated by eye. The positive correlations with age that reached significance were the initial conductance, the shunting coefficient and the initial phase in both the right and left eyes. The negative correlation between age and Tau1 and Tau32 were significant only in the right eye.

Figure 38 shows bar graphs of the parameters' and time constants' mean values for infants and adults in response to the 1.5 c/deg contrast sweep. Infants show different results from adults with this stimulus as well. The mean initial conductance value is larger in adults than in infants (3.55 ± 0.95 , $n=2$ versus 0.77 ± 0.26 , $n=3$). The mean shunting coefficient of $0.25 (\pm 0.14, n=3)$ in infants is in great contrast to the value of $19 (\pm 4, n=2)$ in adults. Adults also show less negative values of initial phase than infants (-188° versus -300°), and adults have shorter time constants than infants (37 ms versus 993 ms for Tau1 and 1.34 ms versus 156 ms for Tau32). Similar trends were also seen when all five infants and six adults who gave reliable data were included in the separate analysis by eye.

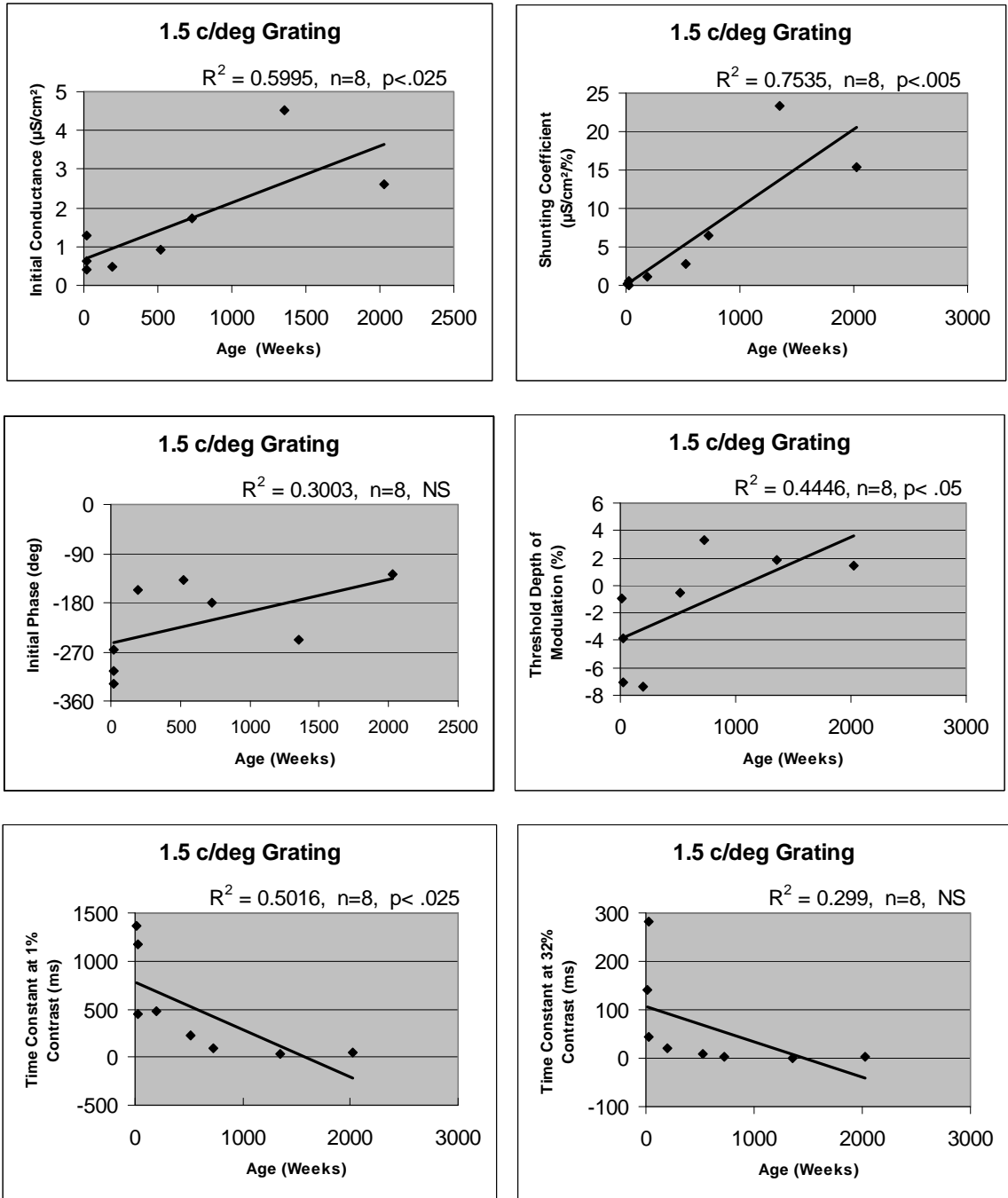


Figure 37. Scatter plots of each of the model's parameters versus age for the 1.5 c/deg contrast sweep responses. Monocular representative data were included in these plots. Regression lines were drawn.

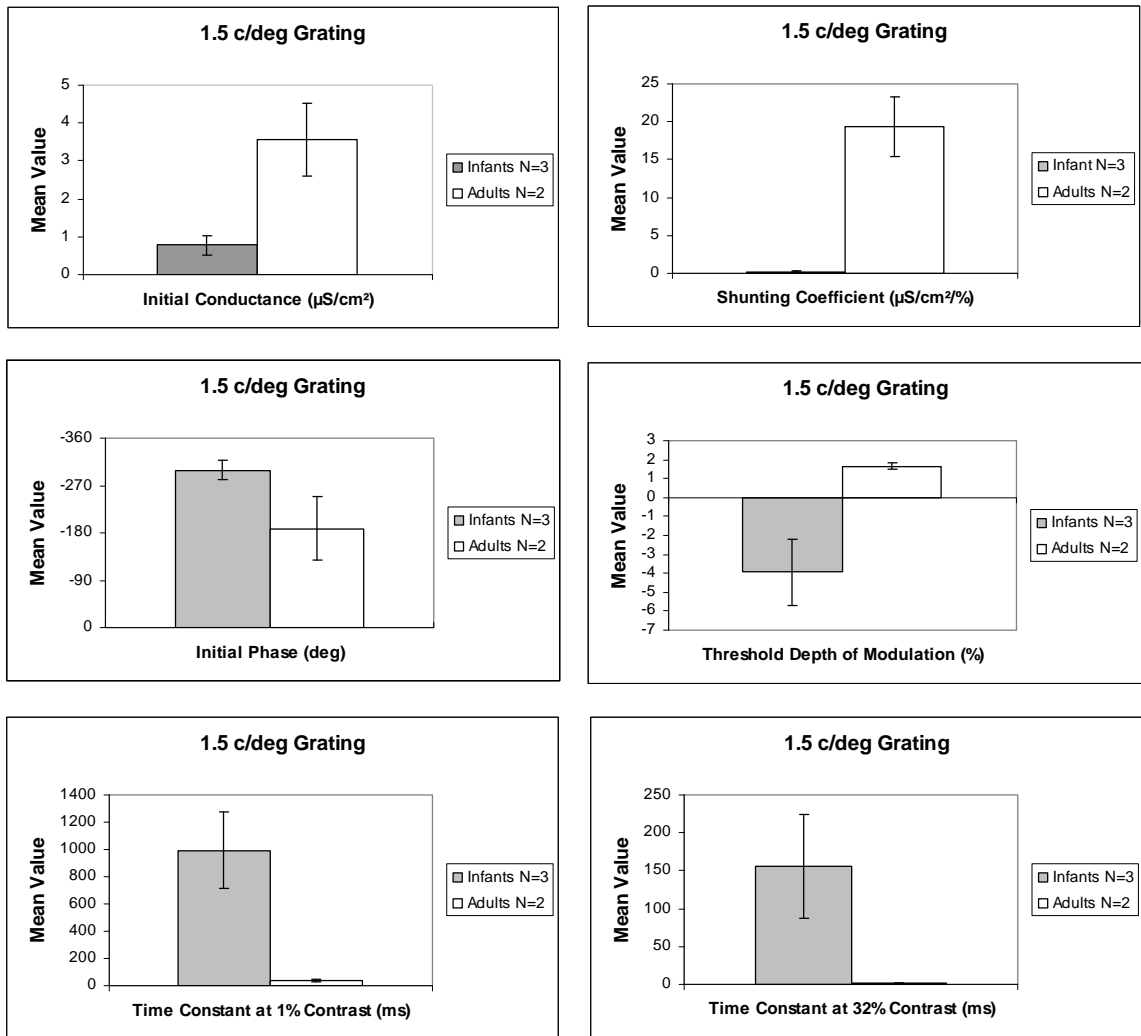


Figure 38. Bar graphs of each of the parameters mean values for adults and infants corresponding to the data shown in Figure 37.

DISCUSSION

This study presents important and significant findings regarding the development of spatial and contrast visual processing in infants. There are marked differences between the responses obtained from infants and adults. The development of inhibitory mechanisms has been incorporated as an explanation for the observed findings.

SPATIAL TUNING FUNCTIONS

The results of this study support previous VEP results (Zemon et al., 1997). In general, infants have lower acuities and show larger response amplitudes, but more response variability than adults. Greater response amplitudes in infants and the subsequent reduction in amplitudes with increasing age have been associated with the increased synaptic density in primary visual cortex around 8 months of age and the following gradual decrease throughout childhood (Huttenlocher et al., 1982; Zemon et al., 1995). The peak of the amplitude in infants is found at lower spatial frequencies than in adults, more often around 1.5 and 3.0 c/deg. In adults, the peak was found mainly at about 3 or 6 c/deg. Zemon et al. (1997) noted that the amplitude peaked at 1 c/deg in a 16-week old, increased to 2 c/deg in a 26- and a 33-week old, and it occurred at 4 c/deg in a 33-year-old adult. The present study is consistent with these results.

Our measure of low spatial frequency fall-off (the log value of the ratio of the signal-to-noise value at the 0.8 c/deg spatial frequency and the signal-to-noise value at the peak of the response) indicated that infants have a more low-pass spatial tuning characteristic than adults. The low frequency attenuation seen in adults is not present in

many of the infants tested in this study. This attenuation has been associated with lateral inhibition (Banks & Salapatek, 1978; Gwiazda et al., 1997; Levine & Shefner, 1991). Lateral inhibition (lateral antagonism) “has the effect of reducing the responses of ganglion cells when they are situated in a broad area of uniform illumination (low spatial frequency)” (Levine & Shefner, 1991). Our results indicate the inhibitory surround mechanism in infants is not fully developed. Whether the reported change in shape of the CSF and the observed fall-off is the result of a central or a peripheral mechanism is open to debate. Devalois, Albrecht and Thorell (1982) found that macaque cortical cells show narrower spatial tuning than LGN cells. Cortical cells show sharp low-frequency as well as high-frequency attenuation, whereas LGN cells are broadly tuned with just a slight decrease in sensitivity to low spatial frequencies. This observation supports a central mechanism.

It has been suggested that data that fail to show an attenuation at low spatial frequencies are obtained because the frequencies used are too high to reveal a decrease in sensitivity (Movshon & Kiorpes, 1988). Some problems arise when testing at very low spatial frequencies. It has been pointed out that 3.5 cycles of a grating stimulus (at least seven bars) is the “minimum number of cycles that a truncated periodic grating must possess in order for it to act effectively as an infinite target” (Kelly, 1975). In a stimulus with less than seven bars, spatial frequency specificity is lost. Participants have to sit very close to the stimulus screen, or the screen has to be big enough to present several cycles of a large pattern. In the present study, the lowest spatial frequency used to obtain responses from infants was 0.8 c/deg. Eight cycles of the stimulus were presented. Although it may be argued that our data do not show more low spatial frequency

attenuation because we did not use stimuli with lower spatial frequencies, we do not believe this to be the case. Figure 39 shows superimposed amplitude and phase of the second harmonic response of an infant and an adult. The plots show an example of the marked differences that exist between infants and adults particularly at the lowest spatial frequencies tested. We believe the striking difference in the low spatial frequency limb of the amplitude plot from infants and adults is caused by further development of lateral inhibition in the maturing visual system.

The acuity estimates from this study compare well to the estimates from previous VEP studies (Norcia & Tyler, 1985; Norcia et al., 1988, 1990; Hamer et al., 1989; Zemon et al., 1997). Figure 40 shows monocular as well as binocular acuity estimates for the present study and previous studies. The top panels in figure 40 present binocular data; the bottom panels show monocular data. For the present study, the right eye results were plotted (Scatter plots of acuity estimates indicated that results for the right and left eye were very similar in both the five- and ten-runs analysis). The panels to the left show the ten-runs analysis graphs; the panels to the right show the five-runs analysis graphs. Although there is a lot of inter-individual variability, in general, there is a trend of increasing acuity with age. From these studies, it can be observed that adult values have not been reached by one year of age. It is important to note that the technique used in this study and the Zemon et al. (1997) study is automated and objective, data collection is synchronous with the stimulus display, and it only requires 6 seconds of data collection per run (a total of 30 seconds per eye with five runs or 60 seconds per eye with ten runs). Moreover, the T^2_{circ} statistic applied uses both amplitude and phase of the response to obtain a more accurate estimate of noise. Using neighboring frequencies to estimate noise

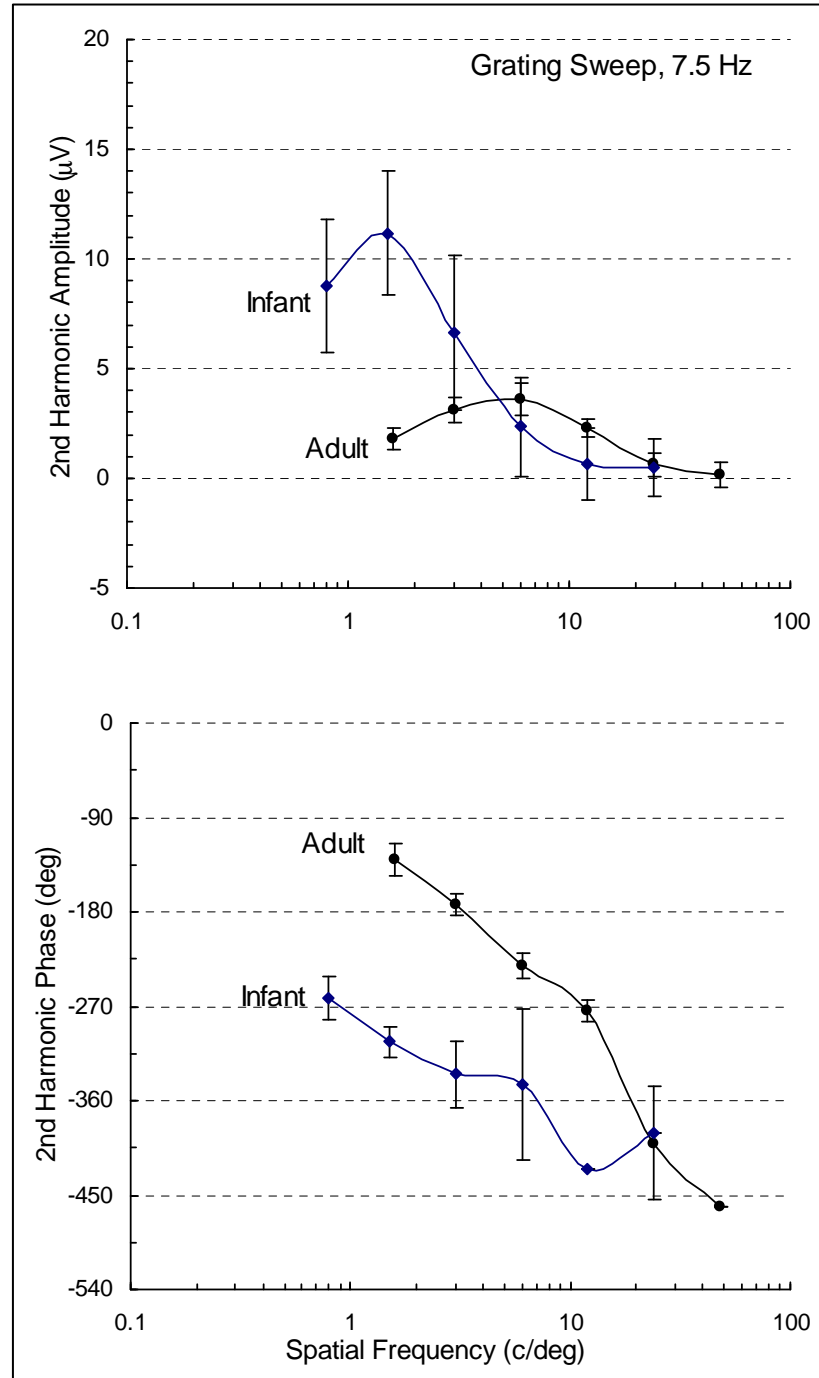


Figure 39. Amplitude and phase of the second harmonic response as a function of spatial frequency from the 16 week-old from Figure 5 (right eye) and the 23 year-old from Figure 9 (left eye) superimposed to emphasize the adult and infant differences.

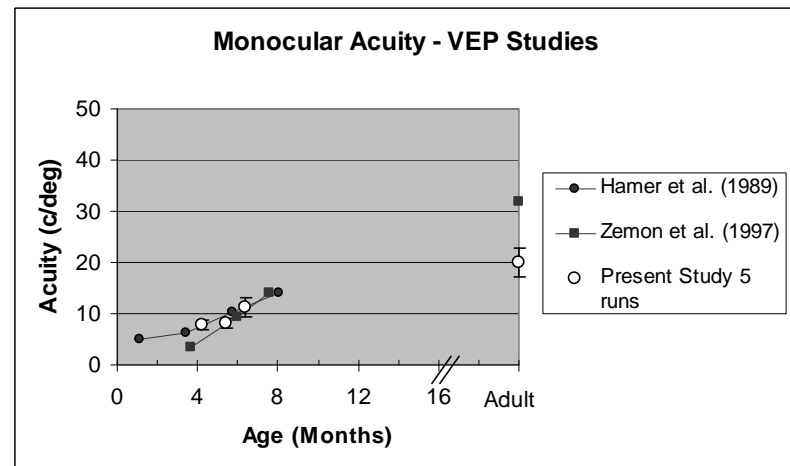
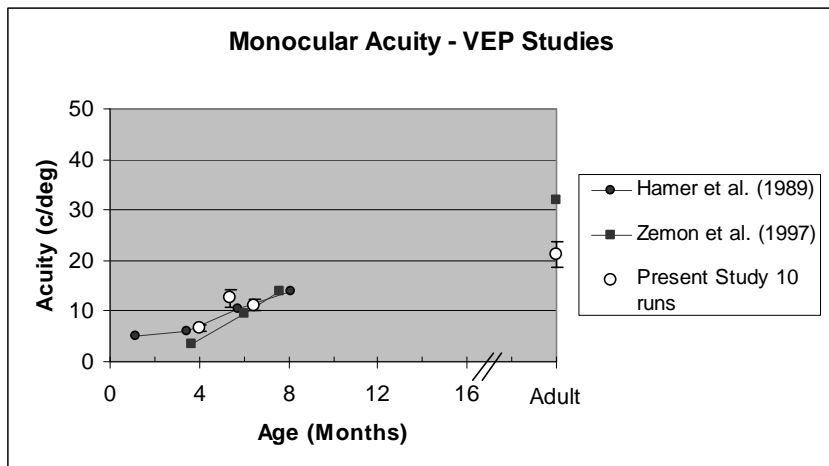
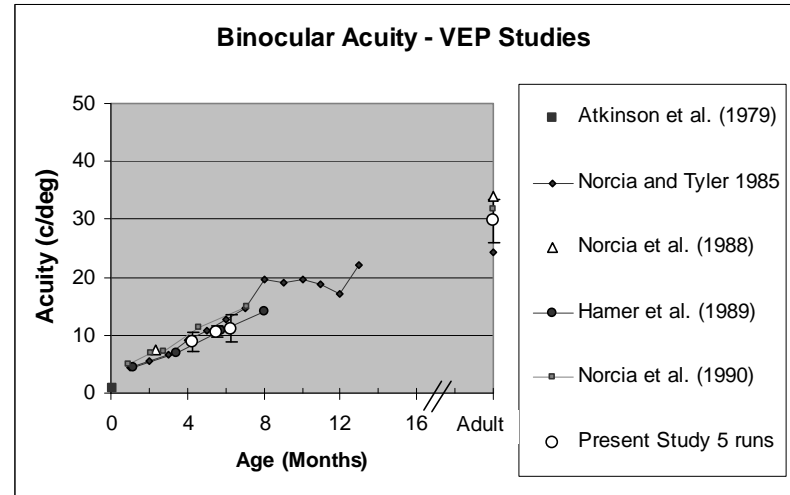
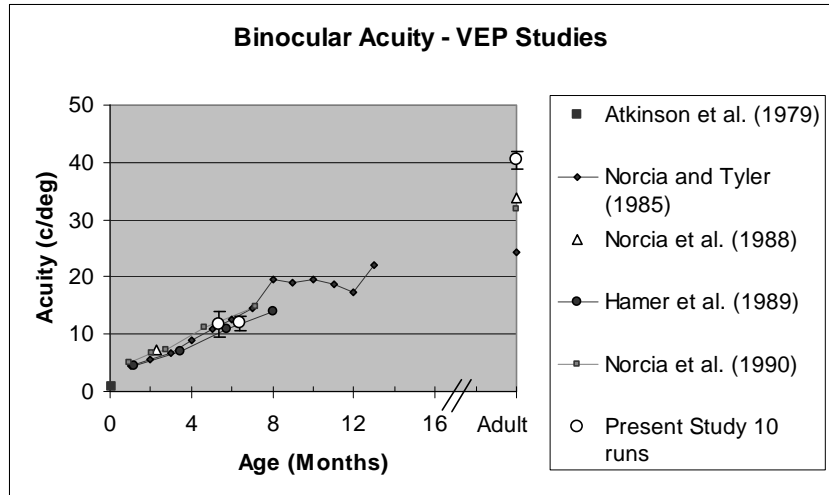


Figure 40. Comparison of mean acuity results from the present study and VEP acuity from previous studies.

at the driven frequency, as is done by Norcia and Tyler (1985) and Norcia et al. (1988, 1990), may underestimate noise level. This study also uses interpolation of the lower confidence limit to zero microvolts to estimate acuity instead of extrapolation of the mean signal to zero microvolts. The latter method requires the subjective selection of a peak in the amplitude of the response, among a number of peaks, to use in the extrapolation process. This procedure assumes that the visual system has no inherent noise and that a linear relation exists between VEP amplitude and spatial frequency (or contrast) of the stimulus (Zemon et al., 1997). Since our estimated acuities compare well to previous studies' results and the method used in this study is rapid, objective, automatic, with a strict criteria for signal-to-noise estimation, this technique is the method of choice for obtaining acuities particularly in infants which have a low attention span.

In scatter plots of right versus left eye acuity, there was a positive significant correlation between the eyes only in the ten-runs ($r=0.608$, $n=15$, $p < 0.01$) but not in the five-runs analysis. These results indicate that on an individual basis, ten runs will produce more reliable data than five runs; however, the fact that similar conclusions have been obtained with either five or ten runs indicates that in some situations where participants are difficult to test or attention span is very short, five runs may be sufficient to draw valid developmental conclusions.

In this study, phase plots in infants are relatively flat with increasing spatial frequency; but in adults there is a steep phase lag. Infant phases at 0.8 c/deg are around -300° , but around -180° in adults. Phase measures are important in understanding the dynamics of the visual system. Phase shifts may be partially due to myelination in the

visual system (Zemon et al., 1997). A light and electron microscopy post-mortem study in 18 infants and children found that optic nerve fibers were virtually myelinated by seven months of age, but sheath thickness around the fibers increased significantly during the first two years of life, and continued to increase modestly thereafter (Magoon & Robb, 1981). Another possible explanation for the phase shift rests on the finding that the magnocellular pathway develops later than the parvocellular pathway; a greater contribution from the magnocellular pathway (higher conduction velocity) to the VEP with increasing age could result in a relative phase advance (Zemon et al., 1997). A change in the balance between cortical excitation and inhibition with increasing age could also cause the phase shifts observed in this study (Zemon et al., 1995; Zemon et al., 1997). A VEP can be represented as a vector sum of excitatory and inhibitory activity. If these processes are not 180° out-of-phase, a change in the relative magnitude between them could result in a phase shift in the summed response (Zemon et al., 1995).

Binocular summation refers to the superiority of binocular performance of a visual task over monocular performance (Legge, 1984; Frisén & Lindblom, 1988). Binocular superiority is believed to be the result of probability summation (the advantage of using two detectors over one) and neural summation (resulting from convergence of monocular inputs in visual cortex) (Blake & Fox, 1973). Based on probability summation, the advantage of using two detectors (two eyes) is equal to the square root of 2 (about 1.41) (Pirenne, 1943). “If performance exceeds predicted probability summation” (any advantage over 1.41), “data are interpreted as evidence of some form of neural summation” (Blake & Fox, 1973). In our study, we obtained a marked difference between monocular and binocular acuity in adults particularly in the ten-runs analysis

(see Figure 20, top left panel and Table 6). Although monocular and binocular acuity was significantly different for infants in some of the analyses, these differences were very small (Figure 19, top panels and Table 6). The binocular summation seen in adults is more than expected by simple probability summation. Hamer et al. (1989) found a small binocular-acuity-superiority (0.17 octaves) in a group of 28 infants under 24 weeks of age, but monocular and binocular acuity were virtually the same in 15 infants over 24 weeks of age. However, the authors did not present any adult data for comparison. In the future, some important insights may be obtained by comparing monocular and binocular measures of other aspects of vision in infants such as the fall-off in spatial tuning functions or differences across spatial frequencies or contrast.

No differences between the acuities of males and females were observed in this study. In their analysis of the infant data collected by Hainline and Abramov (1997), acuity estimates were superior in males versus females (I. Abramov, personal communication, 2006). In other studies, superior visual performance has been observed in females rather than in males. Some studies found higher vernier acuity between 3 and 6 months of age (Gwiazda, Bauer & Held, 1989) and higher mean log sensitivity at the peak of the CSF at 6 months (Peterzell, Werner & Kaplan, 1995) in female than in male infants. Neither Gwiazda et al. (1989) nor Peterzell et al. (1995) found gender differences in the high frequency cutoff of the CSF function of human infants tested with behavioral methods.

General screening methods (i.e. Snellen tests) often fail to detect differences between the eyes, and patients may go undiagnosed. Furthermore, other deficits (i.e. motion deficits, loss of contrast sensitivity, vernier acuity) that may be present in

patients, may not be tested for during screening, which relies heavily on acuity screening. The technique used in this study to assess the development of spatial vision is sensitive to various differences between the eyes, and it may be useful in detecting additional deficits in visual processing other than acuity deficits. As can be observed from the spatial tuning functions of the 46-year-old diagnosed amblyope in Figure 30, acuity estimates from the right and left eyes are virtually the same; however, there are significant differences between the eyes in the amplitude measures at the 3, 6 and 12 c/deg spatial frequencies.

In this study, differences between the eyes were seen in amplitude measures, in phase measures or both. The spatial frequency at which the amplitude and phase measures are significantly different between the eyes is relevant to understanding the kind of deficit that may be present.

Duffy, Snodgrass, Burchfiel and Conway (1976) recorded the responses of visual cortex neurons from monocularly deprived kittens stimulated with moving slits and bars of light. After 8 months of deprivation, they found that all cells responded to stimulation of the normal eye, but only one responded to the amblyopic eye. After they administered bicuculline intravenously, they were able to obtain responses from many cortical neurons after stimulation of the deprived eye. The authors proposed that bicuculline blocked GABA receptors, thus reducing inhibition and restoring binocularity in many of the cells. They suggested that amblyopia may not involve an irreversible loss of visual function. In later studies, in which bicuculline was directly applied to visual cortex in either monocularly deprived (Burchfiel & Duffy, 1981) or surgically induced strabismic cats (Mower, Christen, Burchfiel & Duffy, 1984), it was also found that bicuculline can reverse the effects of deprivation or strabismus in many of the cells tested by presumably

reducing intracortical inhibition. As mentioned previously in the introduction, direct application of bicuculline to the cortex also changes the shape of the VEP response, namely, the negative (N1) wave is greatly increased (exposing excitatory activity), and the positive wave (P2) is diminished or delayed (revealing inhibitory activity) (Zemon, Kaplan & Ratliff, 1980).

Temporal frequency tuning varies depending on the spatial frequency used and vice versa. Spatiotemporal contrast sensitivity surfaces in adults have been studied (Burbeck & Kelly, 1980), but the development of spatiotemporal interactions in infants has not been examined. Generally, responses at particular spatial and temporal frequencies are obtained in infants. It would be interesting to see what changes occur to the spatiotemporal surface with age, but a study of such interactions in infants would not be an easy task.

CONTRAST RESPONSE FUNCTIONS

To date, this is the first study to examine monocular VEP responses of infants as a function of stimulus contrast. Results indicate that processing of contrast in infants differs significantly from processing that occurs in adults. Responses from infants are in general very linear with increasing contrast, and they are similar to responses obtained from neurons in parvocellular-projecting ganglion cells and parvocellular LGN cells in primates (Derrington & Lennie, 1984; Kaplan & Shapley, 1986). They show little amplitude compression, and their phases are relatively constant (flat) with increases in contrast which indicates a lack of contrast gain control. Infants also show bigger responses than adults. The contrast-response functions of adults are similar to the

functions obtained from magnocellular- projecting ganglion cells and magnocellular LGN cells (Derrington & Lennie, 1984; Kaplan & Shapley, 1986): they show amplitude compression and phase advance with increasing contrast. A greater input from the parvocellular pathway early in infancy (due to differential maturation of the magnocellular and parvocellular systems) could contribute to the linear responses obtained from infants.

The results are consistent with greater shunting inhibition in adults than in infants. Infants have lower shunting coefficients (m) than adults in both contrast sweep conditions with the 0.75 and 1.5 c/deg gratings. There were significant positive correlations between m and age in both conditions. Shunting inhibition is mediated by GABA_A receptors. Visual stimulation (increasing contrast) leads to opening of chloride channels which increases the cell's conductance and decreases the integrative time constant (Borg-Graham et al., 1998; Zemon & Gordon, 2006). The relative location of inhibitory inputs with respect to excitatory ones is critical for their shunting efficacy. Inhibitory inputs near the axon hillock (the area with highest number of Na⁺ channels in the cell and lowest threshold for initiation of action potentials) are more effective in shunting excitatory inputs than inhibitory actions at a more distant location, such as in a dendrite (Kandel & Siegelbaum, 2000).

The initial phase is the response phase excluding any phase shift induced by changes in contrast, and in the model, it indicates in great part the phase associated with transmission delay in the system (Zemon & Gordon, 2006). In this study, there is a phase advance with increasing age. There is also a relative phase advance in the phase data

obtained with the 0.75 c/deg grating stimulus compared to the 1.5 c/deg grating phase data.

The initial conductance (G_0) parameter, which is a measure of the contrast gain of the system, as measured with the model did not change much with age for the 0.75 c/deg grating. The shunting coefficient (m) which is a measure of the strength of shunting inhibition in the system showed a marked increase with increasing age. Consistent with this result, the time constant at 1% contrast showed a significant decrease with age.

In contrast to the result for the 0.75 c/deg grating, for the 1.5 c/deg grating stimulus, the initial conductance parameter showed a significant increase with age. This discrepant result may reflect a difference in processing due to the different spatial frequencies used. However, the shunting coefficient, as with the 0.75 c/deg grating, increased while the time constant decreased with increasing age. Lower initial and shunting conductances in infants could lead to longer time constants.

Consistent with the increase in shunting inhibition, in general, there was a trend of decreasing time constants with increasing age, and with increases in contrast. “The time constant of a neuron helps to determine the time course of the synaptic potential and thereby affects temporal summation.” (Kandel & Siegelbaum, 2000). A large time constant gives a neuron a greater capability for temporal summation than a small time constant. With increases in contrast, the time constant decreases; in infants there was often a less than tenfold drop, whereas in adults there was usually a more than twenty-fold decrease in the time constant.

Some participants had negative phase slopes with increasing contrast. Negative time constants were obtained with the model for these observers; negative conductance is

necessary to fit these data with the model. One possible cause for this effect is that at high contrasts, a high level of shunting inhibition is attained in these individuals. Contrast modulation at this high level results in decreases in shunting inhibition (a “ceiling effect”) due to decreases in conductance (closing of channels). Decreasing the conductance leads to longer time constants, and phase lags (Zemon & Gordon, 2006). It has been suggested that negative conductance may play a role in contrast gain enhancement in the visual system via NMDA-receptor activation (Zemon & Gordon, 2006).

Contrast gain control has been shown to be present in cat (Shapley & Victor, 1978, 1981) and monkey (Derrington & Lennie, 1984) retinal ganglion cells, and in cat (Ohzawa, Sclar & Freeman, 1982, 1985) and monkey (Carandini & Heeger, 1994; Sclar, Lennie & DePriest, 1989) cortical cells. Derrington & Lennie (1984) observed amplitude compression and phase advance in magnocellular LGN cells, but Ohzawa et al. (1982, 1985) did not observe contrast gain control in cat LGN cells. Ohzawa et al. (1982, 1985) have used the term contrast gain control to refer to the adaptation mechanism to different contrast levels observed in cat cortical cells. In our study, we observed contrast gain control in the contrast response functions from adults, but it was lacking in most infants. It is possible that we have measured both kinds of contrast gain control in our contrast response functions from adults.

It is believed that shunting inhibition, by nature, has a divisive effect on subthreshold excitatory postsynaptic potentials (Doiron et al., 2000; Holt & Koch, 1997). The VEP is thought to involve the sum of many excitatory and inhibitory postsynaptic potentials on apical dendrites of pyramidal cells in superficial layers of cortex (Zemon,

Kaplan & Ratliff, 1986), and the VEP is thus a sensitive tool to measure the effects of shunting inhibition.

There are major anatomical changes in the visual system in infancy and childhood. These changes are reflected in behavioral and VEP study results. In both the spatial response functions and the contrast response functions obtained from this study, we have shown a developmental sequence that is consistent with increasing cortical inhibition (lateral and shunting inhibition) with age.

REFERENCES

- Abramov, I., Gordon, J., Bibawy, J.N., Abraham, M.J., Bhatt, P., & Feldman, O. (2006). Eye, brain and sex. *Invest. Ophthalmol. Visual Sci.*, **47**, E-Abstract 5358.
- Abramov, I., Gordon, J., Hendrickson, A., Hainline, L., Dobson, V., & LaBossiere, E. (1982). The retina of the newborn human infant. *Science*, **217**, 265-267.
- The American Heritage Dictionary of the English Language (W. Morris, Ed.). (1971). (p. 41) New York, NY: American Heritage Publishing Co., Inc.
- Atkinson, J., Braddick, O., & French, J. (1979). Contrast sensitivity of the human neonate measured by the visual evoked potential. *Invest. Ophthalmol. Visual Sci.*, **18**, 210-213.
- Banks, M.S. (1985). How should we characterize visual stimuli? In G. Gottlieb & N.A. Krasnegor (Ed.) *Measurement of Audition and Vision in the first year of postnatal life: A methodological overview* (pp. 31-51). New Jersey: Ablex Publishing Corporation.
- Banks, M.S. & Salapatek, P. (1978). Acuity and contrast sensitivity in 1-, 2- and 3-month-old human infants. *Invest. Ophthalmol. Visual Sci.*, **17**, 361-365.
- Banks, M.S. & Salapatek, P. (1981). Infant pattern vision: A new approach based on the contrast sensitivity function. *J. Exp. Child Psychol.*, **31**, 1-45.
- Birch, E.E. (1985). Infant interocular acuity differences and binocular vision. *Vision Res.*, **25**, 571-576.
- Blake, R. & Fox, R. (1973). The psychophysical inquiry into binocular summation. *Percept. Psychophys.*, **14**, 161-185.
- Boothe, R.G., Dobson, V. & Teller, D.Y. (1985). Postnatal development of vision in human and nonhuman primates. *Ann. Rev. Neurosci.*, **8**, 495-545.
- Boothe, R.G., Kiorpes, L., Williams, R.A., & Teller, D.Y. (1988). Operant measurements of contrast sensitivity in infant macaque monkeys during normal development. *Vision Res.*, **28**, 387-396.
- Borg-Graham, L.J., Monier, C. & Frégnac, Y. (1998). Visual input evokes transient and strong shunting inhibition in visual cortical neurons. *Nature*, **393**, 369-373.
- Burbeck, C.A. & Kelly, D.H. (1980). Spatiotemporal characteristics of visual mechanisms: excitatory-inhibitory model. *J. Opt. Soc. Am.*, **70**, 1121-1126.
- Burchfiel, J.L., & Duffy, F.H. (1981). Role of intracortical inhibition in deprivation amblyopia: reversal by microiontophoretic bicuculline. *Brain Res.*, **206**, 479-484.

- Burkhalter, A., Bernardo, K.L. & Charles, V. (1993). Development of local circuits in human visual cortex. *J. Neurosci.*, **13**, 1916-1931.
- Carandini, M. & Heeger, D.J. (1994). Summation and division by neurons in primate visual cortex. *Science*, **264**, 1333-1336.
- Chugani, H.T. (1998). A critical period of brain development: studies of cerebral glucose utilization with PET. *Prevent. Med.*, **27**, 184-188.
- Ciuffreda, K.J., Levi, D.M. & Selenow, A. (1991). *Amblyopia: Basic and clinical aspects* (pp. 1-42, 69-144). Boston, MA: Butterworth-Heinemann.
- Courage, M.L. & Adams, R.J. (1990). Visual acuity assessment from birth to three years using the acuity card procedure: Cross-sectional and longitudinal samples. *Optom. Vis. Sci.*, **67**, 713-718.
- Crognale, M.A., Kelly, J.P., Chang, S., Weiss, A.H., & Teller, D.Y. (1997). Development of pattern visual evoked potentials: Longitudinal measurements in human infants. *Optom. Vis. Sci.*, **74**, 808-815.
- Dacey, D.M. (1993). The mosaic of midget ganglion cells in the human retina. *J. Neurosci.*, **13**, 5334-5355.
- Daw, N.W. (1998). Critical periods and amblyopia. *Arch. Ophthalmol.*, **116**, 502-505.
- Derrington, A.M. & Lennie, P. (1984). Spatial and temporal contrast sensitivities of neurones in lateral geniculate nucleus of macaque. *J. Physiol.*, **357**, 219-240.
- De Valois, R.L., Albrecht, D.G. & Thorell, L.G. (1982). Spatial frequency selectivity of cells in Macaque visual cortex. *Vision Res.*, **22**, 545-559.
- Dobson, V. (1993). Visual acuity testing in infants: From laboratory to clinic. In K. Simmons (Ed.) *Early visual development, normal and abnormal* (pp. 318-334). New York: Oxford University Press.
- Dobson, V. (1994). Visual acuity testing by Preferential Looking techniques. In S.J. Isenberg (Ed.), *The Eye in Infancy* (pp. 131-156). St. Louis, MO: Mosby.
- Doiron, B., Longtin, A., Berman, N., & Maler, L. (2000). Subtractive and divisive inhibition: Effect of voltage-dependent inhibitory conductances and noise. *Neural Computation*, **13**, 227-248.
- Duffy, F.H., Snodgrass, S.R., Burchfiel, J.L. & Conway, J.L. (1976). Bicuculline reversal of deprivation amblyopia in the cat. *Nature*, **260**, 256-257.

- Dustman, R.E. & Beck, E.C. (1966). Visually evoked potentials: Amplitude changes with age. *Science*, **151**, 1013-1015.
- Fagiolini, M. & Hensch, T.K. (2000). Inhibitory threshold for critical-period activation in primary visual cortex. *Nature*, **404**, 183-186.
- Famiglietti, E.V., Jr., & Kolb, H. (1976). Structural basis for ON- and OFF-center responses in retinal ganglion cells. *Science*, **194**, 193-195.
- Feldman, D.E. (2000). Inhibition and plasticity. *Nature Neurosci*, **3**, 303-304.
- Fiorentini, A. & Trimarchi, C. (1992). Development of temporal properties of pattern electroretinogram and visual evoked potentials in infants. *Vision Res.*, **32**, 1609-1621.
- Frisén, L. & Lindblom, B. (1988). Binocular summation in humans: Evidence for a hierarchic model. *J. Physiol.*, **402**, 773-782.
- Garey, L.J. & De Courten, C. (1983). Structural development of the lateral geniculate nucleus and visual cortex in monkey and man. *Behav. Brain Res.*, **10**, 3-13.
- Grose-Fifer, J., Zemon, V. & Gordon, J. (1994). Temporal tuning and the development of lateral interactions in the human visual system. *Invest. Ophthalmol. Vis. Sci.*, **35**, 2999-3010.
- Gwiazda, J., Bauer, J. & Held, R. (1989). From visual acuity to hyperacuity: A 10-year update. *Canadian J. Psychol.*, **43**, 109-120.
- Gwiazda, J., Bauer, J., Thorn, F., & Held, R. (1997). Development of spatial contrast sensitivity from infancy to adulthood: Psychophysical data. *Optom. Vision Sci*, **74**, 785-789.
- Hainline, L. & Abramov, I. (1997). Eye-movement based measures of development of spatial contrast sensitivity in infants. *Optom. Vision Sci*, **74**, 790-799.
- Hamer, Norcia, Tyler & Hsu-Winges (1989). The development of monocular and binocular VEP acuity. *Vision Res.*, **29**, 397-408.
- Harris, L., Atkinson, J., & Braddick, O. (1976). Visual contrast sensitivity of a 6-month-old infant measured by the evoked potential. *Nature*, **264**, 370-371.
- Hartline, H.K. (1938). The response of single optic nerve fibers of the vertebrate eye to illumination of the retina. *Amer. J. Physiol.*, **121**, 400-415.
- Hartmann, E.E. (1995). Infant visual development: An overview of studies using visual evoked potential measures from Harter to the present. *Intern. J. Neurosci.*, **80**, 203-235

- Hartmann, E.E. (1996). Functional assessment of Infants. In B. Rosenthal & R. Cole (Eds.) *Functional assessment of low vision* (pp.45-62). St. Louis, MO: Mosby.
- Hartmann, E.E. & Banks, M.S. (1992). Temporal contrast sensitivity in human infants. *Vision Res.*, **32**, 1163-1168.
- Hartmann, E.E., Hitchcox, S.M., & Zemon, V. (1992a). Development of pattern responses to contrast-increment and -decrement stimuli in infants: a VEP measure of functional subsystems in the visual pathway. In: *Noninvasive Assessment of the Visual System Technical Digest, 1992* (Optical Society of America, Washington, D.C., 1992) Vol. 1, pp. 146-149.
- Hartmann, E.E., Hitchcox, S.M., & Zemon, V. (1992b). Development of pattern responses to contrast-increment and -decrement stimuli in infants: a VEP measure of functional subsystems. *Supplement to Invest. Ophthalmol. Visual Sci.*, **33**, 1351
- Harwerth, R.S., Smith III, E.L., Duncan, G.C., Crawford, M.L.J. & von Noorden, G.K. (1986). Multiple sensitive periods in the development of the primate visual system. *Science*, **232**, 235-238.
- Hendrickson, A.E., Wilson, J.R. & Ogren, M.P. (1978). The neuroanatomical organization of pathways between dorsal lateral geniculate nucleus and visual cortex in Old and New World primates. *J. Comp. Neurol.*, **182**, 123-136.
- Hendrickson, A.E. & Yuodelis, C. (1984). The morphological development of the human fovea. *Ophthalmology*, **91**, 603-612.
- Hering, E. (1964). *Outlines of a Theory of the Light Sense*. (pp.30-31). Cambridge, Mass: Harvard University Press (Translated by L.M. Hurvich and J. Jameson).
- Hickey, T.L. (1977). Postnatal development of the human lateral geniculate nucleus: Relationship to a critical period for the visual system. *Science*, **198**, 836-838.
- Holt, G.R. & Koch, C. (1997). Shunting inhibition does not have a divisive effect on firing rates. *Neural Comput.*, **9**, 1001-1013.
- Hubel, D.H. & Wiesel, T.N. (1972). Laminar and columnar distribution of geniculocortical fibers in the macaque monkey. *J. Comp. Neurol.*, **146**, 421-450.
- Huttenlocher, P.R., de Courten, C., Garey, L.J., & Van Der Loos, H. (1982). Synaptogenesis in human visual cortex - evidence for synapse elimination during normal development. *Neurosci. Lett.*, **33**, 247-252.
- Jasper, H.H. (1958). The 10-20 electrode system of the International Federation. *Electroenceph. Clin. Neurophysiol.*, **10**, 371-375.

- Kandel, E.R. & Siegelbaum, S.A. (2000). Synaptic integration. In E.R. Kandel, J.H. Schwartz & T.M. Jessell (Eds), *Principles of Neural Science* (pp. 207-228). New York: McGraw-Hill.
- Kaplan, E. & Shapley, R.M. (1986). The primate retina contains two types of ganglion cells, with high and low contrast sensitivity. *Proc. Natl. Acad. Sci.*, **83**, 2755-2757.
- Kelly, D.H. (1975). How many bars make a grating? *Vision Res.*, **15**, 625-626.
- Kiorpes, L. (2006). Visual processing in amblyopia: Animal studies. *Strabismus*, **14**, 3-10.
- Kiorpes, L. & McKee, S.P. (1999). Neural mechanisms underlying amblyopia. *Curr. Opinion Neurobiol.*, **9**, 480-486.
- Kiorpes, L. & Stavros, K. (2007). Development of temporal contrast sensitivity in monkeys. *Vision Sciences Society Abstracts*, 167.
- Kuffler, S.W. (1953). Discharge patterns and functional organization of mammalian retina. *J. Neurophysiol.*, **16**, 37-68.
- Legge, G.E. (1984). Binocular contrast summation - I. Detection and discrimination. *Vision Res.*, **24**, 373-383.
- Leuba, G. & Kraftsik, R. (1994). Changes in volume, surface estimate, three-dimensional shape and total number of neurons of the human primary visual cortex from midgestation until old age. *Anat. Embryol.*, **190**, 351-366.
- Levi, D.M. (2006). Visual processing in amblyopia: Human studies. *Strabismus*, **14**, 11-19.
- Levine, M.W. & Shefner, J.M. (1991). Spatial frequency representation. In: *Fundamentals of sensation and perception*. (pp.222-223). Pacific Grove, CA: Brooks/Cole Publishing Company.
- Magoon, E.H. & Robb, R.M. (1981). Development of myelin in human optic nerve and tract: A light and electron microscopic study. *Arch. Ophthalmol.*, **99**, 655-659.
- Mayer, D.L, Beiser, A.S., Warner, A.F., Pratt, E.M., Raye, K.N. & Lang, J.M. (1995). Monocular acuity norms for the Teller Acuity Cards between ages one month and four years. *Invest. Ophthalmol. Visual Sci.*, **36**, 671-685.
- McDonald, M., Sebris, S.L., Mohn, G., Teller, D.Y. & Dobson, V. (1986). Monocular acuity in normal infants: the acuity card procedure. *Am. J. Optom. Physiol. Opt.*, **63**, 127-134.

- McKee, S.P., Levi, D.M. & Movshon, J.A. (2003). The pattern of visual deficits in amblyopia. *J. Vision*, **3**, 380-405.
- Mitchell, J.F. & Srinivasan, V. (1969). Release of ^3H - γ -Aminobutyric Acid from the brain during synaptic inhibition. *Nature*, **224**, 663-666.
- Morrone, M.C. & Burr, D.C. (1986). Evidence for the existence and development of visual inhibition in humans. *Nature*, **321**, 235-237.
- Moskowitz, A., & Sokol, S. (1980). Spatial and temporal interaction of pattern-evoked cortical potentials in human infants. *Vision Res.*, **20**, 699-707.
- Movshon, J.A. & Kiorpes, L. (1988). Analysis of the development of spatial contrast sensitivity in monkey and human infants. *J. Opt. Soc. Am. A*, **5**, 2166-2172.
- Mower, G.D., Christen, W.G., Burchfiel, J.L. & Duffy, F.H. (1984). Microiontophoretic bicuculline restores binocular responses to visual cortical neurons in strabismic cats. *Brain Res.*, **309**, 168-172.
- Murphy, K.M., Beston, B.R., Boley, P.M. & Jones, D.G. (2005). Development of human visual cortex: A balance between excitatory and inhibitory plasticity mechanisms. *Dev. Psychobiol.*, **46**, 209-221.
- Murray, I.J., Parry, N.R.A., Carden, D., & Kulikowski, J.J. (1987). Human visual evoked potentials to chromatic and achromatic gratings. *Clin. Vis. Sci.*, **1**, 231-244.
- Norcia, A.M., & Tyler, C.W. (1985). Spatial frequency sweep VEP: Visual acuity during the first year of life. *Vision Res.*, **25**, 1399-1408.
- Norcia, A.M., Tyler, C.W., & Hamer, R.D. (1987). Development of contrast sensitivity in human infants. *Invest. Ophthalmol. Vis. Sci. Suppl.*, **28**, 5.
- Norcia, A.M., Tyler, C.W., & Hamer, R.D. (1988). High visual contrast sensitivity in the young human infant. *Invest. Ophthalmol. Visual Sci.*, **29**, 44-49.
- Norcia, A.M., Tyler, C.W. & Hamer, R.D. (1990). Development of contrast sensitivity in the human infant. *Vision Res.*, **30**, 1475-1486.
- Norcia, A.M., Tyler, C.W., Hamer, R.D., & Wesemann, W. (1989). Measurement of spatial contrast sensitivity with the swept contrast VEP. *Vision Res.*, **29**, 627-637.
- Ohzawa, I., Sclar, G. & Freeman, R.D. (1982). Contrast gain control in the cat visual cortex. *Nature*, **298**, 266-268.
- Ohzawa, I., Sclar, G. & Freeman, R.D. (1985). Contrast gain control in the cat's visual system. *J. Neurophysiol.*, **54**, 651-667.

- Peterzell, D.H. & Kelly, J.P. (1997). Development of spatial frequency tuned “covariance” channels: Individual differences in the electrophysiological (VEP) contrast sensitivity function. *Optom. Vis. Sci.*, **74**, 800-807.
- Peterzell, D.H., Werner, J.S. & Kaplan, P.S. (1995). Individual differences in contrast sensitivity functions: Longitudinal study of 4-, 6- and 8-month old human infants. *Vis. Res.*, **35**, 961-979.
- Pirenne, M.H. (1943). Binocular and unocular thresholds of vision. *Nature*, **152**, 698-699.
- Purpura, D.P., Girado, M. & Grundfest, H. (1957). Selective blockade of excitatory synapses in the cat brain by γ -Aminobutyric Acid. *Science*, **125**, 1200-1202.
- Ratliff, C., Sterling, P. & Balasubramanian, V. (2005). Negative contrasts predominate in natural images. *Supplement to Invest. Ophthalmol. Vis. Sci.*, **46**: 4685.
- Regan, D. (1982). Comparison of transient and steady-state methods. *Ann. NY Acad. Sci.*, **388**, 45-71.
- Regan, D. (1989). *Human brain electrophysiology: Evoked potentials and evoked magnetic fields in science and medicine*. New York: Elsevier Science Publishing Co., Inc.
- Robson, J.G. (1966). Spatial and temporal contrast-sensitivity functions of the visual system. *J. Opt. Soc. Am.*, **56**, 1141-1142.
- Salomao, S.R. & Ventura, D.F. (1995). Large sample population age norms for visual acuities obtained with Vistech-Teller Acuity Cards. *Invest. Ophthalmol. Visual Sci.*, **36**, 657-670.
- Schiller, P.H. (1982). Central connections of the retinal ON and OFF pathways. *Nature*, **297**, 580-583.
- Schiller, P.H., Sandell, J.H. & Maunsell, J.H.R. (1986). Functions of the ON and OFF channels of the visual system. *Nature*, **322**, 824-825.
- Sclar, G., Lennie, P. & DePriest, D.D. (1989). Contrast adaptation in striate cortex of macaque. *Vision Res.*, **29**, 747-755.
- Seiple, W.H., Kupersmith, M.J., Nelson, J.I., & Carr, R.E. (1984). The assessment of evoked potential contrast thresholds using real-time retrieval. *Invest. Ophthalmol Visual Sci.*, **25**, 627-631.

- Shapley, R. (1982). Parallel pathways in the mammalian visual system. *Ann. NY Acad. Sci.*, **388**, 11-20.
- Shapley, R.M. & Victor, J.D. (1978). The effect of contrast on the transfer properties of cat retinal ganglion cells. *J. Physiol.*, **285**, 275-298.
- Shapley, R.M. & Victor, J.D. (1981). How the contrast gain control modifies the frequency responses of cat retinal ganglion cells. *J. Physiol.*, **318**, 161-179.
- Simons, K. (2005). Amblyopia characterization, treatment and prophylaxis. *Surv. Ophthalmol.*, **50**, 123-166.
- Slaughter, M.M., & Miller, R.F. (1981). 2-amino-4-phosphonobutyric acid: A new pharmacological tool for retina research. *Science*, **211**, 182-184.
- Sokol, S. (1976). Visually Evoked Potentials: Theory, techniques and clinical applications. *Surv. Ophthalmol.*, **21**, 18-44.
- Sokol, S. (1978). Measurement of infant visual acuity from pattern reversal evoked potentials. *Vision Res.*, **18**, 33-39.
- Sokol, S. (1982). Infant visual development: Evoked potential estimates. *Ann. NY Acad. Sci.*, **388**, 514-525.
- Sokol, S. & Moskowitz, A. (1990). Development of ON & OFF brightness pathways in human infants. *Supplement to Invest. Ophthalmol Visual Sci.*, **31**, 251.
- Sokol, S., Zemon, V. & Moskowitz, A. (1992). Development of lateral interactions in the infant visual system. *Vis. Neurosci.*, **8**, 3-8.
- Somogyi, P., Cowey, A., Halasz, N. & Freund, T.F. (1981). Vertical organization of neurones accumulating 3H-GABA in visual cortex of rhesus monkey. *Nature*, **294**, 761-763.
- Swanson, W.H. & Birch, E.E. (1990). Infant spatiotemporal vision: dependence of spatial contrast sensitivity on temporal frequency. *Vision Res.*, **30**, 1033-1048.
- Tessier-Lavigne, M. (2000). Visual processing by the retina. In E.R. Kandel, J.H. Schwartz & T.M. Jessell (Eds), *Principles of Neural Science* (pp. 507-522). New York: McGraw-Hill.
- Victor, J.D. & Mast, J. (1991). A new statistic for steady-state evoked potentials. *Electroenceph. Clin. Neurophysiol.*, **78**, 378-388.
- Von Békésy, G. (1967). Sensory inhibition. (p. 24). Princeton, NJ: Princeton University Press.

Wilson, H.R. (1988). Development of spatiotemporal mechanisms in infant vision. *Vision Res.*, **28**, 611-628.

Wu, C. & Hunter, D.G. (2006). Amblyopia: Diagnostic and therapeutic options. *Am. J. Ophthalmol.*, **141**, 175-184.

Wurtz, R.H. & Kandel, E.R. (2000). Central visual pathways. In E.R. Kandel, J.H. Schwartz & T.M. Jessell (Eds), *Principles of Neural Science* (pp. 523-547). New York: McGraw-Hill.

Yuodelis, C. & Hendrickson, A. (1986). A qualitative and quantitative analysis of the human fovea during development. *Vision Res.*, **26**, 847-855.

Zemon, V., Eisner, W., Gordon, J., Grose-Fifer, J., Tenedios, F. & Shoup, H. (1995). Contrast-dependent responses in the human visual system: Childhood through adulthood. *Int. J. Neurosci.*, **80**, 181-201.

Zemon, V. & Gordon, J. (1988). Spatial tuning characteristics of functional subsystems in the visual pathways of humans. *Supplement to Invest. Ophthalmol. Visual Sci.*, **29**, 297.

Zemon, V. & Gordon, J. (2006). Luminance-contrast mechanisms in humans: Visual evoked potentials and a nonlinear model. *Vision Res.*, **46**, 4163-4180.

Zemon, V., Gordon, J., Greenstein, V., Holopigian, K. & Seiple, W. (1990). Properties of chromatic and luminance channels measured electrophysiologically in humans. *Supplement to Invest. Ophthalmol. Visual Sci.*, **31**, 263.

Zemon, V., Gordon, J. & Welch, J. (1986). ON- and OFF-center pathways in humans examined using VEPs. *Supplement to Invest. Ophthalmol. Visual Sci.*, **27**, 280.

Zemon, V., Gordon, J. & Welch, J. (1988). Asymmetries in ON and OFF visual pathways of humans revealed using contrast-evoked cortical potentials. *Visual Neurosci.*, **1**, 145-150.

Zemon, V., Hartmann, E.E., Gordon, J. & Prünke-Glowazki, A. (1997). An electrophysiological technique for assessment of the development of spatial vision. *Optometry Vision Sci.*, **74**, 708-716.

Zemon, V., Kaplan, E. & Ratliff, F. (1980). Bicuculline enhances a negative component and diminishes a positive component of the visual evoked cortical potential in the cat. *Proc. Natl. Acad. Sci.*, **77**, 7476-7478.

Zemon, V., Kaplan, E. & Ratliff, F. (1986). The role of GABA-mediated intracortical inhibition in the generation of visual evoked potentials. In R.Q. Cracco and I. Bodis-

Wollner (Eds.), *Frontiers of Clinical Neuroscience, Vol. 3: Evoked Potentials* (pp. 287-295). New York: Alan R. Liss, Inc.

Zemon, V. & Ratliff, F. (1982). Visual evoked potentials: Evidence for lateral interactions. *Proc. Natl. Acad. Sci.*, **79**, 5723-5726.

Zemon, V., Siegfried, J. & Gordon, J. (1991). Magno and parvo pathways in humans studied using VEPs to luminance and chromatic contrast. *Supplement to Invest. Ophthalmol. Visual Sci.*, **32**, 1033.